LABORATORY STUDIES OF THE ROUGHNESS AND SUSPENDED LOAD OF ALLUVIAL STREAMS

Vito A. Vanoni and Norman H. Brooks

Final Report to
Corps of Engineers, U. S. Army
Missouri River Division
Contract DA-25-075-eng-3866

Sedimentation Laboratory
CALIFORNIA INSTITUTE OF TECHNOLOGY
Pasadena, California

Report No. E-68 December 1957

Corps of Engineers, U. S. Army
Missouri River Division
Contract DA-25-075-eng-3866

LABORATORY STUDIES OF

THE ROUGHNESS AND SUSPENDED LOAD OF ALLUVIAL STREAMS

Vito A. Vanoni
Norman H. Brooks

FINAL REPORT

Sedimentation Laboratory
California Institute of Technology
Pasadena, California

Report No. E-68

December 1957

ABSTRACT

This report describes research work done under Contract No. DA-25-075-eng-3866 with the U. S. Army, Corps of Engineers, Missouri River Division, Cmaha, during the period 1954-1957, on problems of suspended load transport in alluvial streams.

A total of 94 experimental runs were made in two laboratory flumes charged with fine sand of several size distributions. Special attention was given to the variation of the friction factor caused by the changing bed configuration and the damping effect of suspended sediment. The relationship between the sediment transportation rate and the hydraulic variables was also investigated. Most of the runs (General Studies, Chap. V) were made with the bed of the flume completely covered with loose sand but some special runs (Special Studies, Chap. VII) were made with the sand bed chemically solidified in place to prevent sediment transport while preserving the bed configuration previously generated by a natural flow of the same velocity with loose sand. The principal laboratory results are as follows:

1. The friction factor f for a stream with a movable sand bed may vary several fold, being highest at low or medium flow velocities and lowest at high velocity.

2. The principal cause of the variation in f is the appearance of dunes at low or medium velocities and disappearance at high velocities.

3. A secondary cause for the reduction in f for high sediment transport rates is the damping effect of the suspended sediment on the turbulence, and the concomitant reduction in the turbulent diffusion coefficients. The maximum observed reduction due directly to the sediment load was only about 28 percent.

4. The discharge and sediment transportation rate are not unique functions of depth and slope because of the variable roughness. Slope (or shear) must probably be considered a dependent variable for alluvial streams because several equilibrium flows can yield the same slope and shear stress.

The laboratory data are compared with similar data for natural streams, and the most promising existing analyses for roughness and sediment load are discussed in the light of the present findings. In addition, a critical review of early and recent literature on the resistance of sediment-laden streams is presented in Chapter II.

CONTENTS

CONTENTS
(cont'd)

LIST OF FIGURES

LIST OF FIGURES
(cont'd)

LIST OF FIGURES
(cont'd)

LIST OF TABLES

I. INTRODUCTION

This report describes some sediment transportation studies made in two laboratory flumes charged with fine sand. The sediment was fine enough to be transported primarily as suspended load, with the bed being movable so that under certain conditions dunes and bars appeared. The research was carried out under Contract No. DA-25-075-eng-3866 with the U. S. Army Corps of Engineers, Missouri River Division, Omaha, Nebraska, and this report is the final one for the sponsor.

A. The Problems

In natural alluvial streams with loose beds of sand there are two major unsolved problems facing river engineers: how can the channel roughness be predicted inasmuch as it varies with the bed configuration and the amount of sediment load; and how can the rate of sediment transport be predicted from the flow conditions? While it may be said that for any given stream these quantities can be measured, nevertheless it is vital for engineers to be able to solve these problems when man-made changes in the stream regimen are being planned, such as for flood control, power, navigation and water supply. The research conducted in the laboratory flumes was directed at these two problems. Because of the extreme complexity of them, the problems are still by no means solved, but the results reported herein should increase the engineer's general understanding of the processes involved.

The resistance to flow of clear water in a channel with fixed boundaries has been studied extensively and can be predicted with a satisfactory degree of certainty. Values of friction factors to be used in the flow equations such as the Manning or Darcy-Weisbach formulas have been determined and are given in reference works on hydraulics as a function of the texture or roughness of the channel walls and the Reynolds number.

However, when a stream has a movable bed, and sediment is being transported, the problem of determining the resistance is much more complicated than in the simple case of clear water flowing in a channel with fixed walls. Observations have shown that the friction factors for such sediment-bearing or alluvial streams vary over appreciable ranges.

However, the problem has not been studied sufficiently to enable hydraulic engineers to predict a friction factor for given conditions.

The fact that the friction factors for alluvial streams vary has been known for a long time. Despite this, the problem is not discussed at any length in the literature, and textbooks are particularly silent on this point. This leaves all but the expert in this field with the erroneous impression that the friction factor of streams is constant and can be determined once for all time. The lack of discussion in the literature of the resistance of alluvial streams may be explained by the fact that the problem is not well understood, and information on it is often conflicting. For instance, some evidence presented shows that the friction factor of a stream increases as the sediment load increases, while other evidence supports the opposite conclusion.

The variation of roughness of sediment-laden streams is caused by two distinct processes: (1) appearance of dunes and bars which may increase the roughness several fold because of the additional form resistance of the bed; and (2) the damping effect of the suspended sediment on the turbulence in the stream tending to reduce the hydraulic roughness. Because of these two opposing processes, there has often been confusion about the effect of sediment load on roughness. Indeed, it is very difficult to separate the two effects because, for streams in which a significant amount of bed material is carried in suspension, the two processes are always acting together, but with differing relative effects. For example, in a sediment-laden stream flowing at high velocity over a flat bed of sand, the friction factor or roughness coefficient will probably be lower than that for a clear flow over a fixed bed of comparable grain roughness because of the damping effect of the suspended load. On the other hand, at a lower velocity with light suspended load, dunes may grow, and the net result will appear to be an increase in the friction factor over that for a fixed flat bed of the same sand roughness.

To investigate these two processes two kinds of experiments were made; these will be designated hereinafter as "General Studies" and "Special Studies". In the General Studies the beds of the flumes were covered with sand, and the water was circulated, allowing the sediment to be transported and the bed configuration to become adjusted to the flows.

In other words, in the General Studies the flume was allowed to behave as much as possible like a stream (except for fixed walls and straight channel), and the hydraulic roughness was affected by both the processes described above.

In the Special Studies an effort was made to separate the two processes in order to determine qualitatively their relative order of magnitude. To accomplish this, runs were made with suspended load and a movable bed, and then with clear water but with no change in the bed configuration. This necessitated the development of a procedure for solidifying a natural bed configuration in place so that the clear water could be made to flow over exactly the same bed as the sediment-laden flow. A comparison of friction factors then showed directly the damping effect of the sediment separately from the effect of changing bed configuration.

The problem of determining the law of transportation of suspended sediment cannot be solved independently of the roughness problem. On any stream the depth, velocity and shear for any discharge are determined by the roughness, which itself depends on the sediment load. But, on the other hand, the sediment discharge is intimately related to the depth and velocity; thus it is seen that the two problems are closely interlocked and that they should, therefore, be attacked simultaneously. This, in fact, was the case for all the experiments described under "General Studies".

B. Organization of the Report

Although the report deals with two distinct investigations, it has been organized together as a single report to avoid duplication of text and figures which apply equally well to both the General and Special Studies.

In Chapter II previous investigations of the resistance of alluvial streams will be briefly reviewed. Following that, Chapters III and IV will describe the laboratory apparatus and procedure common to both sets of experiments. The experimental results of the General Studies appear in Chapter V, and discussion of them is in Chapter VI. Presented in Chapter VII are the results of the Special Studies, as well as special items of procedure; discussion follows in Chapter VIII. The conclusions are summarized in Chapter IX. Acknowledgments, appendices, and a list of references may be found at the very end of the report.

II. PREVIOUS STUDIES OF RESISTANCE OF SEDIMENT-LADEN STREAMS

A. Early Studies of the Resistance Problem

One serious obstacle to the understanding of the resistance of alluvial streams by the hydrodynamicist of the latter part of the last century was the theory developed to explain the phenomenon. The reasoning back of the theory started out with the logical idea that the loss in energy head between any two stations on a stream is merely the difference in elevation between the stations. It was then argued that this drop or head loss was used up in two ways: (1) in overcoming the hydraulic friction of the flow, and (2) in transporting sediment. According to this concept, the more energy used in transporting sediment the less was available to overcome friction, and vice versa. Since the hydraulic slope is merely the energy consumed in overcoming friction per unit length of stream, it was argued that a reduction of this energy or slope would also reduce the mean flow velocity, which result could be obtained from the Chezy formula for mean velocity in a channel. Finally, from this it was concluded that a clear stream would flow faster than a comparable one carrying a sediment load.

In view of present knowledge of flow problems, it is clear that some of the ideas upon which the above conclusion was based were incorrect. To begin with, much of the energy to transport sediment comes from the turbulence which itself results from the expenditure of energy in overcoming the friction. Therefore, this energy of turbulence is no longer available to overcome friction, and the fact that some of it is used to transport sediment should not necessarily affect the dissipation of the main energy head. Apparently it was not recognized that the friction or roughness factor of sediment-bearing streams varies widely with load and flow rate, and that because of this the mean velocity can vary even without a change in energy gradient or depth.

The energy concept held by the hydraulicians of the last century, and the deductions resulting from it, were so firmly established that they influenced the thinking of many workers of that era, and some vestiges of the ideas are to be found even in relatively recent literature. It appears from his early publications that G. K. Gilbert (1, 2)* adhered firmly to

*Numbers in parentheses refer to list of references at end of report.

this concept. This, no doubt, had an important influence in the thinking of his time because of the excellent reputation he had rightfully earned in his active and productive career. Latham, in 1886 (3), reported that observations of a storm sewer four feet in diameter in Croydon, England, over a period of years showed that the mean velocity for a given water depth was always greater when the water was clear than when it was turbid. He concluded that the retardation of the turbid water was due to the load of sediment it was carrying. Hooker (2, p. 288) in commenting on Latham's conclusions, noted that Gilbert also reached the same conclusion. Hooker also went on to state, "The law of conservation of energy will not admit any other decision in this matter, though the statement has sometimes been made that such a retardation of velocity does not exist." One statement contradicting the belief that a stream at a given stage would flow faster when clear than when turbid, was made by McMath, and was included in the paper by Hooker (2, footnote p. 289). McMath (4) was apparently citing some observations of the Mississippi River which contradicted the accepted views of the time.

In his classical flume experiments in sediment transportation, Gilbert (5, p.229) expected to confirm the idea that a clear stream offers less resistance to flow than a loaded one. He selected pairs of runs from his experiments which had the same depth and slope except that one of them carried sediment and the other did not. The bed in both cases was composed of a pavement of sand grains which did not move. According to the then prevalent theory, the mean velocity of the clear flow should exceed that of the loaded flow. However, the opposite result was found in eleven of the sixteen pairs of runs selected for the comparison. The depth measurements in these runs were apparently not as reliable as desired, and it was thought that this may have introduced a systematic error into the results. Therefore Gilbert selected thirteen more sets of comparable runs, eleven of which showed higher velocity for the clear flows than for the loaded flows. However, it was also noted that the reduction in mean velocity due to sediment transport was greater for small load than for large, for gentle slopes than for steep, for low velocity than for high, and for large depths than for small. As a result of these data Gilbert was forced to admit that the theory was not supported and that there was probably some physical

law which escaped his analysis.

A valuable contribution to the resistance problem was made by Buckley (6) in his work on the Nile. He made elaborate continuous observations of slope, mean velocity and cross-sectional area at several stations on the river which showed an appreciable fluctuation of the coefficient of roughness. Typical values of these are shown in Table 1.

TABLE 1. Measurements at the Khannaq Nile Discharge Station by Buckley (6)

Date	River elev. meters	Cond. of flood	Flow rate meter^3/sec.	Sed. conc. grams/meter^3 (parts per million)	Mean vel. meter/sec
Aug.16,1920	87.54	rising	7200	1900	1.48
Sept.16,1920	87.54	falling	6400	1000	1.32

Data applying to this station on both dates:-

Cross-sectional area	4850 square meters
Slope	0.000072
Hydraulic radius	8.6 meters

These data show clearly that at the given stage the mean velocity of the river is larger on the rising than on the falling stage, while other channel characteristics remain unchanged. The reduction in mean velocity represents an increase in the Manning friction factor of 12 percent. A further pertinent point to be noted is that the sediment concentration like the velocity is higher on the rising than on the falling flood.

Figure 1 shows the measurements made by Buckley (6) in 1921 at Beleida Station on the Nile, which is about 28 miles upstream from Cairo and about 40 miles upstream from the Delta Barrage or diversion dam which diverts water to the canals of the delta system. The variation in slope shown is due to the change in level of the water at the Delta Barrage required to feed the canals. The value of Kutter's roughness coefficient is seen to decrease appreciably as the discharge and mean velocity increase. For example, the following extreme values are obtained from Fig. 1:

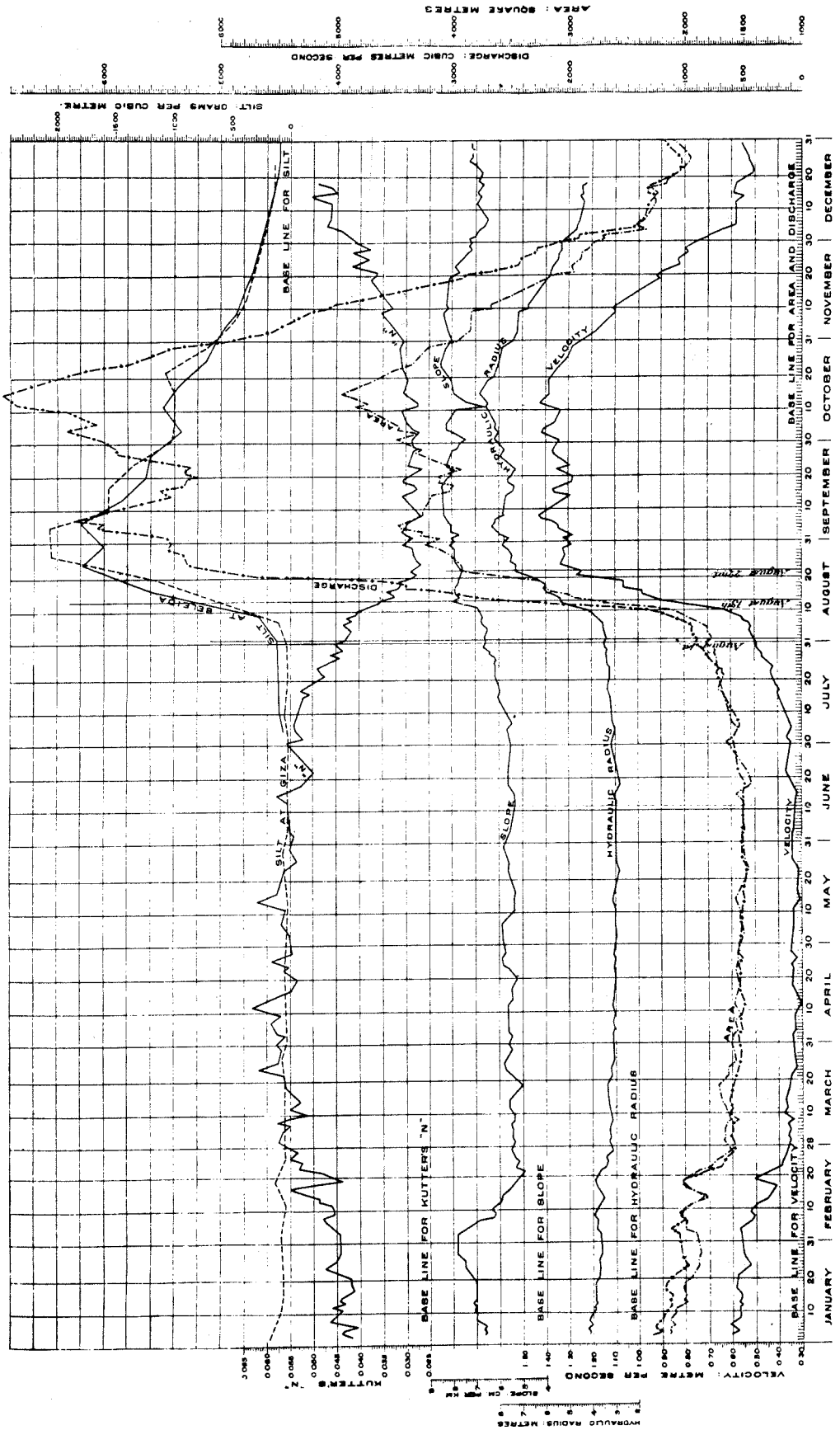

Fig. 1. Measurements on the Nile River at Beleida, reported by Buckley (6).

	April 12, 1921	Sept. 8, 1921
Discharge, cu. meters/sec	500	6200
Kutter "n"	.063	.027
Hydraulic radius, meters	3.1	7.8

Such great reduction in channel roughness during the flood must have been due primarily to smoothing out of dunes and bars on the river bed, with the damping effect of the suspended sediment being secondary, as will be seen from the laboratory experiments described in later chapters.

In discussing Buckley's paper (6, p. 231), Lacey pointed out that in the report of the Indus River Commission covering the period 1906 to 1910, it was stated that the velocity and discharge for a rising river were higher than for a falling river for the same stage, and the reverse was true for the water cross section of the stream.

Kantlack (6, p. 265) cited evidence which disagreed with that obtained by Buckley. He called attention to the result of research on rivers by Swiss and French engineers which showed that the stream velocity was decreased in every case as the sediment concentration increased. According to Kantlack, this had been demonstrated prior to 1870. He also stated that in his experience in the Punjab Canal system of India there was never an excess of flow during the time of high sediment load, as would be expected from Buckley's findings on the Nile and as was reported by other workers in India.

In the opening paragraph of his paper Buckley also called attention to some laboratory work by Duponchel which showed that a sediment load tended to increase the mean valocity of flow.

B. Recent Studies of the Resistance Problem

Interest in the resistance problem in the past two or three decades has been stimulated by both laboratory and field studies of the sediment problem. One of the main objectives of research in sedimentation is to develop a theory which will enable one to predict the sediment load of a stream as a function of the water discharge and other pertinent variables. Once the discharge is given it is necessary to calculate the flow velocity and depth, which requires that one know the roughness coefficient of the

channel. Thus the need for knowledge of the resistance problem arises naturally in dealing with sedimentation problems.

Flume experiments by Vanoni (7, 8) on transportation of suspended load showed that a flow with suspended load had a smaller friction factor than a clear water flow of the same depth in the same channel, with fixed artificially roughened bed in both cases. These experiments were made first with clear water and then with various small amounts of sand, so that the sediment load was controlled. Experiments by Ismail (8) in a rectangular pipe showed a decrease in friction factor in some cases but the opposite trend in others, thus duplicating the conflicting results reported by field observers. The apparent paradox was probably due to the fact that in some runs the bed became roughened with small dunes, making the roughness increase instead of decrease when sediment was added to the system.

Figure 2 shows graphs of velocity profiles measured by Vanoni (8) at the center of a flume for two flows of the same slope and depth, one with clear water and the other with a mean sediment concentration of 15.8 grams per liter of 0.1 mm sediment. It is clear that the sediment-laden flow which has the higher velocity has the lower friction factor. Figure 2b, in which the relative distance up from the bed is plotted on a logarithmic scale, shows that the velocity profile follows the von Karman logarithmic law. For two-dimensional flow, profiles can be expressed by

$$u = \bar{u} + \frac{1}{k}\sqrt{\frac{\tau_o}{\rho}} + \frac{2.3}{k}\sqrt{\frac{\tau_o}{\rho}}\ \log_{10}\frac{y}{d} \qquad (1)$$

where u is the point velocity at a distance y up from the bed, $\bar{u}$ is the mean velocity at the profile, τ_o is the shear stress at the bed, ρ is the mass density of the fluid, d is the flow depth, and k is the von Karman constant. From Eq. 1 one can write,

$$u_2 - u_1 = \frac{2.3}{k}\sqrt{\frac{\tau_o}{\rho}}\ \log_{10}\frac{y_2}{y_1} \qquad (2)$$

where u_1 and u_2 are the velocities at levels y_1 and y_2, respectively. Since τ_o can be calculated from the measured slope and depth, one can calculate k from a pair of points on the velocity profile by Eq. 2. The

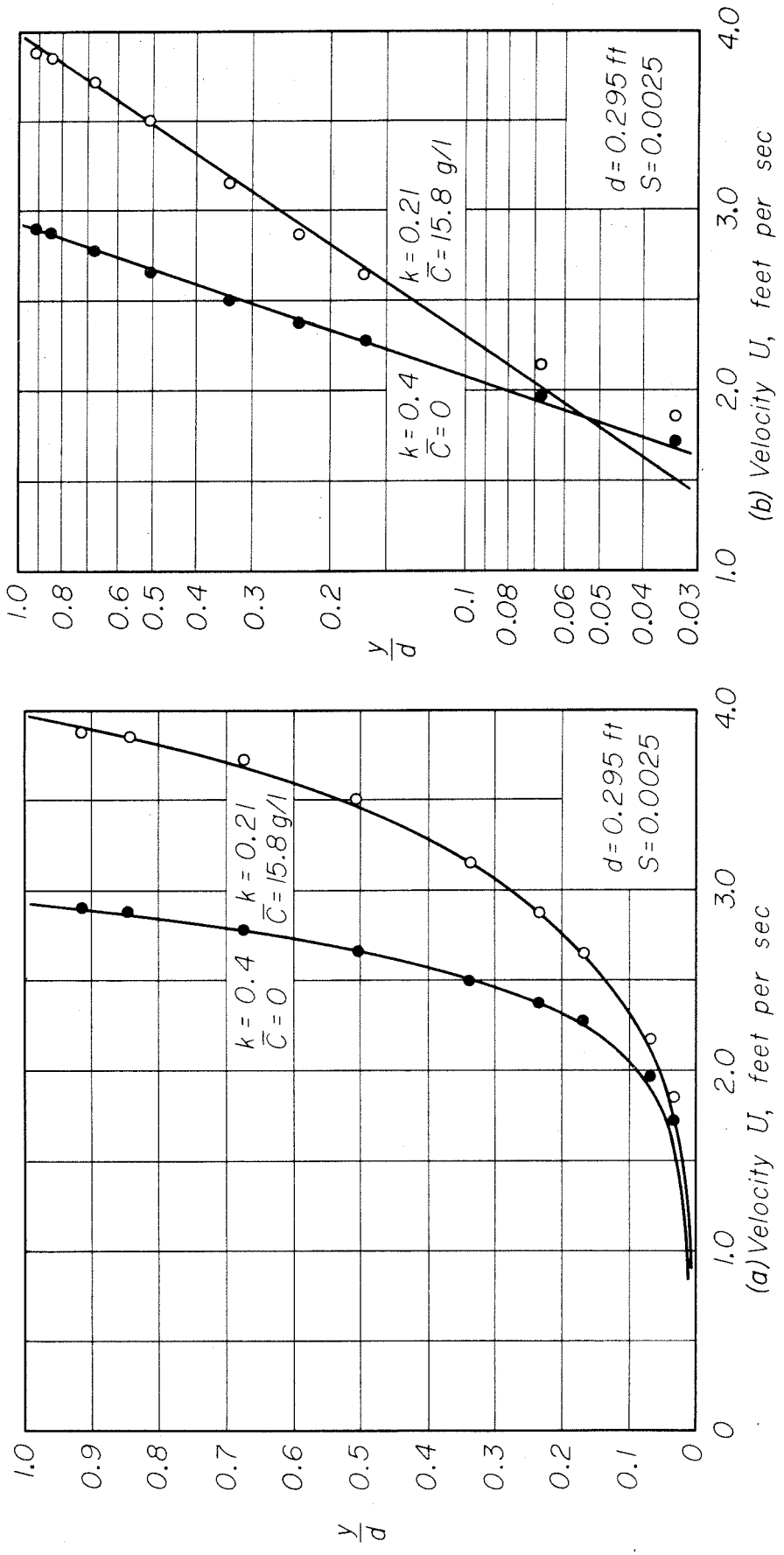

Fig. 2. Linear and semi-logarithmic graphs of velocity profiles in a flow 0.295 feet deep and 33.5 inches wide with clear water and with a heavy suspended load of 0.1 mm sand.

effect of the suspended sediment in reducing k, as indicated by Fig. 2, is a general one which occurs at all times (8) in the laboratory as well as in the field.

Recent experiments by Brooks (9) demonstrated clearly how the friction factor is affected by the dunes which develop on the sand bed of a stream. He obtained friction factors for dune-covered beds which were as much as seven times as large as for flat sand beds of the same material. Studies by Ali and Albertson (10), and Barton and Lin (11) also showed clearly the importance of dunes on the channel roughness.

Recent studies of rivers have contributed appreciably to the understanding of the resistance problem. Leopold and Maddock (12) presented detailed observations of streams which show that at a given discharge high sediment loads are associated with high mean velocities and low water depths. This means that high loads are also accompanied by low friction factors, as was found on the Indus River system by Lacey (6) over thirty-five years ago.

Eden (13) made a study of Manning's roughness coefficient "n" as a function of river stage for the lower Mississippi River. He found that n varied from about 0.040 at low stages to about 0.030 or less at flood stages. Carey and Keller (14) have recently investigated the bed configuration of the bed of the lower Mississippi River by means of a sonic fathometer and found that sand waves were present at all times and that the largest waves were formed at the highest flow rates. They concluded that these waves must be a major factor in determining the friction coefficient of the river, although they were unable to measure it during their investigations. The fact that a loop exists in the rating curve of the river was explained, at least partially, by a lag in the adjustment of the sand waves to the flow, i.e., during the rising flood the waves are growing and hence have a smaller resistance than they do at the same flow rate during the receding flood when the sand waves are diminishing.

Harrison (15) presented data on the Missouri River near Fort Randall which showed that the Manning roughness coefficient diminished with increase in discharge. The minimum roughness coefficient obtained by him was about equal to that which would be expected by a sand roughness equal to the sand grain size, so it seemed reasonable to conclude that dunes

existed on the bed at lower discharges.

As explained in greater detail in Chapter VI, Sec. C, Einstein and Barbarossa (16) divide the total resistance to flow into two parts, one due to the sand grain roughness and the other due to the sand bars and dunes. Large values of the latter component of resistance have been found to occur at low flow rates or stages where, according to the findings of Eden (13) and Harrison (15), the friction factor is the highest, thus indicating that the effect of sand dunes is largest in this region, as was found by laboratory experiments (9) and (11).

III. APPARATUS

The experiments described in Chapters V and VII were carried out in two laboratory flumes, one being 10.5 inches wide and 40 feet long, the other being 33.5 inches wide and 60 feet long. Both of these flumes are of the closed circuit type; that is, the flow of water and sediment was recirculated continuously during the runs. Consequently, no sand-feeding apparatus was needed. Sections A and B, below, describe in more detail the two flumes which were used.

A. 10.5-Inch Flume

The 10.5-inch flume is shown schematically in Fig. 3. It is equipped with an axial-flow pump with a variable speed drive, venturi meter, transparent section in the return pipe, and electric immersion heaters to control the temperature of the water. At the entrance to the flume section there is an adjustable diffuser, and one or more coarse screens (4- to 16-mesh per inch) to improve the inlet condition. The flume is made of hot rolled steel and the interior of the flume itself is painted with a smooth bitumastic paint. Along the top of the channel are mounted steel rails and a movable instrument carriage which can measure vertical elevations relative to the flume to the nearest 0.001 foot. The entire flume is mounted on a truss, the slope of which can be easily adjusted even during the course of a run. There is no end-gate or weir needed inasmuch as the amount of water in the flume and the speed of the pump are adjusted to give a level in the forebay over the pump which does not produce either backwater or drawdown. Although

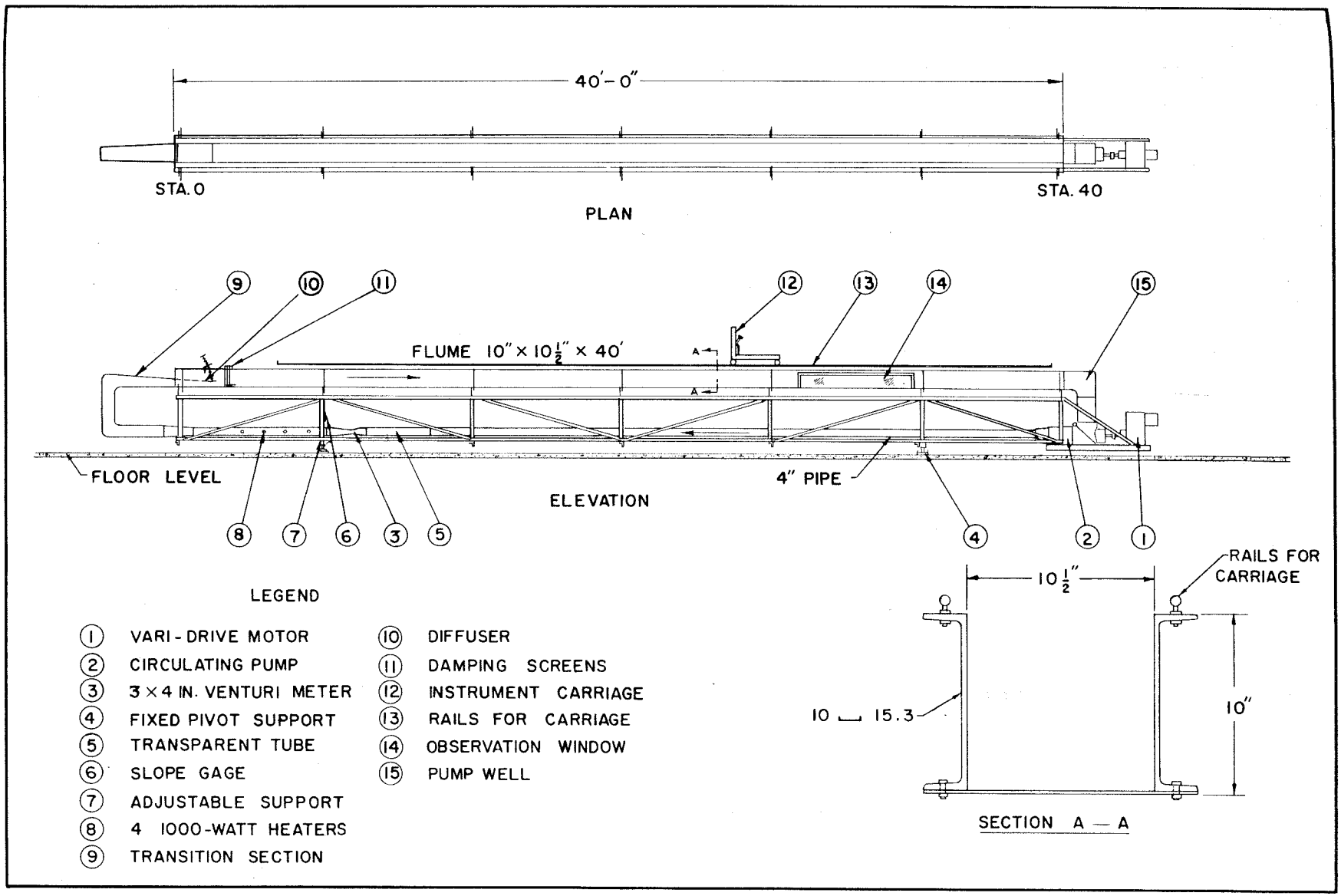

Fig. 3. Schematic diagram of 10.5-inch flume.

the channel itself is ten inches deep, experiments were made with depths of flow less than four inches to avoid excessive wall effects on the velocity and shear distribution of the flow.

During the period of this contract no significant modifications of this flume were undertaken.

B. 33.5-Inch Flume

The features described above for the 10.5-inch flume proved so successful that modifications were made in the 33.5-inch flume to provide essentially the same facilities. The 33.5-inch flume was originally built in 1937, and a description of it has been given by Vanoni (7). The major drawback of the flume as it existed was the difficulty in changing the slope, because it was supported on a system of jacks, while the motor, pump and return piping were fixed. Thus a change in the slope required a careful readjustment of a number of jacks with the loosening and retightening of two joints in the flow circuit. Hence, at the initiation of the contract it was decided to build a truss for this flume which would support not only the flume itself, but all of the appurtenances, and that this truss would be supported on only two supports, making the adjustment of slope possible during the progress of a run. It has been found in the 10.5-inch flume that it is very difficult and time-consuming to predetermine the slope and try to set the discharge or depth to match when working with a movable bed of sand. Experiments were greatly facilitated by setting the desired depth and discharge first and then making the final adjustment in the slope as required to give uniform flow.

Progress in installation of the new trusses for the 33.5-inch flume is shown in Figs. 4, 5 and 6. The new jacking system at the movable support is illustrated in Fig. 7. A schematic diagram of the reconstructed flume is shown in Fig. 8. Additional modifications included the installation of adjustable steel rails and the construction of an instrument carriage. The size of the return pipe was also reduced from ten inches to eight inches to increase the velocities and reduce the possibility of deposition at low rates of flow. Furthermore, the artificial bed roughness previously used by Vanoni (7) was removed for the current series of tests. During the period of this contract a temperature control system was designed, but has not been built.

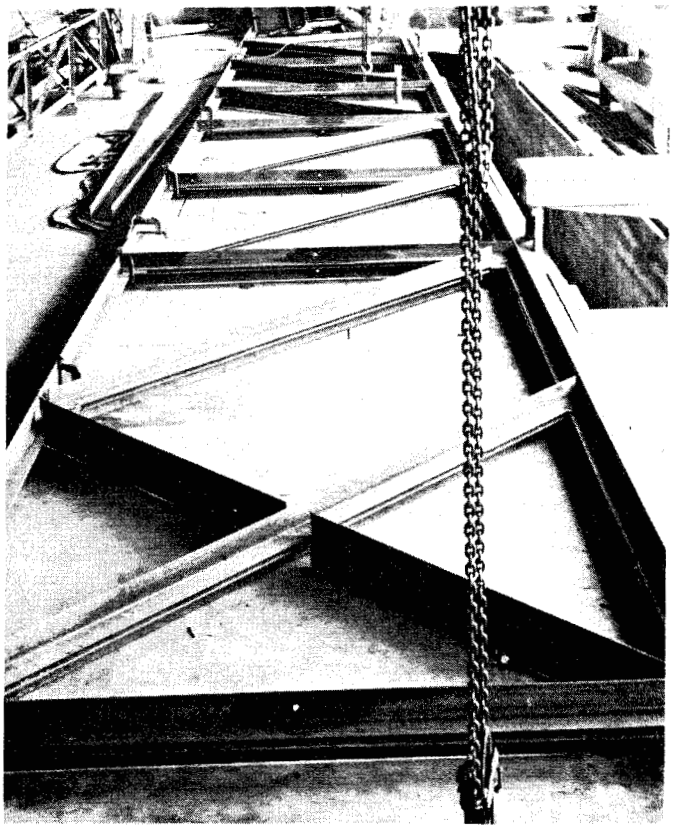

Fig. 4. Trusses for 33.5-inch flume during fabrication.

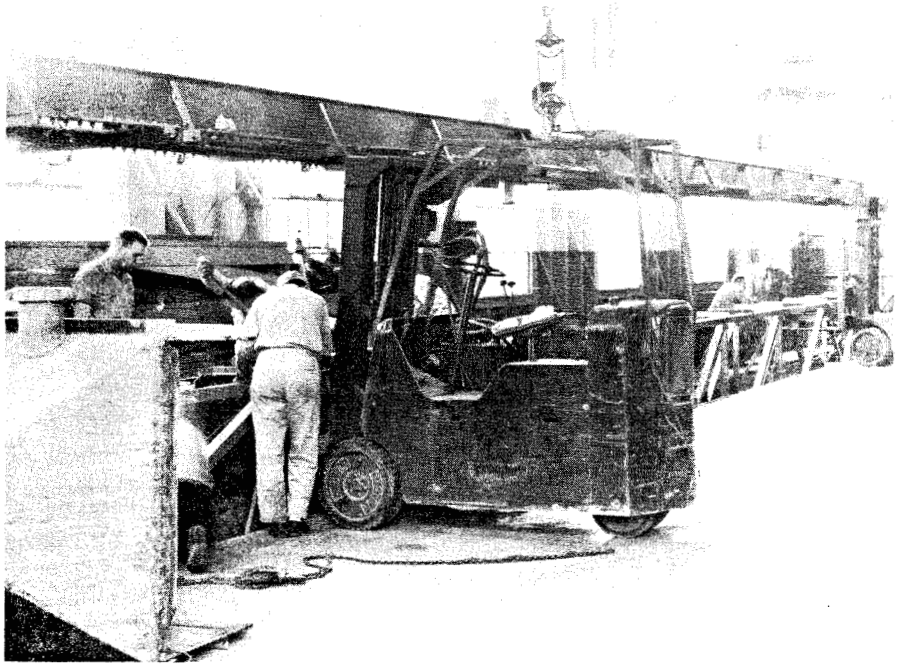

Fig. 5. Lowering trusses into place under 33.5-inch flume.

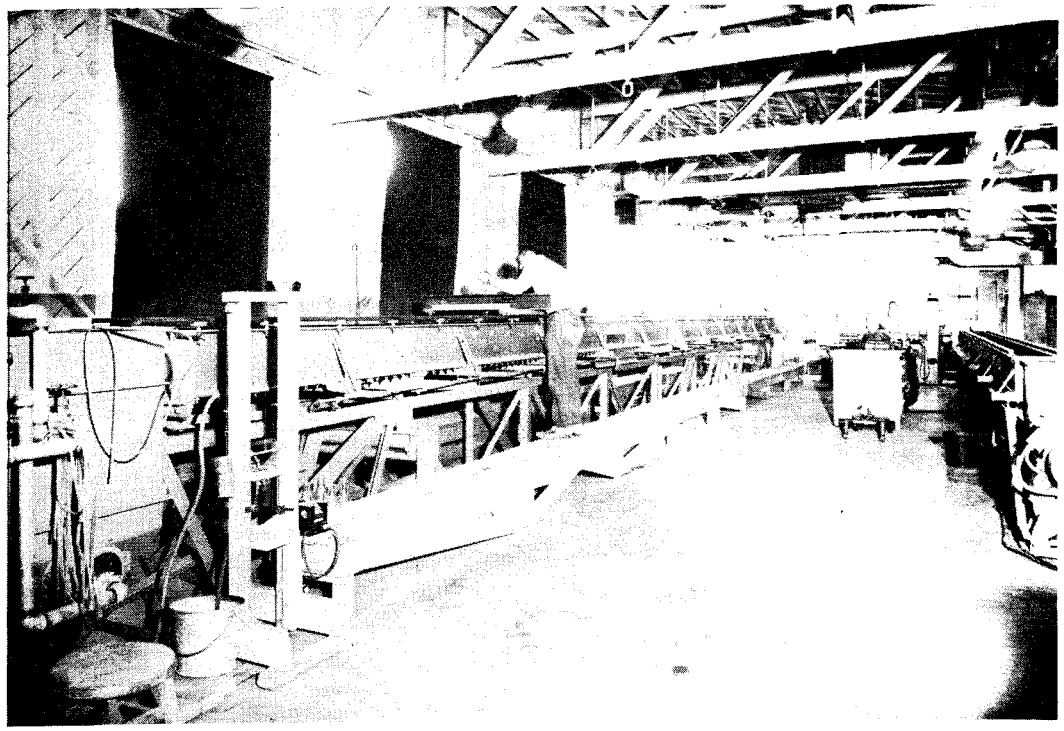

Fig. 6. View of 33.5-inch flume after completion of modifications. Note 10.5-inch flume at far right.

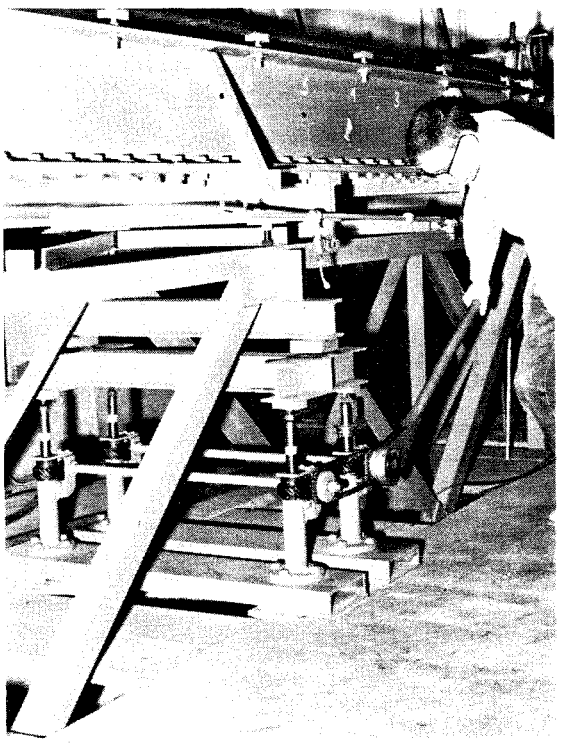

Fig. 7. Jacking system for 33.5-inch flume.

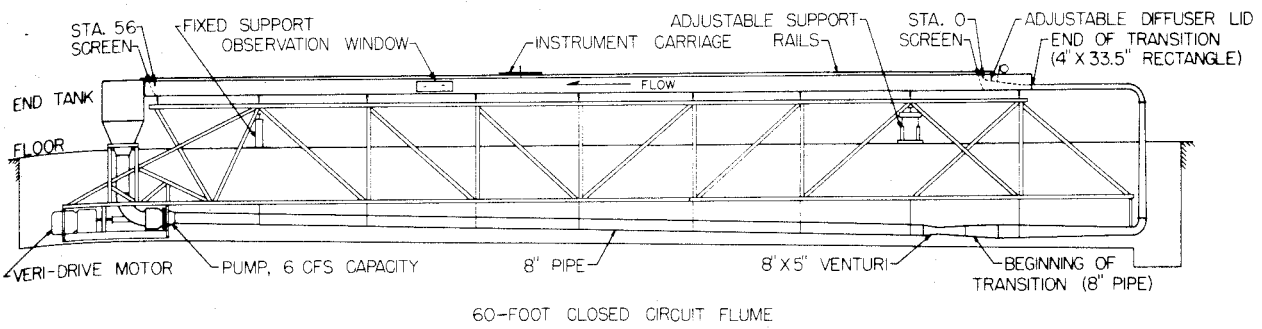

(a) Elevation

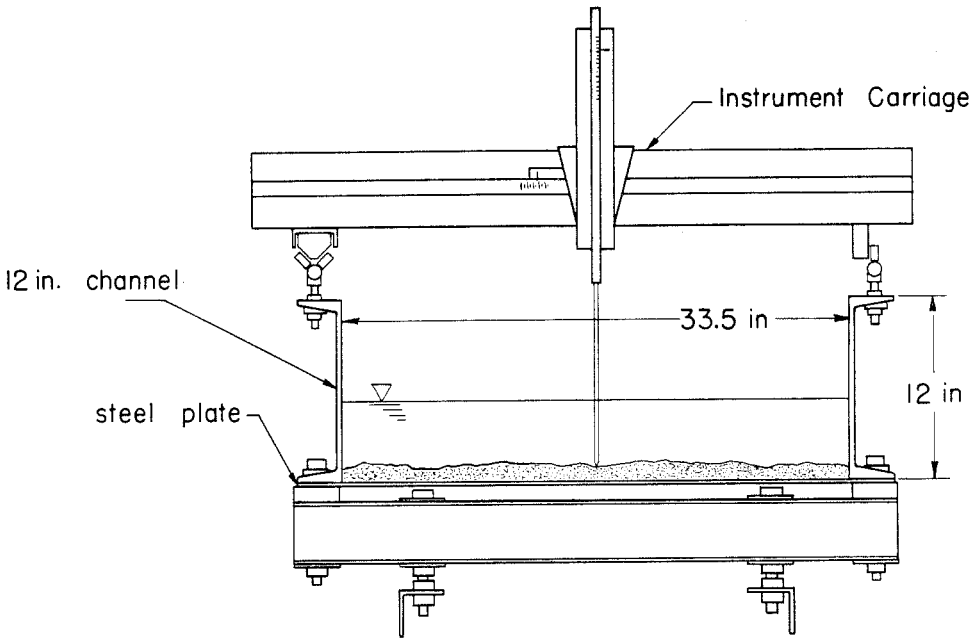

(b) Cross section of flume

Fig. 8. Schematic diagram of 33.5-inch flume after modifications.

With the modifications described above, the 33.5-inch flume proved to be an extremely valuable research tool for studies of the kind reported in this report.

C. Sediment Samplers

For the runs reported herein, only the total sediment discharge was measured. In both flumes samples were withdrawn from a vertical section of pipe at the end of the flume above the pump. The samplers used to accomplish this are shown in Figs. 9 and 10. They were designed to convey the sample from sampling point to bottle at high enough velocity to prevent any sand storage in the sampler. For the wide range of discharges possible in the 33.5-inch flume, it was necessary to build three samplers, as shown, in order to operate the samplers by means of a simple siphon. Each sample was drawn into the upturned intakes of the sampler at the same velocity that the water flowed downward in the pipe; then the sample was conveyed upward to the surface, over the side of the flume, and down into a sample bottle. The head on the siphon was adjustable so that the correct rate of flow was easily obtainable. A summary of the operating characteristics of the samplers is given in Table 2.

TABLE 2

Operating Characteristics of Total Load Samplers

Flume width, inches		33.5			10.5
Sampler		A	B	C	
No. of intakes		4	3	2	1
Flume discharge, Q:	Min.	0.48	0.98	1.8	0.17
	Max.	1.04	2.2	4.4	0.58
Time required to collect 1 liter sample, seconds:	Max.*	99	74	53	205
	Min.*	45	33	22	60

*Maximum time corresponds to minimum Q, and vice versa.

At the locations where the samples were taken, the settling velocity was always small compared with the downward water velocity, and it is

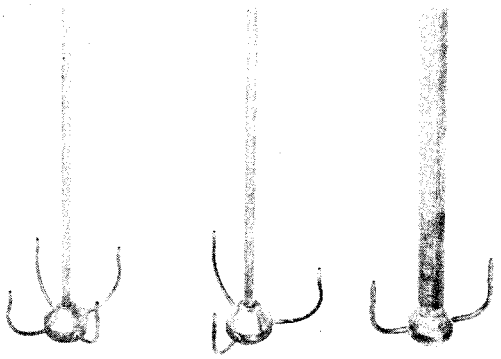

Fig. 9. View of total load samplers for 33.5-inch flume. (Flow is downward at sampling point.)

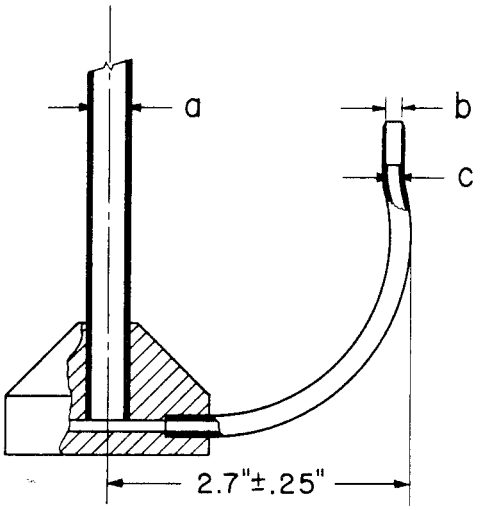

Flume width	Sampler	Dimensions			No of inlets
		a in.	b in.	c in.	
33.5 in.	A	0.305	0.136	0.089	4
	B	0.353	0.129	0.129	3
	C	0.416	0.136	0.194	2
10.5 in.	-	0.188	0.312	0.188	1*

*No manifold - simple bent tube

Fig. 10. Diagram of typical sampler.

believed that the sediment concentration at the cross section sampled was fairly uniform; nevertheless, the samplers are moved around laterally in a gentle fashion to insure getting representative samples.

Sediment samples in the flume cross section were taken by siphoning groups of three to six samples of one liter each from the flume at various positions. The sampler which was mounted on the instrument carriage was made from a brass tube of 3/16-inch outside diameter with the open end facing upstream. The end was flattened to inside dimensions of 0.040 inch by 0.217 inch, with the short dimension vertical. The velocity at the sampler tube was made the same as the local flow velocity by adjusting the head on the syphon. Concentration profiles were determined only for some of the runs under "Special Studies" (Chapter VII).

D. Instrument Carriage

The instrument carriage built for the 33.5-inch flume is shown in Fig. 11. It runs longitudinally along the flume on rails and the instrument can be run either up or down and crosswise with the carriage in any position. Thus with a point gage, pitot tube or point sampler it is possible to reach any position in the flume. There is a similar carriage for the 10.5-inch flume which is not shown in the figure.

For both flumes, photographs of the sand bed configurations were taken with a camera mounted on a stand which slid on the rails. Without any delay for aiming or focusing the camera, excellent photographs of the bed configuration at any place in the flume could be easily taken at any time. The photographs were all taken on 5 x 7-inch negatives. For the 33.5-inch flume the film showed the full width of the flume and about 50 inches along the flume; for the 10.5-inch flume the film covers the full width and about 18 inches along the flume. In all cases, photographs were taken without draining the water from the flume, but the flow of water was usually stopped to make the bed more visible. The turbidity of the water was controlled by careful washing of the sand and frequent changes of the water.

E. Bed-Levelers

In order to determine mean bed elevations and mean depths, it was necessary to have a device to level off the dunes generated by the flowing

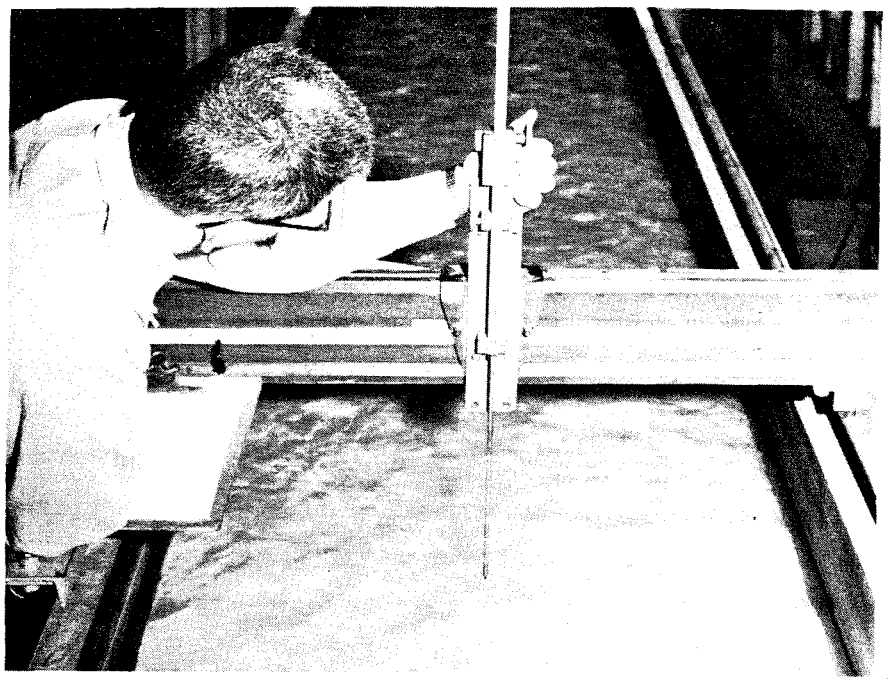

Fig. 11. View of instrument carriage for 33.5-inch flume.

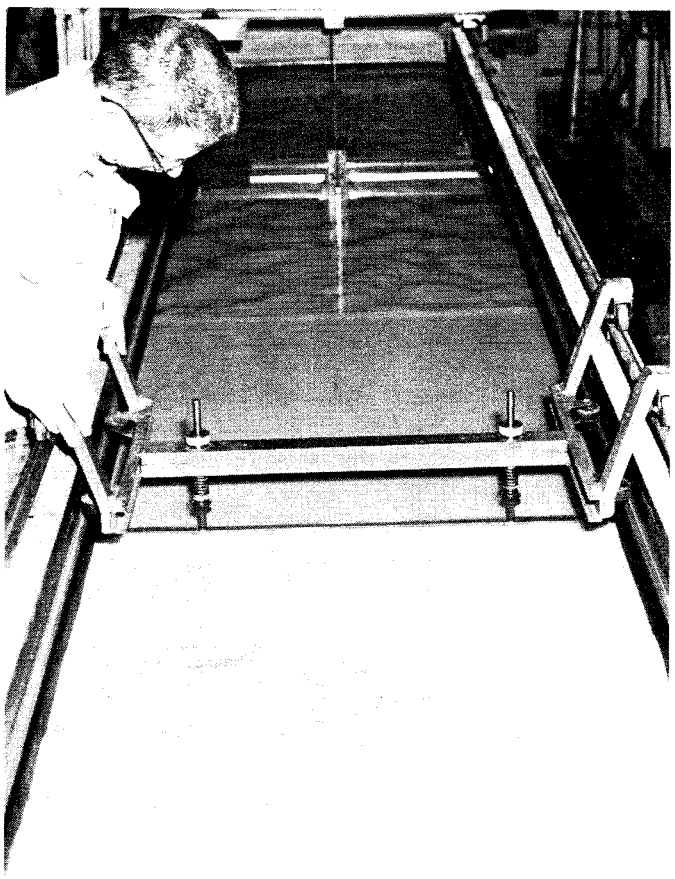

Fig. 12. View of bed-leveler for 33.5-inch flume.

water. The bed-leveler built for the 33.5-inch flume is shown in operation in Fig. 12. By working this leveler back and forth in short reaches of two to four feet, the sand that is originally in that reach is replaced in the same reach but with a plane surface. The elevation of this surface, or the mean bed elevation, is then easily determined with the point gage. A similar bed leveler was used for the 10.5-inch flume.

F. Operating Ranges of the Flumes

Each flume has various limitations in its operation. For example, there is a maximum discharge determined by the capacity of the pump and a minimum discharge governed by the minimum permissible velocity in the return pipe to prevent significant deposition of sand. Depths are restricted somewhat by the inlet arrangement and the ratio of width to depth which is tolerable for experiments. The slopes are restricted by the design of the equipment. The possible range for all these quantities for each of the two flumes is summarized in Table 3.

TABLE 3

Operating Characteristics of Experimental Flumes

Flume width, inches		10.5	33.5
Width, feet		0.875	2.79
Length, feet		40	60
Maximum feasible depth, feet		0.30	0.60
Discharge Q, cfs:	Min.	0.17	0.5
	Max.	0.60	5.7
Discharge per unit width, q, cfs/ft:	Min.	0.195	0.18
	Max.	0.69	2.05
Maximum slope		0.008	0.017

IV. PROCEDURE

Several series of runs were made in the two flumes. In each run a particular uniform flow was established which became stably adjusted with its bed and remained so during a period of several hours during which the run was made. The actual performance of an individual run often required several working days to cover all the necessary trial runs, test for stability, make the final run and take and reduce the necessary measurements.

The following sections of the chapter will describe briefly the procedure for the individual measurements. Some of the less important procedural problems are passed over here because they are discussed in greater detail by the writers elsewhere (17, 18).

A. Discharge

In both flumes the discharge was measured with a venturi meter connected to an air-water or water-mercury differential manometer. Both meters had smoothly curving walls and diffusers with slide slopes of 1 to 20 (or a total included angle of about 6°). The coefficients for the venturi meters were determined by testing in a volumetric tank setup, over a range of Reynolds numbers. The error in the discharge measurement is believed to be less than 0.5 percent, because of the good location of the meters in the flow circuits, and good calibrations.

B. Depth

The mean depth was defined as the average difference between the water surface and bed elevation in that part of the flume in which the flow was uniform. In other words, those portions of the flume which were disturbed by the inlet or outlet are excluded from determinations of the mean depth.

The water surface elevations were measured to the nearest 0.001 or 0.0005 ft with a point gage mounted on a movable carriage. Readings were usually taken every four feet over the entire length of the flume and were plotted to give a water surface profile relative to the plane of reference established by the rails on which the carriage moves. An example of such a water surface profile is given in Fig. 13 for Run 2-1.

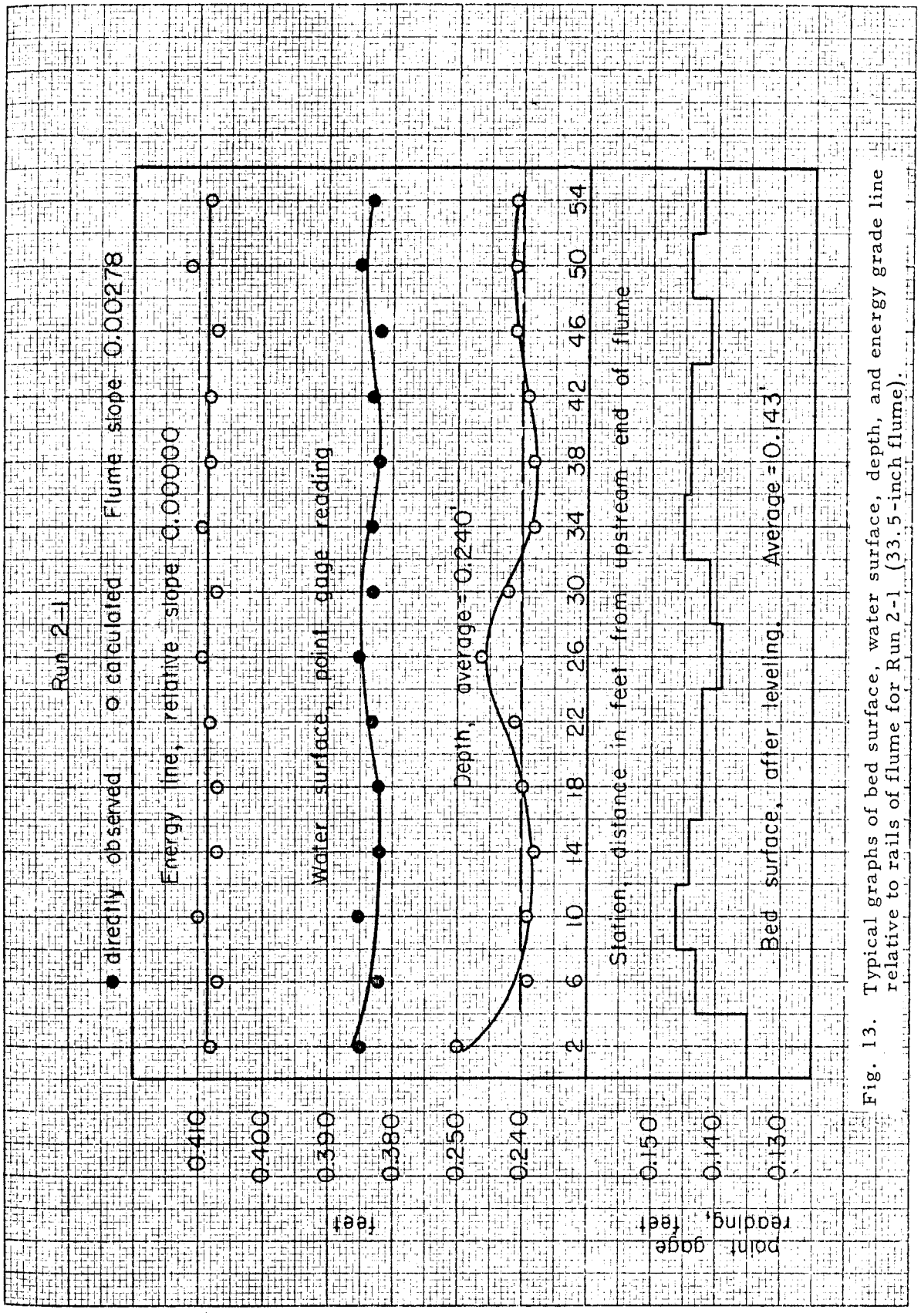

Fig. 13. Typical graphs of bed surface, water surface, depth, and energy grade line relative to rails of flume for Run 2-1 (33.5-inch flume).

It was found that the simplest test of stability for a run was the measurement of the water surface profile at relatively frequent intervals (one-half hour to one hour). Unless the velocity is very low, a significant change in the bed elevation is directly reflected in a change in the water surface profile. For tranquil flow the water surface will rise slightly if the bottom elevation drops relative to the flume. Knowing this, the usual procedure was to start the flume at some predetermined value of the discharge with a fixed amount of water, run the flume for several hours taking intermittent surface profiles, and when the surface profile had stopped changing and had stayed constant for an hour or two the flow was then stopped and the bed leveled with the specially built bed-leveler in reaches of four feet. Once leveled, the bed elevation was then determined with the point gage for each reach, and a bed profile could be plotted as shown for Run 2-1 in Fig. 13. The profile is not, of course, a true profile of the bed, but a profile of the average values by 4-foot sections.

From these two profiles(for the water surface and bed), the depth curve is plotted as the difference. In Run 2-1 (Fig. 13) the depth appears to be uniform with only random fluctuations from station 6 to station 54. When studying Fig. 13 it is well to keep in mind the extreme exaggeration; the vertical scale is magnified to four times actual, while the horizontal scale is reduced by a factor of ninety-six from actual. It is interesting to note that the average elevation of the sand bed varies only from 0.139 to 0.146 ft, a variation of only slightly more than 1/16 inch.

Since the pointgage is adjusted to read approximately 0.000 ft on the bed of the flume, the average thickness of the sand bed was about 0.14 ft or 1.75 in. The bed remained completely covered everywhere in the flume for all the runs with rare exceptions.

C. Slope

With the water surface profile and the depths established as indicated in the foregoing section, it was possible to calculate the mean velocities and add the corresponding velocity heads to the water surface profile to obtain an energy grade line. This is illustrated for Run 2-1 in Fig. 13. However, it should be noted that, since the coordinate system of the point gage

is relative to the flume, the calculated energy slope is also relative to the flume. If the slope of the flume is properly adjusted the relative slope becomes zero, as it did in the case illustrated in Fig. 13. Otherwise, the small relative slope measured from the graph (usually less than 0.0001) is added to the slope which is read from the gage on the movable support of the truss. Inasmuch as slope is one of the most difficult quantities to measure, frequent checks were made of the slope gage, and the slight differential truss deflections of the order of $\pm$ 0.001 ft were determined and corrected for by taking point gage readings of the perfectly still water surface in the 33.5-inch flume. With these precautions, it is believed that the probable error in the values of the slope does not exceed 0.00002 for the 33.5-inch flume and 0.00005 for the 10.5-inch flume.

For each trial the depth and slope were determined as explained above. The amount of water in the flume was then adjusted to produce the desired depth, if different from the observed depth, and the slope of the flume was adjusted to conform to the slope of the energy grade line. The flume was then started again, and the dunes which were erased by the bed-leveler were again generated. This process was repeated until stable, uniform flow was obtained.

D. Velocity Profiles

For a few of the runs, vertical velocity profiles were measured. A 3/16-inch Prandtl pitot tube connected to an air-water manometer was used in the 10.5-inch flume. A 1/4-inch Prandtl pitot tube was used in the 33.5-inch flume.

To determine the von Karman constant k, the measured velocities on the centerline were plotted on semi-logarithmic graph paper and fitted with a straight line which represents von Karman's logarithmic law, as given in Eqs. (1) or (2). If m is the slope of the line in units of velocity per cycle of 10, then the von Karman constant at the centerline (k_{cl}) is simply:

$$k_{cl} = \frac{2.30\, u_{*cl}}{m}, \qquad (3)$$

where u_{*cl} is the shear velocity ($\sqrt{\tau_o/\rho}$) at the centerline. Recognizing that the shear stress is variable around the boundary of a rectangular open channel, the mean shear was not used as the basis for the calculation of k.

From the velocity profile the mean velocity ($\bar{u}_{cl}$) was first determined, and then u_{*cl} was computed by the relation

$$u_{*cl} = \sqrt{\frac{f}{8}}\,\bar{u}_{cl}\,, \tag{4}$$

considering that the flow in the central portion is essentially two dimensional. The value of u_{*cl} thus computed is almost always slightly less than $\sqrt{gdS}$, the shear velocity for two-dimensional flow; however, if the former happens to exceed the latter, then $\sqrt{gdS}$ is used for u_{*cl}.

E. Sediment Discharge

In the current series of experiments the total sediment discharge was measured. The samples were withdrawn from the downward-flow pipe at the end of the flume with samplers which are described and illustrated in Chapter III, Section C, above. One liter samples were withdrawn in groups of three or four, with the groups being spaced one or several hours apart. The time required to withdraw a one-liter sample was usually of the order of one to two minutes. By taking the samples in this grouping it was possible to get information on the short-term fluctuation of the sediment load from minute to minute, and also the long-range variation from hour to hour. The latter variation was usually greater than the former.

The samples thus obtained were filtered and the sand was then dried and weighed. For simplicity, the concentrations are all given in grams per liter of suspension. The probable error in the measured average concentration is generally of the order of two to three percent. Individual samples, of course, are subject to considerably larger error. The main difficulty is not in the processing of the samples, but in the procurement of truly representative samples from a flow in which the sediment is surely not uniformly distributed owing to the turbulence. Nevertheless, since the over-all variations in the concentration from run to run are of several orders of magnitude, an error of five or even ten percent is not of great importance.

The samples were taken in such a way that bed load is included with the suspended load. No attempt was made to separate the two, although it appears from visual observations for most of the runs that the suspended-load discharge was far greater than the bed-load discharge. Only for those

runs at the lowest velocities did it appear that the bed-load discharge amounted to as much as the suspended load discharge.*

The concentration measured as described above will hereinafter be called the sediment discharge concentration, $\overline{C}$. If $\overline{C}$ in lbs per cu ft is multiplied by the water discharge, Q in cu ft/sec, the amount of sediment discharge in lbs per sec is obtained. Because of the variation of the velocity and concentration with depth in the flume section, this sediment discharge concentration is not identical to the mean concentration in the vertical in the open channel section.

Only a few concentration profiles were measured in the flume during this experimental program. The problem of obtaining good representative values of the concentration close to a dune-covered bed has not yet been resolved. It is hoped that future research can be directed toward the problem of measuring concentration profiles for runs with dunes.

F. Inlet and Outlet

It was found by trial and error that the inlet condition could be improved by the use of one or several screens ranging from four meshes to sixteen meshes per inch. The improvement was manifested by the adjustment to uniform flow conditions (as described in the foregoing section) nearer to the inlet; in other words, the depth of water and the depth of the sand bed reached their equilibrium values sooner. Presumably the screen has the effect of damping out some of the large scale turbulence generated in the elbows (in spite of the vanes) and making a more uniform inlet velocity distribution.

At the lower discharges and lower depths the equilibrium was sometimes obtained even without the screens in distances of only four to six feet downstream from the inlet; at the other extreme, for runs using screens sometimes the inlet disturbance would be noticeable for twenty or even thirty feet in the larger flume. Because of the inlet disturbance, it is imperative to have long flumes for sediment transportation studies, and even the sixty-foot flume in use was not entirely adequate for all conditions.

---

*Note that a distinction is being made between sediment load (the material itself) and sediment discharge (the rate of transportation of the sediment load). Since the suspended load generally travels at higher velocities than the bed load, the ratio of the amount of suspended load to bed load is not the same as the ratio of the suspended load discharge to the bed load discharge.

There was little difficulty associated with the outlet except occasional slight pulsations in the water level in the forebay over the pump. A single screen at the end of the channel was found helpful in isolating the flume from this vibration. Furthermore, the downstream screen allowed the sand bed to wash uniformly over the end of the flume without sliding off in chunks which tend to make the sediment discharge measurement erratic.

G. Temperature

Several investigators have found that the temperature affects the suspended load (see Chap. VI, Sec. D). In the 10.5-inch flume the temperature was maintained at $25^{\circ} \pm 1^{\circ}C$ for all of the runs reported except those in which the temperature was purposely varied. In the 33.5-inch flume it was not possible to control the temperature because temperature control equipment has not yet been built; the experiments were conducted over a range from $16.5^{\circ}C$ to $27.4^{\circ}C$. Some of the scatter in the results for the 33.5-inch flume is certainly due to this uncontrolled temperature variation.

H. Side-wall Corrections

Laboratory streams almost inevitably have a smaller width-to-depth ratio than natural streams. The results of flume experiments cannot be expected to correspond to field experiments unless a correction for the shear on the walls is made. Moreover, as the resistance of the bed of the stream varies, the relative distribution of shear between the bed and walls of a flume also varies. Consequently, a procedure called "side-wall correction" was used in order to determine a hydraulic radius, r_b, shear velocity, U_{*b}, and friction factor, f_b, which would apply to the bed itself. Essentially the method covered by Johnson (19), employing the Darcy-Weisbach resistance equation, was used. Since the reader may not be familiar with all the details and also because some modifications in the procedure were made, a full derivation and explanation of the equations used is given in Appendix A with an example.

J. Equilibrium and Reproducibility

Before making the final measurements for a run, it was first necessary to establish uniform flow in equilibrium with its sand bed. Equilibrium as used hereafter implies (1) that the mean depth of flow stays constant over

a working section of the flume, and (2) that the pattern and distribution of sand on the bed has stopped changing. Equilibrium was achieved by adjusting the slope of the flume for given depth and discharge after one or several trial runs.

The reproducibility of the runs was found to be excellent. Those runs which were inherently stable in their equilibria could be repeated as many times as desired and with identical results. Those which appeared to be inherently unstable due to long sand waves in the system always remained so and could never be made to be stable; in fact, one might even say that the nature of the instability was reproducible. Unstable flows do not settle down to a constant water surface and bed profile regardless of how long the flume is run.

The closeness of agreement between repeated runs is well demonstrated by some of the preliminary runs for Run 2-1 performed in the 33.5-inch flume. Table 4 shows the most important measured values for trial A, trial B, and the final run. In order to obtain the full information for each trial the sand bed is leveled in sections (see Sec. B), thereby destroying the configuration that had been built up. Consequently, each run was started from essentially a flat bed. In this particular instance the establishment of equilibrium of the water surface and the bed required about two hours. The various reported values changed somewhat between trials A and B because the depth of flow was intentionally reduced about 2.5 percent to obtain the desired value of depth in trial B.*

---

*It may be noted here that it is not possible to tell exactly what depth has been achieved in a run until the final reduction of bed and water surface profiles has been made. The depth of still water in the flume gives only an approximate indication of depth, inasmuch as the mean thickness of the sand bed and its distribution in the flume and storage in several spots in the return circuit make it impossible to predetermine the depth any closer than about 0.01 foot.

TABLE 4

Example of Reproducibility of Runs

	Trial A July 25, 1956	Trial B July 27, 1956	Final Run 2-1 July 30, 1956
Q, discharge, cfs	0.845	0.854	0.855
d, depth, ft	0.248	0.242	0.240
S_f, slope of flume	0.00270	0.00284	0.00278
S, slope of energy line	0.00276	0.00278	0.00278
U, average velocity, fps	1.22	1.26	1.28
f, friction factor	0.101	0.092	0.090
T, water temperature, °C.	25.5	25.5	25.5
$\overline{C}$, sediment discharge concentration, gr/ℓ	---	1.90	1.88
Number of sediment samples	0	6	12

Note: Bed covered with dunes.

Between trial B and the final run no changes were intentional except reduction of the flume slope to match the measured energy slope of trial B. The value of the friction factor f = 0.090 for the final run, checks the value of 0.092 for trial B rather well. The difference of two percent is easily attributable to the various experimental errors. The lack of variation in the values of the water temperature is attributable more to the uniformity of the Pasadena climate on the days listed than to the skill of the operator; indeed, on each of the days the water temperature varied by about 3°C during the run, with the average being 25.5°C as listed in the table.

K. Summary of Procedure

By careful measurements and adjustments the flow in each run was made stable and could be maintained for a number of hours without significant change in characteristics, both as regards channel friction and sediment discharge except as hereinafter noted. Because both the flumes are of the closed recirculating type, there was no necessity for sand feeding, and hence no practical restrictions on the length of time taken to make a run. The detailed procedure for measuring discharge, depth, total

sediment discharge and slope are outlined in detail in the foregoing sections, along with other items of procedure. The equations for applying the sidewall correction are given in Appendix A.

It is believed that the procedures followed here are, in general, some of the most exacting procedures that have ever been used on experiments of this type. Although the experimental results do not cover an extremely wide range of variables, the investigators believe that the reader may have considerable confidence in the validity and accuracy of the data presented.

V. GENERAL STUDIES

A. Objectives

Briefly stated, the objectives of the experiments described in this chapter were as follows: (1) to study the hydraulic roughness of movable sand beds in two laboratory flumes under various flow conditions, and (2) to study the relationship of the sediment transportation rate to the hydraulic characteristics and the physical properties of the sediment for streams carrying substantial suspended loads.

Inasmuch as both of these problems are extremely complex, no quantitative solutions or usable formulas have been obtained; nevertheless, the data show many interesting qualitative relationships that greatly increase our understanding of the whole problem. Some existing theories have been analyzed, and their strong points and weaknesses demonstrated, at least on the basis of the laboratory results.

The behavior of the dunes which cause the wide variations in the channel roughness has been the subject of a simultaneous study conducted under Research Grant No. G 1709 from the National Science Foundation. Detailed measurements of the characteristics of the dunes were made under that grant for most of the same runs reported herein. However, the reader is referred to a forthcoming paper which will present this additional information (20).

B. Characteristics of Sands Used

Three new sands were used in these studies. The distribution of sieve sizes for these three sands, designated by the numbers 3, 4 and 5,

are shown graphically in Fig. 14. Sands 1 and 2, also shown in Fig. 14, were used in the earlier work by Brooks (9), as well as by Vanoni (7) and Ismail (21). The characteristics of the size distribution for all five of the sands are summarized in Table 5. Although the geometric mean sieve diameters (D_g) for Sands 3, 4 and 5 are very close to those for Sand 1, the geometric standard deviations (σ_g) are considerably larger. Values of the mean sedimentation diameter (D_s) are presented in Table 5 only for Sands 1 and 2 where σ_g is quite small. For the other sands the spread in grain sizes is so large that a mean sedimentation diameter has little meaning.

All the sands used are predominantly quartz. Sands 3 and 4 were obtained from a local foundry supply company and were not further processed except for washing. Sand 5 was a synthetic preparation designed to give a logarithmically normal size distribution with $D_g = 0.15$ mm and $\sigma_g = 1.8$. Under microscopic analysis Sand 4 was found to contain more than 99 percent quartz grains of subrounded shape. The other sands are believed to be similar in composition.

In order to get an idea of the degree of sorting taking place during the experiments, sieve analyses of the sediment load were made for most of the runs. The usual procedure was to composite all of the dried sand from the sediment discharge samples and perform one sieve analysis for the composite. Generally the sediment load was considerably finer than the bed material and usually had a higher geometric standard deviation.

C. Summary of Experimental Results

The principal data obtained in both of the flumes are summarized in Tables 6, 7, 8 and 9. With the explanations of procedure in Chapter IV and Appendix A, the tables should be entirely self-explanatory except for the column entitled "Bed Condition", which will be explained below (Sec. D.) The experiments in the 10.5-inch flume (Tables 7 and 8) were all performed by Dr. George Nomicos, and those in the 33.5-inch flume (Tables 6 and 9) by the writers.

Tables 6 and 7 give summaries of experiments with movable sand beds in the 33.5-inch and 10.5-inch flumes, respectively. The runs are arranged in the tables in order of increasing velocity for the depths and sands listed in the headings. The runs were actually performed in numerical order.

TABLE 5

Summary of Sand Size Distributions

Sand No.	D_g Geom. Mean mm	σ_g Geom. Std. Deviation	D_{35} (35% finer) mm	D_{65} (65% finer) mm	D_s Mean Sed. Diameter mm
1	0.145	1.11	0.140	0.151	0.16
2	0.088	1.17	0.084	0.094	0.10
3	0.145	1.30	0.130	0.159	-
4	0.137	1.38	0.123	0.155	-
5	0.152	1.76	0.123	0.191	-

Note: $D_g = \sqrt{D_{84} D_{16}}$; $\sigma_g = \sqrt{D_{84}/D_{16}}$

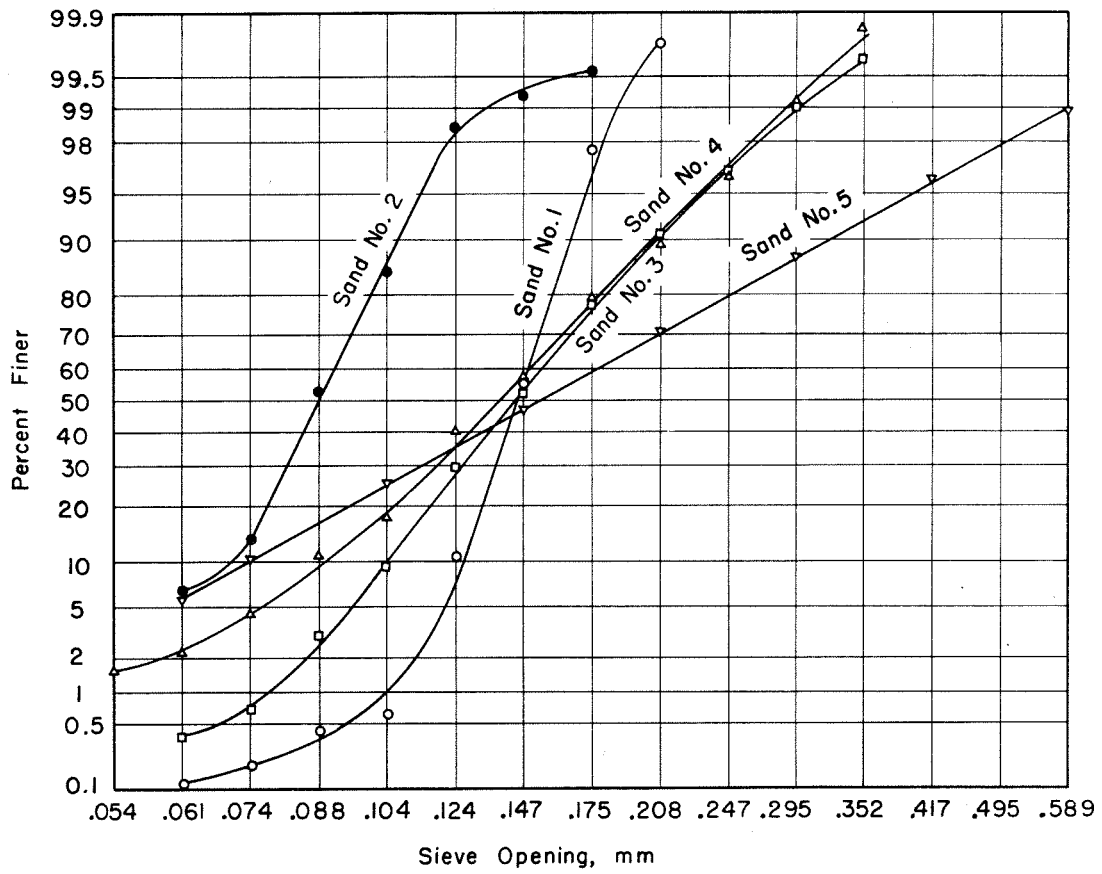

Fig. 14. Sieve analyses of the sands used in present investigation (Nos. 3, 4 and 5) compared to sands (Nos. 1 and 2) used by Brooks (9).

TABLE 6

SUMMARY OF EXPERIMENTS BY VANONI AND BROOKS IN 33.5-INCH FLUME, 1956

Sand No. 4, D_g = 0.137 mm, σ_g = 1.38

Run No.	Q Discharge cfs	d Depth ft	r Hydr. Radius ft	S Slope	U_* Shear Vel. ft/sec	U Ave. Vel. ft/sec	f Frict. Factor	T Water Temp. °C	r_b Bed Hydr. Radius ft	U_{*b} Bed Shear Vel. ft/sec	f_b Bed Frict. Factor	No. of Sed. Disch. Samples	$\bar{C}$ Sed. Disch. Conc. gr/l	G Sed. Discharge lb/min	Analysis of Sediment Load D_g mm	Analysis of Sediment Load σ_g	F Froude No.	Bed Condition	Run No.
Depth Range: 0.203-0.302 ft																			
2-9	0.510	0.238	0.203	0.00141	0.096	0.77	0.124	23.4	0.230	0.102	0.140	20	0.037	0.071	0.086	1.44	0.28	Dunes	2-9
2-3	0.615	0.243	0.207	0.00204	0.117	0.90	0.133	24.5	0.238	0.125	0.153	13	0.24	0.54	0.094	1.53	0.32	Dunes	2-3
2-8	0.715	0.240	0.205	0.00280	0.136	1.07	0.129	25.2	0.233	0.145	0.147	16	1.15	3.1	0.096	1.49	0.38	Dunes	2-8
2-1	0.855	0.240	0.205	0.00278	0.135	1.28	0.090	25.5	0.231	0.144	0.101	12	1.9	6.0	0.086	1.56	0.46	Dunes	2-1
2-7	0.930	0.237	0.203	0.00277	0.134	1.40	0.074	22.4	0.227	0.142	0.083	20	2.2	7.6	0.086	1.54	0.51	Dunes	2-7
2-6	1.00	0.249	0.211	0.00246	0.129	1.44	0.064	27.4	0.236	0.137	0.072	8	1.4	5.3	0.086	1.64	0.51	Dunes (s.w)	2-6
2-17D*	1.17	0.302	0.248	0.00201	0.127	1.39	0.067	18.9	0.284	0.136	0.077	4	2.2	9.8	0.092	1.49	0.44	Dunes (s.w)	2-17D*
2-17F*	1.17	0.203	0.177	0.00276	0.125	2.07	0.029	18.9	0.186	0.133	0.031	8	3.0	13	0.097	1.46	0.81	Flat (s.w)	2-17F*
2-2	1.38	0.233	0.200	0.00205	0.115	2.13	0.0235	23.5	0.208	0.117	0.024	22	2.5	13	0.095	1.60	0.78	Flat (s.w)	2-2
Depth Range: 0.524-0.553 ft																			
2-12	1.21	0.541	0.390	0.00039	0.070	0.80	0.061	24.6	0.488	0.078	0.076	16	0.0033	0.015	0.097	1.66	0.19	Dunes	2-12
2-5	1.54	0.528	0.383	0.00070	0.092	1.04	0.063	23.4	0.480	0.104	0.079	16	0.068	0.39	0.085	1.60	0.25	Dunes	2-5
2-10	1.87	0.549	0.394	0.00105	0.116	1.22	0.072	21.9	0.505	0.131	0.092	16	0.21	1.5	0.084	1.49	0.29	Dunes	2-10
2-11	2.23	0.536	0.387	0.00122	0.123	1.49	0.055	25.2	0.485	0.138	0.069	16	0.67	5.6	0.078	1.52	0.36	Dunes	2-11
2-13D*	2.65	0.553	0.396	0.00102	0.119	1.72	0.038	20.7	0.482	0.126	0.046	4	1.45	14	0.088	1.50	0.41	Dunes (s.w)	2-13D*
2-16F*	3.50	0.524	0.381	0.00107	0.115	2.39	0.0185	16.5	0.408	0.119	0.0195	-	-	-	-	-	0.59	Flat (s.w)	2-16F*
2-4	3.84	0.544	0.391	0.00107	0.116	2.53	0.0170	24.9	0.416	0.120	0.0180	16	1.15	16.5	0.124	1.45	0.60	Flat	2-4

* D Dune section in runs with a long sand wave.

* F Flat section in runs with a long sand wave.

s.w. Sand wave(s) in system.

TABLE 7

SUMMARY OF EXPERIMENTS BY NOMICOS IN 10.5-INCH FLUME, 1956

Run No.	Q Discharge cfs	d Depth ft	r Hydr. Radius ft	S Slope	U_* Shear Vel. ft/sec	U Ave. Vel. ft/sec	f Frict. Factor	T Water Temp. °C	r_b Bed Hydr. Radius ft	U_{*b} Bed Shear Vel. ft/sec	f_b Bed Frict. Factor	No. of Sed. Disch. Samples	$\bar{C}$ Sed. Disch. Conc. gr/l	G Sed. Discharge lb/min	Analysis of Sediment Load D_g mm	Analysis of Sediment Load σ_g	F Froude No.	Bed Condition	Run No.
Series I, Sand No. 3, D_g = 0.145 mm, σ_g = 1.30																			
A	0.435	0.241	0.156	0.0021	0.103	2.06	0.020	25.0	0.166	0.106	0.021	9	1.85	3.0	-	-	0.74	Flat	A
B	0.269	0.242	0.156	0.0027	0.116	1.27	0.068	25.0	0.187	0.136	0.092	10	1.2	1.2	-	-	0.45	Dunes	B
C	0.193	0.241	0.156	0.0021	0.103	0.91	0.101	25.0	0.218	0.121	0.141	5	0.23	0.17	-	-	0.33	Dunes	C
Series III, Sand No. 4, D_g = 0.137 mm, σ_g = 1.38																			
H-2	0.436	0.233	0.152	0.0025	0.111	2.13	0.0215	24.3	0.167	0.116	0.0235	7	2.3	3.8	0.155	1.35	0.78	Flat	H-2
H-3	0.387	0.223	0.148	0.00225	0.104	1.97	0.022	24.0	0.162	0.108	0.024	12	3.3	4.7	0.096	1.60	0.73	Flat(s.w)*	H-3
H-7	0.293	0.237	0.154	0.00275	0.117	1.41	0.054	24.1	0.199	0.133	0.071	12	2.0	2.2	0.093	1.56	0.51	Sand Wave#	H-7
H-7a	0.293	0.243	0.156	0.00275	0.118	1.38	0.059	24.6	0.210	0.136	0.078	-	-	-	-	-	0.49	Dunes	H-7a
Series II, Sand No. 5, D_g = 0.152 mm, σ_g = 1.76																			
2b	0.170	0.241	0.156	0.0020	0.100	0.80	0.124	26.0	0.220	0.119	0.175	6	0.30	0.19	0.070	1.7	0.29	Dunes	2b
2a	0.180	0.241	0.156	0.0021	0.102	0.85	0.115	25.6	0.219	0.122	0.162	6	0.59	0.40	0.072	1.9	0.31	Dunes	2a
2	0.193	0.241	0.156	0.0024	0.110	0.91	0.115	25.5	0.220	0.130	0.163	12	0.82	0.59	0.069	2.1	0.33	Dunes	2
3a	0.207	0.241	0.156	0.0026	0.114	0.98	0.108	25.0	0.219	0.136	0.153	7	1.15	0.88	0.065	1.7	0.35	Dunes	3a
3	0.219	0.241	0.156	0.00275	0.118	1.04	0.103	25.0	0.220	0.140	0.145	7	1.8	1.5	0.061	1.9	0.37	Dunes	3
4	0.253	0.241	0.156	0.0027	0.116	1.20	0.075	25.0	0.214	0.136	0.103	7	2.5	2.4	0.062	1.6	0.43	Dunes	4
5	0.292	0.241	0.156	0.0024	0.109	1.38	0.050	25.0	0.203	0.125	0.065	14	3.4	3.8	0.064	1.7	0.50	Dunes	5
6	0.327	0.241	0.156	0.00225	0.106	1.55	0.038	25.0	0.195	0.119	0.047	14	2.9	3.5	0.065	1.7	0.55	Sand Wave#	6
7	0.358	0.241	0.156	0.0021	0.102	1.69	0.029	25.0	0.185	0.112	0.035	14	3.3	4.4	0.071	1.8	0.61	Sand Wave#	7
8	0.387	0.241	0.156	0.0020	0.100	1.83	0.024	25.0	0.176	0.106	0.027	7	3.2	4.7	0.073	1.8	0.66	Flat	8
1	0.435	0.241	0.156	0.00225	0.106	2.06	0.0215	25.0	0.171	0.112	0.0235	6	3.4	5.6	0.085	2.3	0.74	Flat	1
9	0.561	0.241	0.156	0.0039	0.140	2.66	0.022	25.0	0.177	0.149	0.025	7	5.6	12	0.163	1.7	0.95	Flat	9

* Data for Run H-3 apply only to the flow over the flat section of the sand wave, which covered major part of flume.

\# Data for Runs H-7, 6, and 7 are composites for flat and dune-covered sections together.

TABLE 8

SUMMARY OF EXPERIMENTS WITH VARIABLE TEMPERATURE BY NOMICOS IN 10.5-INCH FLUME, 1956

Run No.	Q Discharge cfs	d Depth ft	r Hydr. Radius ft	S Slope	U_* Shear Velocity ft/sec	U Ave. Velocity ft/sec	f Friction Factor	T Water Temp. ^oC	r_b Bed Hydr. Radius ft	U_{*_b} Bed Shear Velocity ft/sec	f_b Bed Friction Factor	No. of Sed. Disch. Samples	$\overline{C}$ Sed. Disch. Conc. gr/ℓ	G Sed. Discharge lb/min	F Froude No.	Bed Condition
D_1	0.435	0.240	0.155	0.0024	0.110	2.07	0.022	15.3	0.170	0.115	0.025	6	3.24	5.27	0.74	Flat
A	0.435	0.241	0.156	0.0021	0.103	2.06	0.020	25.0	0.166	0.106	0.021	9	1.87	3.0	0.74	Flat
D	0.435	0.241	0.156	0.0023	0.107	2.06	0.022	25.0	0.171	0.113	0.024	6	2.14	3.48	0.74	Flat
D_2	0.435	0.242	0.156	0.0022	0.105	2.05	0.021	38.0	0.173	0.111	0.023	6	1.66	2.70	0.73	Flat
G_1	0.193	0.242	0.156	0.00235	0.108	0.91	0.114	15.0	0.229	0.129	0.162	6	0.31	0.22	0.33	Dunes
C	0.193	0.241	0.156	0.0021	0.103	0.91	0.101	25.0	0.218	0.121	0.141	5	0.23	0.17	0.33	Dunes
G	0.193	0.241	0.156	0.0021	0.103	0.91	0.101	25.0	0.218	0.122	0.142	6	0.22	0.16	0.33	Dunes
G_2	0.193	0.240	0.155	0.0019	0.097	0.92	0.090	35.6	0.216	0.115	0.126	7	0.11	0.08	0.33	Dunes

TABLE 9

SUMMARY OF EXPERIMENTS WITHOUT SEDIMENT BY VANONI AND BROOKS IN 33.5-INCH FLUME, 1956

Run. No.	Q Discharge cfs	d Depth ft	r Hydr. Radius ft	S Slope	U_* Shear Vel. ft/sec	U Ave. Vel. ft/sec	f Friction Factor	T Water Temp. ^oC	R Reynolds Number	k von Karman Universal Constant*	b/d Width-Depth Ratio	F Froude Number
1-3	0.688	0.199	0.174	0.00069	0.062	1.24	0.0202	22.2	0.84×10^5	-	14.0	0.49
1-4	1.06	0.256	0.216	0.00069	0.069	1.48	0.0174	22.8	1.26	-	10.9	0.52
1-7	1.93	0.377	0.297	0.00069	0.081	1.83	0.0157	22.0	2.10	0.345	7.4	0.52
1-1	2.52	0.450	0.340	0.00068	0.086	2.01	0.0148	25.4	2.86	-	6.2	0.53
1-2a	1.90	0.332	0.268	0.00095	0.090	2.05	0.0156	23	2.15	-	8.4	0.63
1-2b	1.92	0.333	0.269	0.00098	0.092	2.07	0.0158	21.8	2.12	0.340	8.4	0.63
1-2c	1.92	0.335	0.270	0.00093	0.090	2.06	0.0152	24.3	2.27	0.342	8.3	0.63
1-5a	4.35	0.599	0.419	0.00093	0.112	2.60	0.0148	21.2	4.14	-	4.7	0.59
1-5b	4.25	0.597	0.418	0.00092	0.111	2.61	0.0144	20.2	4.06	0.38	4.7	0.60
1-5c	4.35	0.604	0.422	0.00092	0.112	2.52	0.0158	21.8	4.10	0.40	4.6	0.57
1-6	3.64	0.248	0.210	0.00688	0.216	5.26	0.0135	24.4	4.51	0.401	11.3	1.87

* At Station 42 on center line

Detailed discussion and interpretation of these data will be deferred to the next chapter.

Table 8 gives some runs which show the effect of temperature variation in the 10.5-inch flume for Sand 3. It is easily seen that with either a flat bed or a dune-covered bed an increase in temperature is accompanied by a substantial decrease in the sediment transport without very significant changes in the roughness of the bed. It was not the object of the current investigation to study the effect in temperature; hence, only these few runs are reported to show the general trend of the effect of temperature and to indicate what errors are involved if temperature is not controlled during flume experiments.

Finally, Table 9 presents data for some runs with clear water made in the 33.5-inch flume after reconstruction. The purposes of these runs were: (1) to check the equipment; (2) to determine the hydraulic roughness of the newly painted interior of the flume; (3) to study the velocity distribution in the flume throughout cross-sections at various stations along the flume; and (4) to measure a few values of the von Karman constant, k. The values of the friction factor measured were on the average only three percent higher than those commonly used for hydraulically smooth pipe. Studies of the velocity distribution showed evidence that secondary currents were present by deviations from what would be expected in simple shear flow at a station and also by unexplained small variations in the profile at various stations along the flume. Vanoni (7, 17) has given a good discussion of this problem previously and the writers are satisfied that although this is not necessarily a desirable condition it is nonetheless unavoidable in all flumes of this type. Furthermore, some of the von Karman k-values determined, as reported in Table 9, are paradoxical and seem to depend on the width-to-depth ratio. The variation of these k-values is presumed to be the effect of secondary circulation.

Similar data obtained by Brooks (9) and Barton and Lin (11) are presented in the same form in Tables 15 and 16 in Appendix B. For Barton and Lin's data, sidewall calculations were computed as well as other quantities needed for the table.

D. Observations of the Sand Bed

The major cause of the extreme variations in the channel roughness is the changing configuration of the sand bed of the flume. At the lower velocities the beds are typically covered with dunes yielding high values of bed friction factor, f_b, while at higher velocities the dunes are swept away, resulting in much lower values of f_b. The condition of the bed for each run is indicated by an appropriate term in columns labelled "Bed Condition" in Tables 6, 7 and 8.

In this report only a brief summary of dune and bed observations will be presented, inasmuch as a separate paper (20) will present a detailed discussion of the observations and analysis carried out simultaneously with a grant from the National Science Foundation.

On the basis of observations in both the flumes with the various fine sands used, the following general description of changes of the bed configurations may be given. If the flow velocity is sufficient to move the grains at all, and if sufficient time is allowed, large dunes will develop. During this development stage the total shear for the channel increases because of the increasing roughness, and the total amount of sediment transportation gradually increases. In effect, the dunes are an aid to the entrainment of sediment by the flowing water. Fully developed dunes at low velocity are characterized by relatively short wavelengths and limited lateral extent. Single dunes do not extend very far to the left or right before they give way to other dunes, forming a rather haphazard pattern without dune crests extending from one wall to the other. Such a dune pattern is illustrated in Fig. 15 for Run 2-12. For this run the velocity is 0.80 fps, and the sediment discharge concentration is only 0.0033 gr/ℓ (or 3.3 ppm).

As the velocity is increased the dune pattern changes very gradually in comparison to the rate at which the sediment load increases. A fifty percent increase in velocity may bring a fifty-fold increase in the sediment discharge but only small order changes in the bed friction factor, usually downward. The dunes themselves become more rounded on their crests, their wavelengths increase slightly and their lateral extent also increases. A more definite system of passes is developed which is probably influential in reducing the friction factor. The height of the dunes seems to stay about the same, or to decrease slightly, being on the average about 1/2 to 3/4 inch

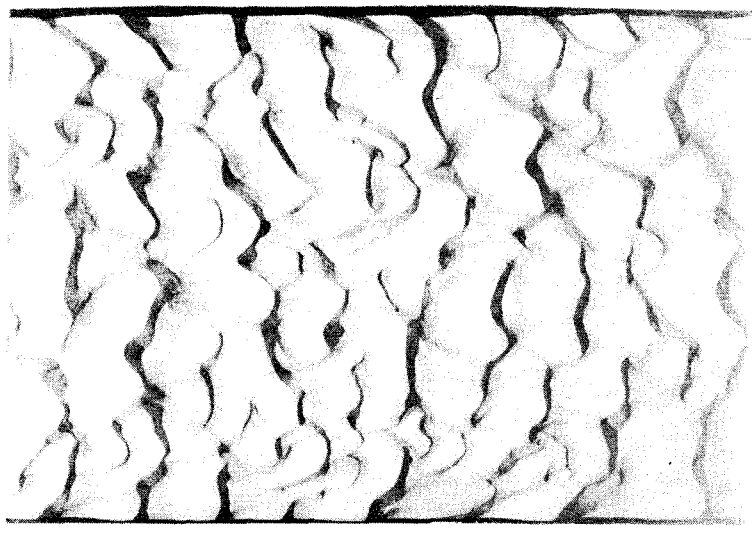

Flow direction ⟶
U = 0.80 fps, d = 0.541 ft, f_b = 0.076, $\overline{C}$ = 0.0033 gr/ℓ

Fig. 15. Dune configuration at a low rate of sediment transportation (Run 2-12). (Full 33.5-inch width of the flume shown.)

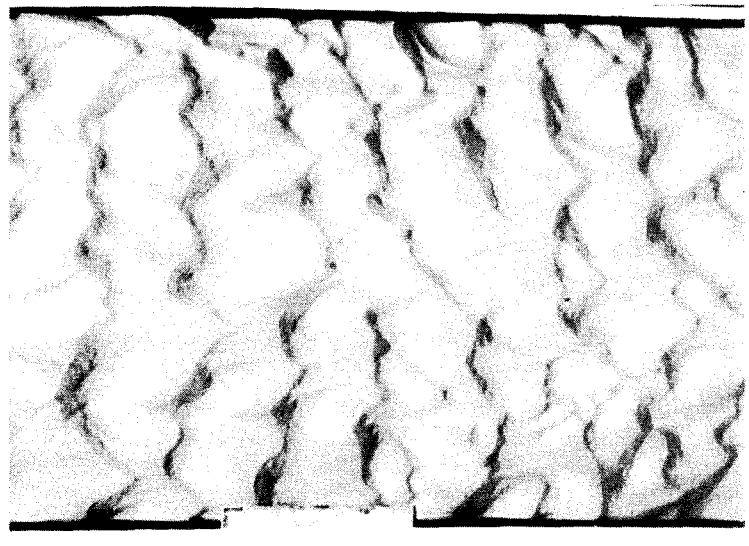

Flow direction ⟶
U = 1.40 fps, d = 0.237 ft, f_b = 0.083, $\overline{C}$ = 2.2 gr/ℓ

Fig. 16. Dune configuration at a high rate of sediment transportation (Run 2-7). (Full 33.5-inch width of the flume shown.)

for the runs reported herein, with maxima of the order of 1 to 1.5 inches. Figure 16 is an illustration of this type of configuration (Run 2-7). For this photograph and all following ones, the flow of water was stopped before the photograph was taken.

Further increases in the velocity bring forth a very strange phenomenon at a velocity of around 1.4 fps in the 10.5-inch flume and 1.5 or 1.6 fps in the 33.5-inch flume. At these velocities the sand becomes nonuniformly distributed in the flume, creating a reach with generally thick sand bed and another reach with a thinner sand bed. Over the thick section the depth is reduced, the velocity is increased, and the bed flat; whereas over the thinner part of the bed the depth is more, the velocity is less, and the bed is dune-covered with a high friction factor. In this report this phenomenon is called a sand wave. A typical front of a sand wave is shown for Run 2-17 in Fig. 17. This front or transition from flat to dune-covered bed moves downstream in a regular fashion and recirculates through the pipe and starts over again at regular intervals. The transition from rough to flat at the other end of the wave is much more gradual and may occur over an interval of ten to twenty feet. Figure 18, for Run 2-6, is an illustration of the chaotic nature of the bed in this upstream transition section of a sand wave. For some of the runs in the large flume several small secondary sand fronts or sand bars were sometimes observed in addition to the main one, usually following behind it.

As indicated by the footnotes in Tables 6 and 7, the data listed for runs with sand waves apply separately either to the flat section (Runs H-3, 2-17F, and 2-16F) or the dune section (Runs 2-17D and 2-16D), or for a composite of flat and dune sections (Runs H-7, 6 and 7).

As the velocity of the flow is further increased, to about 2 fps or more depending on the depth, the sand wave disappears. Careful observation shows that as the discharge is increased the relative length of the flume covered by the flat section gradually increases, while that for the dune section gradually decreases until the dune section disappears altogether leaving a uniformly flat bed. The converse is true at the transition between the condition of a completely dune-covered bed and the initiation of a short sand wave.

With the flat bed condition, illustrated by Fig. 19, there are usually

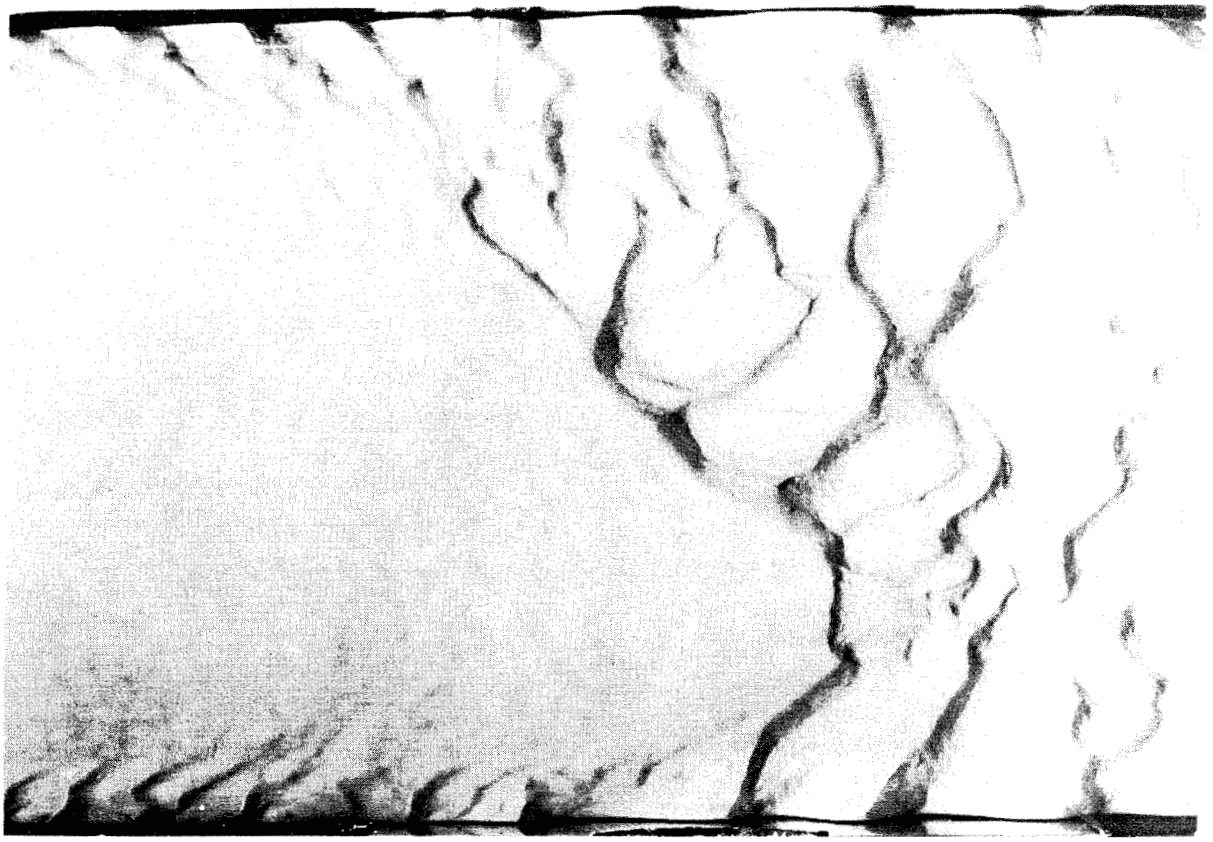

Flow direction ⟶

Flat Section		Dune Section
0.203	Depth d, ft	0.302
2.07	Mean velocity, U, fps	1.39
0.031	Bed friction factor, f_b	0.077
0.15	Avg. thickness of sand bed, ft	0.10

Fig. 17. Typical front of a sand wave (Run 2-17). (Full 33.5-inch width of the flume shown.)

Flow direction ⟶

Fig. 18. View in transition zone from rough to flat for sand wave in Run 2-6. (Compare with abrupt flat-to-rough transition in Fig. 17. Full 33.5-inch width of the flume shown.)

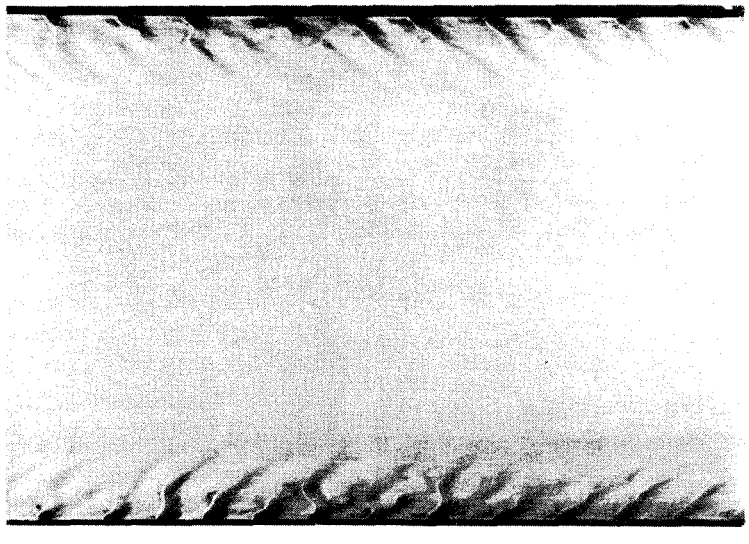

Flow direction ⟶

U = 2.13 fps, d = 0.233 ft, f_b = 0.024, $\overline{C}$ = 2.5 gr/ℓ

Fig. 19. Flat bed at a high transportation rate (Run 2-2). (Full 33.5-inch width of the flume shown.)

very slight ripples near the wall because of the reduced local velocity. Otherwise the bed gives the impression of being exceedingly flat with variations in thickness of only a very few thousandths of a foot. The sediment discharge is higher but the sediment discharge concentration has usually not changed very much from the maximum concentration for beds entirely covered with dunes.

If the velocity is increased still further to reach a critical Froude number of around 0.8, standing surface waves start to form and are reinforced by long wavelength undulations of the bed. When the velocity is increased so that the Froude number exceeds 1.0, the surface waves become exceedingly high, as do the corresponding undulations of the bed; occasionally the surface waves break and the peaks of the corresponding waves in the bed are rapidly scoured. This condition is characterized by rapid and convulsive changes in the bed configuration. These waves on the bed are often called anti-dunes. Because of the unstable nature of the flow no experiments in this regime were carried on, although it is a spectacular demonstration experiment. Unlike supercritical flow of clear water, the flow never becomes stable again as the Froude number is further increased (unless all the bed sand is carried into suspension).

VI. DISCUSSION OF RESULTS OF GENERAL STUDIES

The principal findings of the General Studies will be discussed under four headings below: A. Choice of Independent Variables for Flume; B. Comparison with Field Data for Rio Grande River; C. Channel Friction; and D, E. Sediment Transport. The principal findings of the General Studies have already been published by Brooks (22) as the closing discussion to his earlier paper (9). Some of the text figures and tables below have been taken directly from that closing discussion.

A. Choice of Independent Variables for Flume

In the past it has usually been presumed that the problem of flow in alluvial channels could be solved by choosing as independent variables the slope, channel geometry, depth, and bed material size. However, in the flume studies it has often been found that more than one equilibrium flow is possible for given depth d, slope S, and bed material. These equilibria occur at substantially different velocities, discharges, and sediment loads. Consequently, the velocity U, for example, cannot be considered a unique function of d and S. On the other hand, it was found that the inverse relation is unique when U and d are chosen as independent variables and S is taken as dependent.

Since it is awkward for engineers to deal with multiple solutions to a problem for which it is not clear which is the correct answer, the proper choice of the independent variables is essential for clear thinking. Furthermore, dimensional analysis cannot determine which dimensionless numbers should be considered independent and which ones dependent. The objective of this section is, therefore, to discuss the results in a direct way to illustrate the effects of the several variables on each other and to indicate which functional relationships may be expected to be unique, and hence most useful.

To facilitate discussion of this uniqueness problem, Figs. 20, 21, and 22 have been prepared from the data presented in Tables 6 and 7. No dimensional analysis has been made, but rather the data have been plotted directly to show some of the simple relationships. For example, Fig. 20 shows how the slope S, bed shear velocity U_{*b}, and bed friction factor f_b, vary with the mean velocity U when the depth is held constant at about 0.24 feet with

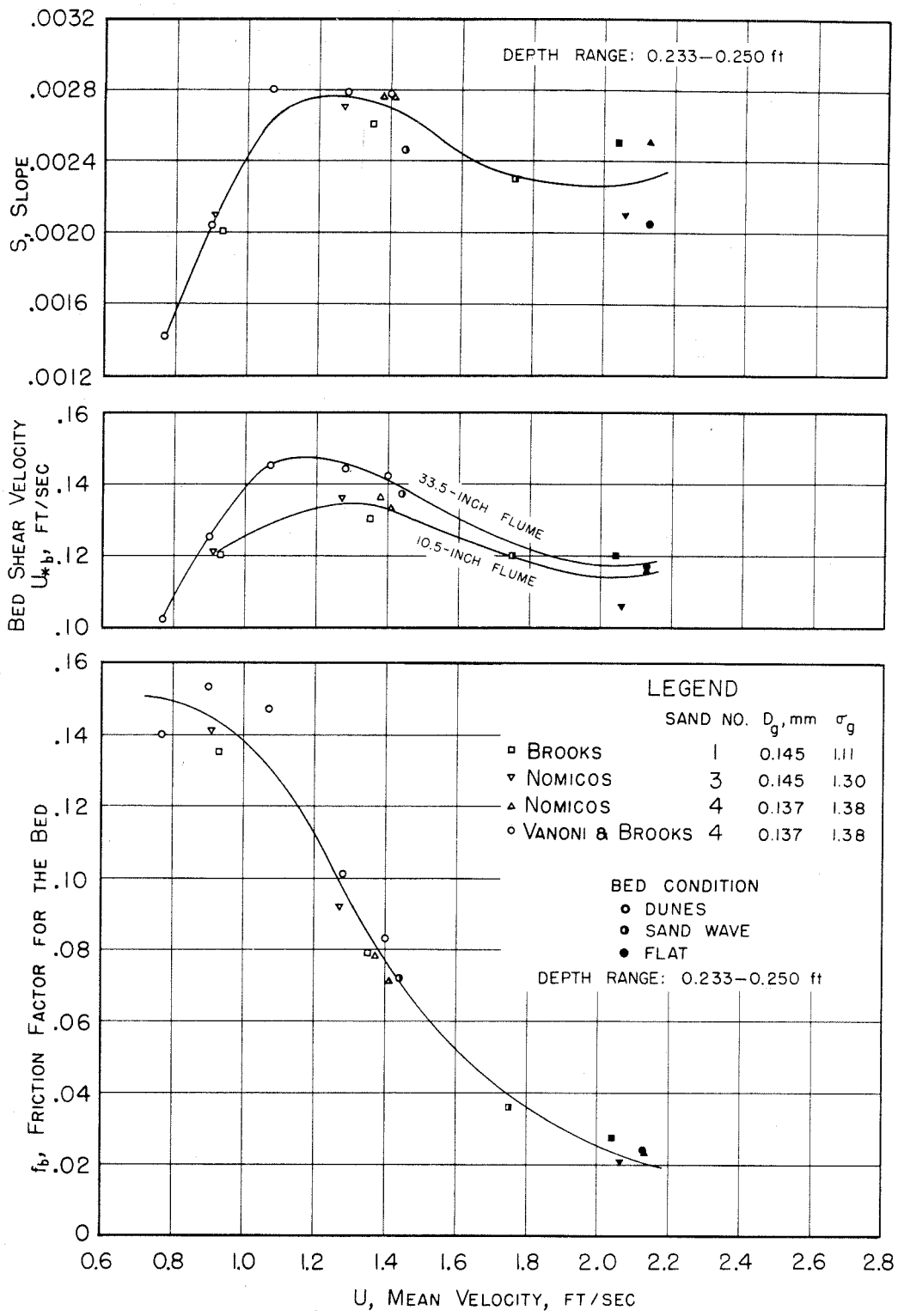

Fig. 20. Variation of S, U_{*b} and f_b with U for depth = 0.233 to 0.250 ft for Sands 1, 3 and 4 in 10.5-inch flume (Brooks, Nomicos) and Sand 4 in 33.5-inch flume (Vanoni and Brooks).

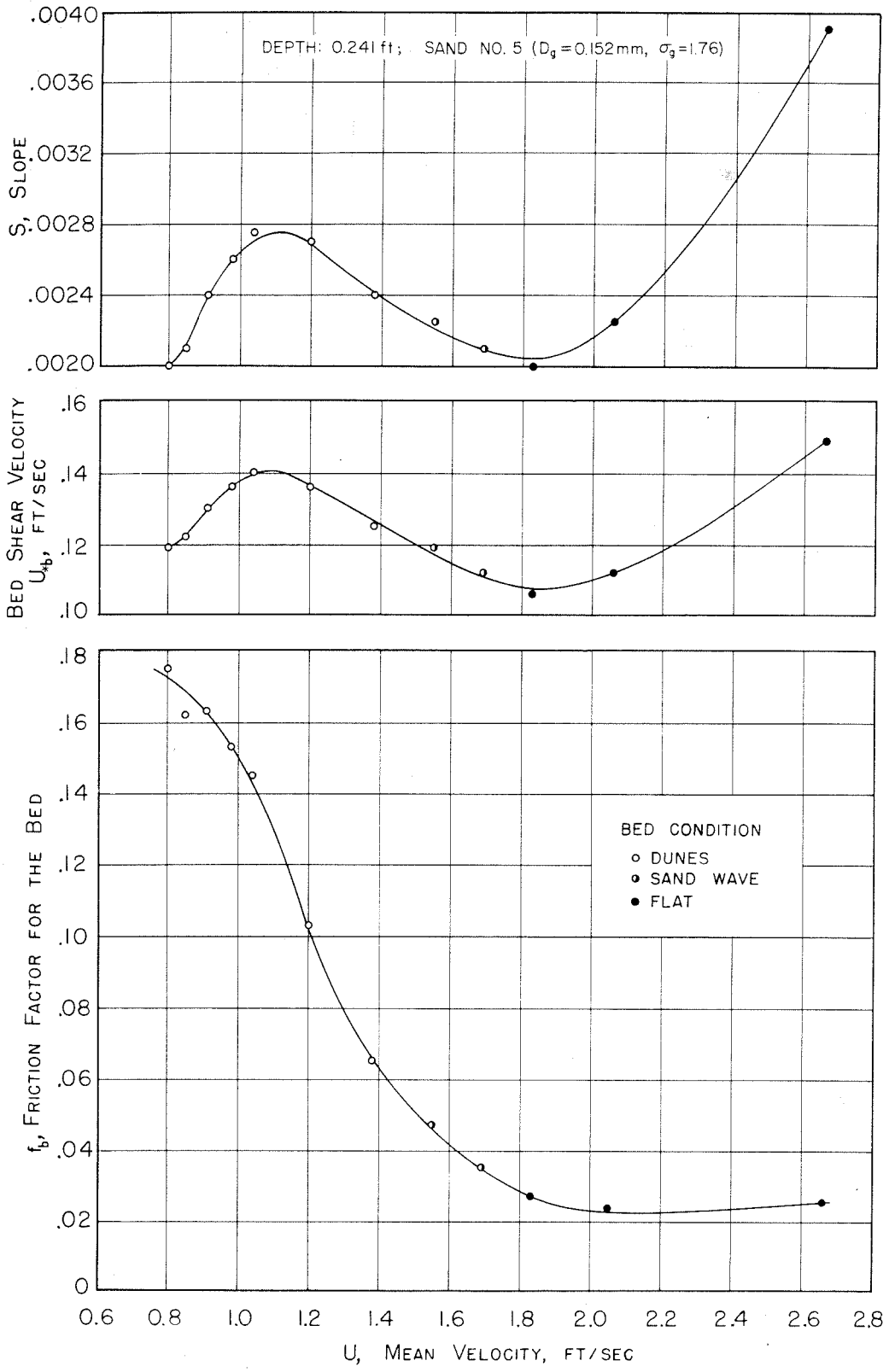

Fig. 21. Variation of S, U_{*b} and f_b with U for depth = 0.241 ft for Sand 5 in the 10.5-inch flume.

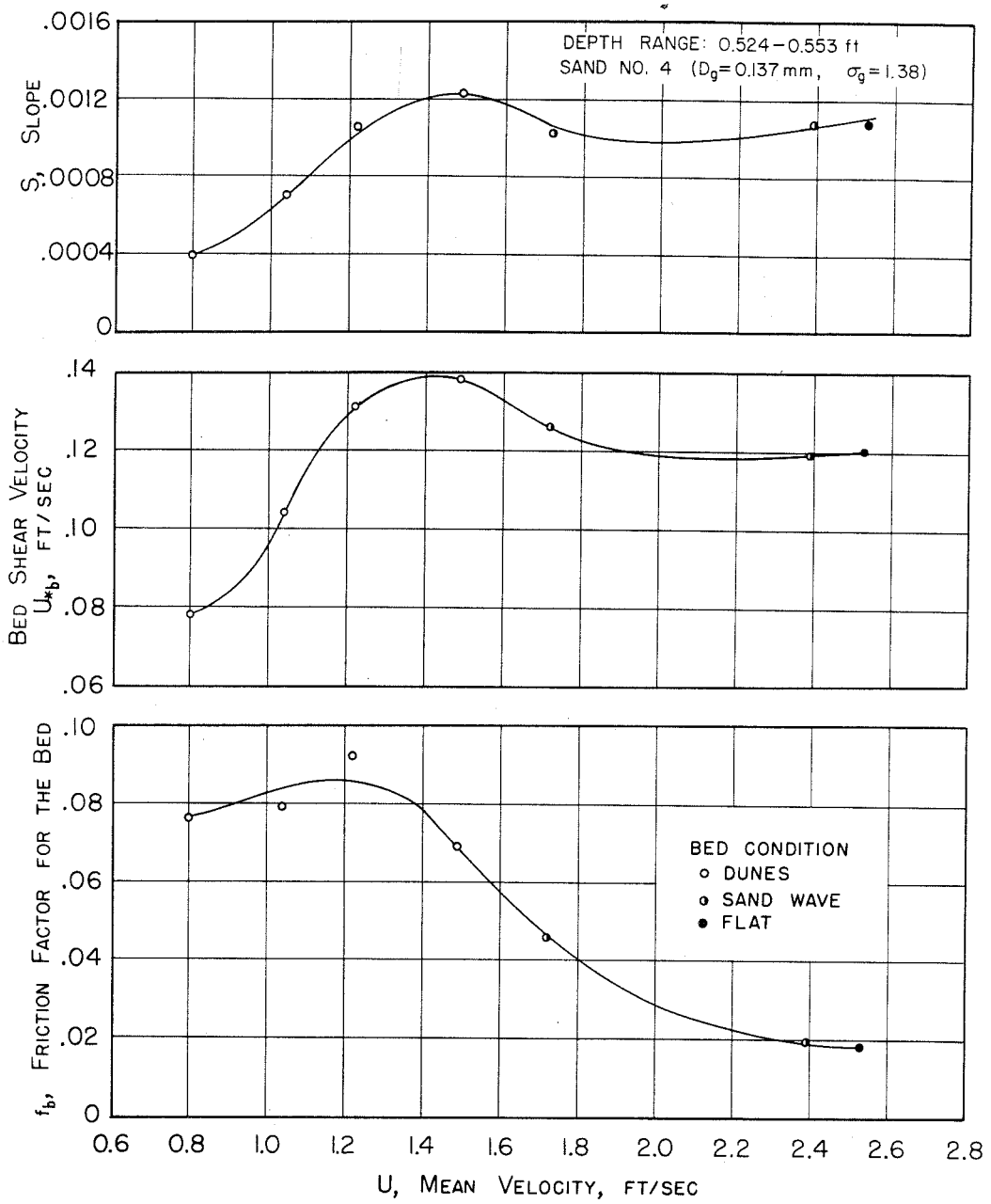

Fig. 22. Variation of S, U_{*b} and f_b with U for depth = 0.524 to 0.553 ft for Sand 4 in 33.5-inch flume.

the bed-material size kept constant at D_g = 0.14 mm. In this category fall not only some runs by Nomicos in the 10.5-inch flume and by the writers in the 33.5-inch flume, but also some earlier runs by Brooks for Sand 1 (see Appendix B).

From Fig. 20 it is seen that the bed friction factor f_b decreases markedly from 0.15 to 0.025 when the velocity U is increased from 0.8 to 2.0 fps. The points which are half blacked-in in the figure apply to those runs in which a sand wave was observed, and the individual data points may apply to either the dune section or the flat section, or may be a composite of both, as indicated in Tables 6 and 7. As previously pointed out, the cause for this tremendous variation in roughness is the reduction of the rugosity of the dunes as the velocity increases. The same sort of variation in f_b is shown in Fig. 21, which is for the same depth (d = 0.24 ft) using Sand 5 which has a very large geometric standard deviation (σ_g = 1.76) with approximately the same median grain size (0.15 mm). However, when the depth is increased to about 0.54 ft (Fig. 22) the friction factor is no longer as large even at its maximum value which is less than 0.10. Furthermore, there appears to be a slight increase in f_b with increase in U in the range 0.8 to 1.2 fps before the friction factor drops finally to 0.02. The cause of these differences is not understood, except that the reduction in the maximum friction factor when the depth is increased is due to the fact that the dunes do not increase appreciably in size when the depth is increased; therefore, the relative roughness of the bed is diminished, making a corresponding drop in f_b. Further discussion of channel friction will be given in Sec. C.

Perhaps the most surprising result of these studies is the variation of slope S with velocity. In all cases (Figs. 20, 21 and 22) S first increases with U, holding depth constant, as would be expected, but then drops during a further increase in U when the dunes are swept from the bed, and finally rises again with U when the bed becomes flat. The S-shaped curve thus obtained indicates that for a given depth and slope it is actually possible to find more than one equilibrium velocity. In particular, from Fig. 21 it would appear that there may be as many as three equilibrium velocities for a slope such as 0.0024, namely, U = 0.9, 1.4, and 2.1 fps. However, at a higher or lower value of slope there may still be only one solution; for example, using a slope of 0.0032 in Fig. 21, we find that U = 2.45 fps is the only

possible velocity. As previously mentioned, the cause of this reversal in the slope-velocity curve is the tremendous reduction in the friction factor resulting from the disappearance of the dunes.

Considering now the shear on the bed as expressed by the bed shear velocity U_{*b}, we find the same general results. The velocity is not uniquely determined by the shear stress, as it would be for the flow in a channel with a rigid rough bed and fixed friction factor. Here again Fig. 21 shows the possibility of having three different velocities for $U_{*b} = 0.12$ fps. In Fig. 20 it is apparent that there is a slight difference between the 10.5-inch and the 33.3-inch flumes. This is presumed to be an effect of the walls which is not accounted for in a sidewall correction procedure. However, the differences in U_{*b} are small, being always less than 10 percent and on the average only about 4 percent.

Figures 20-22 illustrate that whereas depth and slope cannot be considered independent variables because more than one velocity is possible, on the other hand depth and velocity can be readily used as the independent variables with slope, bed shear stress, and friction factor being dependent variables. In other words, given d and U, then S, U_{*b} and f_b are uniquely determined. The points in Fig. 20 scatter more than those in Figs. 21 and 22; the latter figures are each for a single sand in one flume, thus indicating that the scatter in Fig. 20 is due probably to the slight differences in the sands and the flumes used. Also, it should be noted that there was no temperature control for all the runs in the 33.5-inch flume (Sand 4) and for the runs by Brooks (Sand 1) in the 10.5-inch flume.

Although it is not apparent in Figs. 20, 21, and 22, there are some combinations of depth and velocity which are impossible to achieve in the flume. Instead of the problem of multiple solutions, we now have no solutions. It is impossible, for example, to obtain experimental points in the gap between U = 1.8 and 2.4 fps in Fig. 22. If an attempt is made, a sand wave develops which yields one section of high-velocity, low-depth, flat-bed flow, and another of lower-velocity, higher-depth, rough-bed flow. Hence neither the correct depth nor velocity is obtained. Although the average of the two conditions is the desired combination of depth and velocity, it is apparently an unstable situation in which the flow equilibrium splits and "slides" off both ways from the desired depth and velocity. It would be

interesting to know if such conditions prevail in the field.

Since the velocity U is not uniquely determined by d and S, it is apparent from Fig. 23 that the sediment discharge concentration $\overline{C}$, is also not uniquely determined by these variables. For example, in Fig. 21 (which shows results for Sand 5) we find that when $U_{*b} = 0.12$ fps the velocity may be 0.8, 1.5, or 2.2 fps. At U = 0.8 fps we find from Fig. 23 that $\overline{C} = 0.30$ grams/liter for Sand 5, while for the two higher velocities $\overline{C}$ is between 3 and 4 grams/liter. Similarly, the discharge and the sediment transportation rate per unit width (q and q_s, respectively) cannot be considered unique functions of depth and slope, or bed shear (assuming fixed bed material size and width). However, it is seen from Fig. 24 that q and q_s may indeed be taken as independent variables with d and U being uniquely determined dependent variables; moreover, it was found that f_b and S are also uniquely fixed by q and q_s. Of course, the grain size of the material is also considered an independent variable, and the width is fixed. Thus, from Fig. 24 one may estimate that given q = 0.5 cfs/ft and q_s = 1.0 lbs/ft min., it is required that the depth be about 0.4 ft for Sand 4. Using q and q_s as the independent variables, no multiple solutions to this problem have been found. In fact, considering how natural rivers must operate, it is perhaps reasonable to consider the water and sediment discharge as being the independent variables and the depth and roughness being the response of the stream to the applied q and q_s.

The multiplicity of the relation between sediment discharge and depth and slope, encountered in the present experiments, was first pointed out by Brooks (9) and has not been observed by other investigators. Either this multiplicity caused by the variable roughness has not been noticed, or else it has not been nearly so pronounced (if existent at all) for some of the other sand sizes used heretofore in sediment transportation experiments.

With coarse material, the sediment moves primarily as bed load; although dunes have been observed, it is possible that the roughness may not undergo nearly such radical changes. In this case, the bed-load transportation rate would be more or less directly related to the shear, as first suggested by DuBoys, and checked by countless investigators during the past several decades. However, the large scatter of the points in all graphs of bed-load transportation rates (which is usually ignored) is evidence that

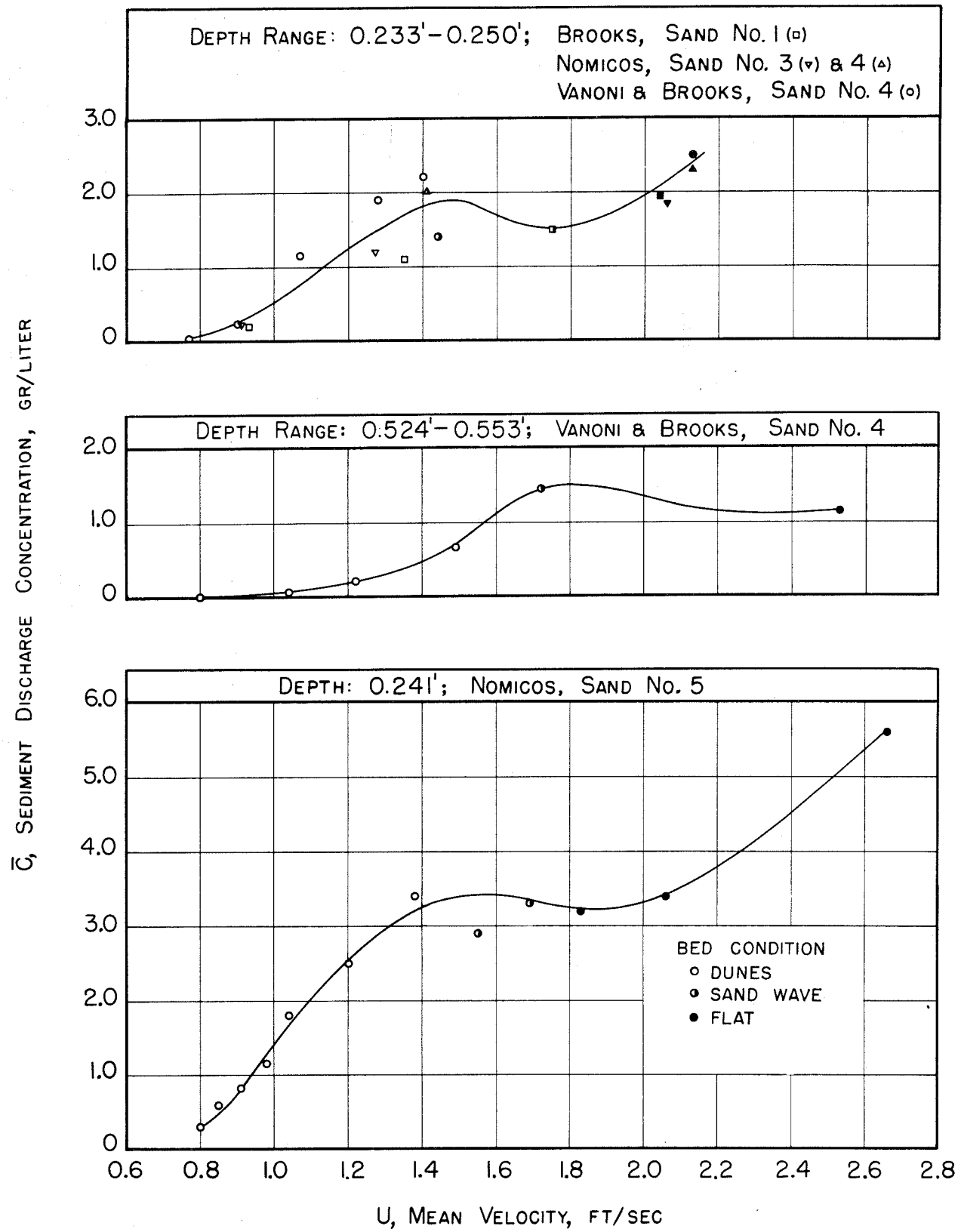

Fig. 23. Variation of $\overline{C}$ with U for various sands at constant depths as indicated.

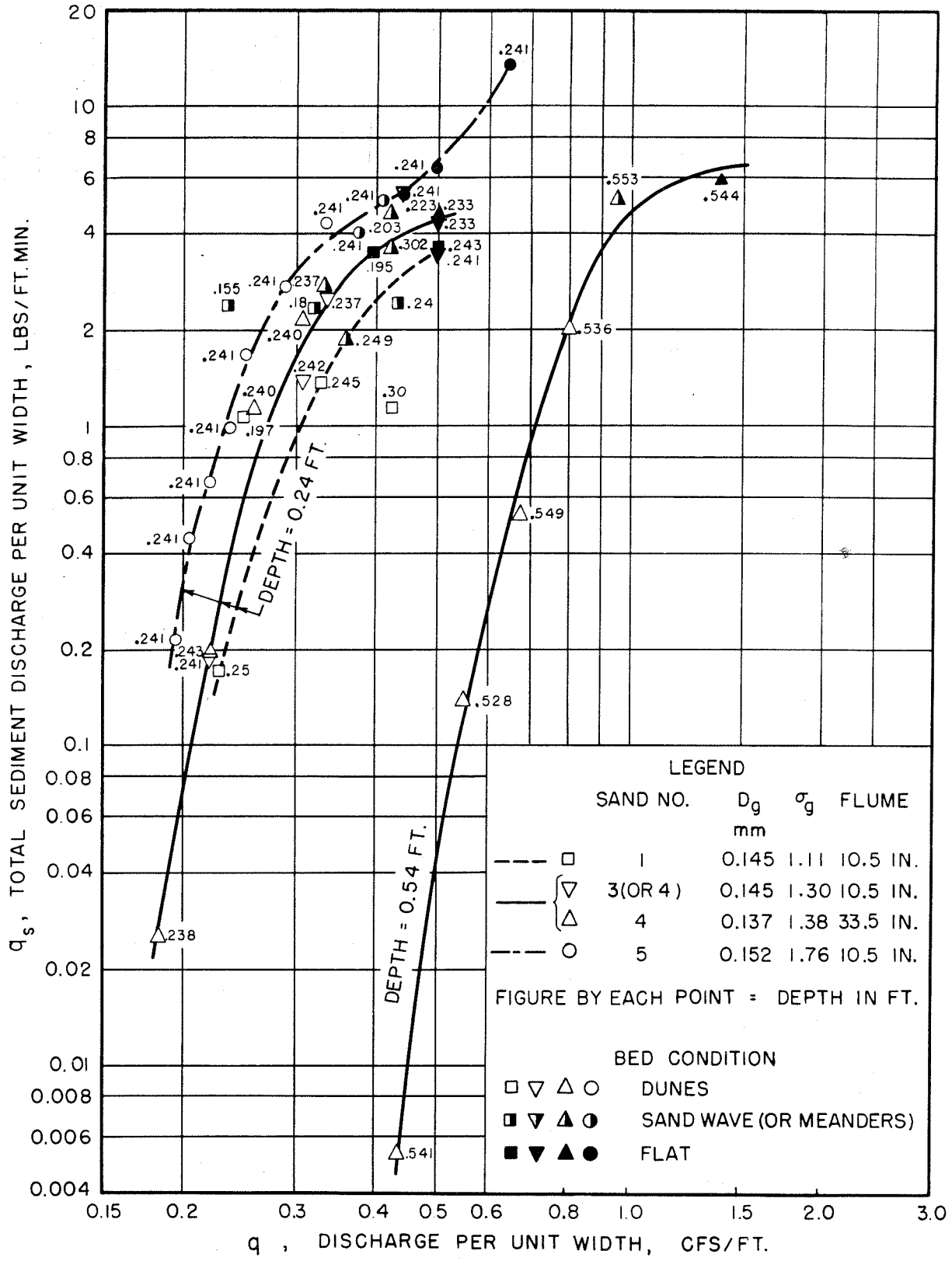

Fig. 24. Relation of depth to q and q_s for various sands.

some other effect, such as roughness has not been taken full account of. In some bed-load formulas, notably that of the Waterways Experiment Station (Vicksburg), the Manning roughness coefficient n has been included in the formula as an independent variable; however, a method for predicting n is then needed. Einstein's bed-load theory (23) takes account of variable channel roughness and uses the method given by Einstein and Barbarossa (16) for determining it. This method of predicting channel friction will be discussed in Sec. C.

It is doubtful whether changes in roughness play a very significant part in the mechanics of streams with beds of silt or clay, or the finely ground silica flour used by Kalinske and Hsia (24). It seems that dunes may never become very large in this material because it is so easily moved by flowing water even at very low velocities. For nine different flows over a bed covered with this extremely fine material, Hsia found that the Manning n varied only from 0.0119 to 0.0098, with one of the highest values being for the run with the smallest sediment concentration (0.64%) and the smallest n for the run with the largest concentration (11.1%). He found that the transportation rate did have a direct relation to the bed shear, increasing when the shear increased.

Consequently, it may be that the multiple relationship between sediment transportation rate and bed shear occurs only for some intermediate range of sediment sizes under ordinary circumstances, or possibly it would occur only at unusually large shears for coarse material and at extremely small shears for fine material.

Experiments with movable beds of fine sand have only recently been made because of the difficulty of making them, even though this material is commonly found on the beds of large rivers. Notable among recent experiments are those at the Colorado State University reported by Barton and Lin (11). (For tabular summary of data, see also Appendix B.) On the basis of these experiments, Barton (25) disagrees with the conclusion noted above that discharge and sediment transport rate are not uniquely determined by the depth, slope and grain size. Not finding such a conclusion is probably the result of the way in which the runs were scheduled and analyzed.

If the experimental results of Barton and Lin are plotted, as shown in Fig. 25, with discharge Q as abscissa, depth d as ordinate, and slope S

as the third variable, contours of equal slope may be drawn in the figure. These curves for constant slope are, in effect, rating curves for the flume used by Barton and Lin, considering the depth as equivalent to the stage. For some values of S, there appears to be an inflection in the contour which would indicate the possibility of finding more than one equilibrium Q for a given depth and slope. On the other hand, for a given Q and S, there appears to be no difficulty in determining the depth. Although this is contrary to a conclusion given by Brooks (9, p. 16, 4(b)), no new data were obtained in these studies to resolve the disagreement.

Other extensive experiments with suspended load have also been made recently at the University of Iowa by E. Laursen (26), but his report was not available in time to be discussed herein.

In summary, the current experiments bear out in general the conclusions given by Brooks (9) in 1955 for streams carrying suspended loads of bed material. As they apply here, they may be enumerated as follows:

(1) In the laboratory flumes it was found that neither the velocity nor the sediment transportation rate could be expressed as a single-valued function of the bed shear stress, or any combination of depth and slope, or bed hydraulic radius and slope. This contradicts assumptions which have commonly been held for some years, to the effect that knowledge of the slope, channel geometry, and bed material of a stream were sufficient to predetermine its flow and sediment-transporting characteristics.

(2) The cause of the nonuniqueness cited in Conclusion (1), above, is the extreme variation in channel roughness caused by the variable nature of the bed configuration. In general, the runs at low velocity were accompanied by high, rugged dunes, while those at high velocity were associated with flat beds, with sand wave phenomena occurring at intermediate velocities.

(3) On the basis of experiments to date, it appears that the depth and velocity may logically be used as independent variables along with the grain size of the bed material. Knowing these quantities, it is found for the flumes that the slope, bed shear, friction factor, and sediment discharge are all uniquely determined.

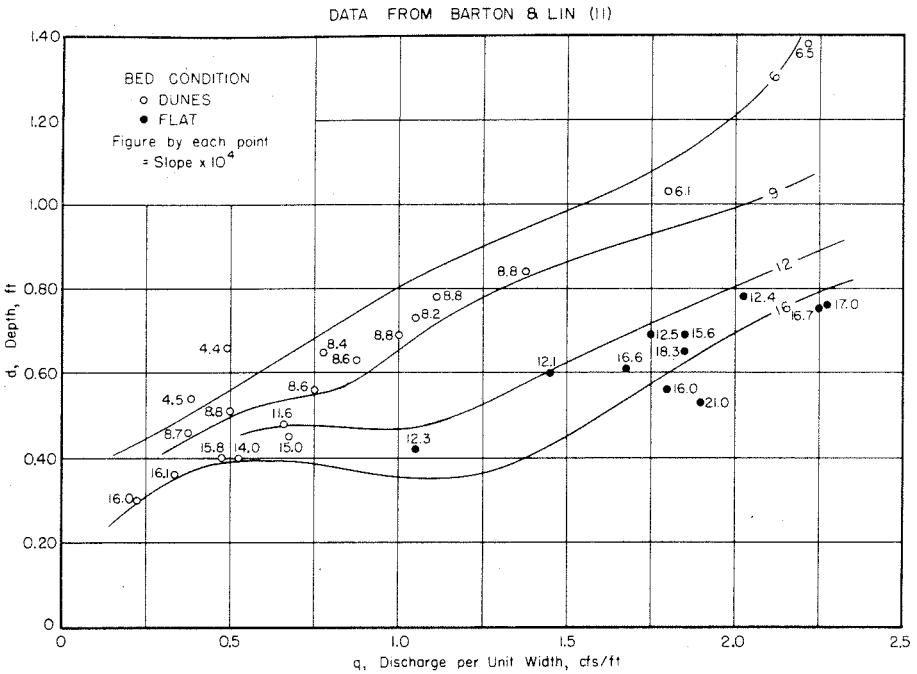

Fig. 25. Relation between slope, depth and discharge for Barton and Lin flume data (11). (Mean sand size = 0.18 mm.)

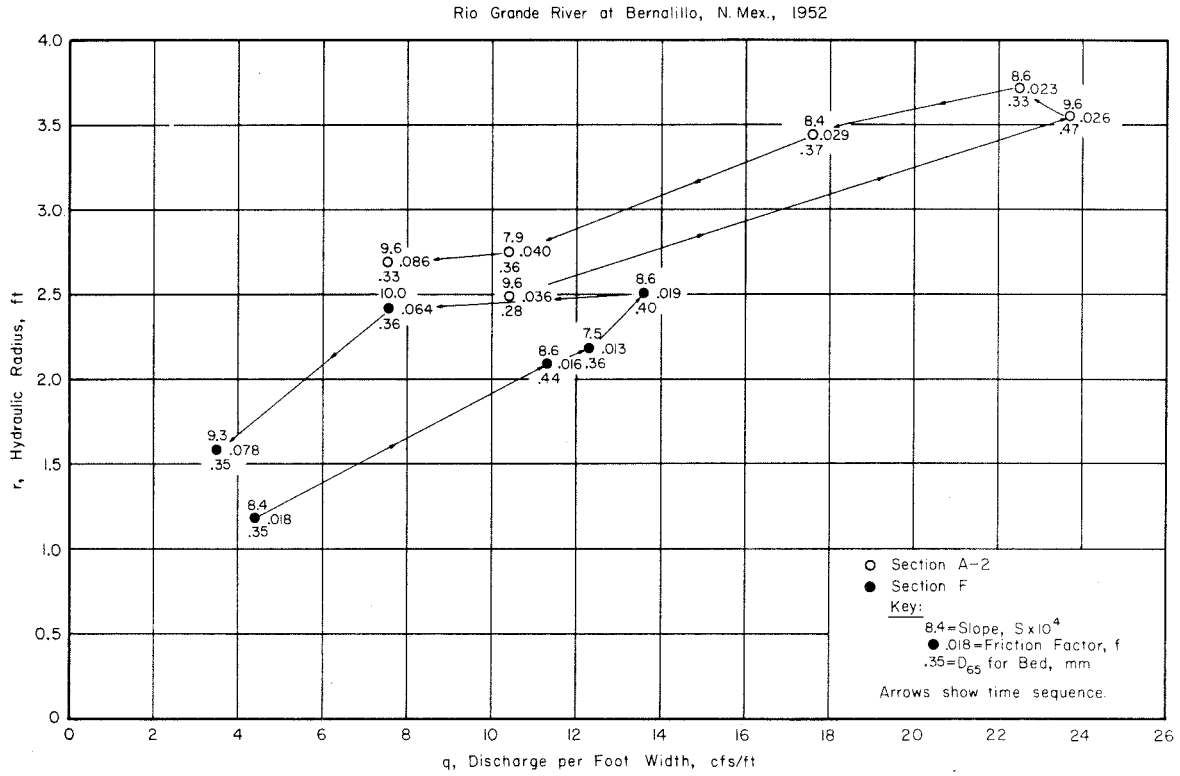

Fig. 26. Variation of hydraulic radius, slope, friction factor and bed-material size with changing discharge for Rio Grande River at Bernalillo, New Mexico, April-July, 1952.

It was also found possible to consider the water and sediment discharges as independent variables, and from these to determine the depth, velocity, friction factor, and slope. These relationships are all illustrated in Figs. 20-24.

(4) From an examination of Figs. 20-24 the following general relationships are apparent:

a. For a constant discharge, q, an increase in sediment discharge, q_s, requires a decrease in the depth, d.

b. If q is to be increased without changing q_s, then an increase in d is necessary, although this increase is relatively less than in q.

c. When the velocity, U, increases with depth d constant, the bed friction factor, f_b, generally drops, the slope, S, and bed shear velocity, U_{*b}, may either increase or decrease and the concentration, $\overline{C}$ increases until the sand wave stage is reached.

d. When d is increased with U constant, f_b and $\overline{C}$ both decrease.

e. The bed shear velocity U_{*b} appeared to change less than any other quantity. It may be expected, therefore, that U_{*b} is not a good variable from which to attempt to determine the flow and sediment transportation characteristics.

f. The conclusions above are unaffected by the geometric standard deviation of the bed sand, which ranges from $\sigma_g = 1.11$ for Sand 1 to $\sigma_g = 1.76$ for Sand 5 with insignificant change in the geometric mean size.

B. Comparison with Field Data for Rio Grande River

Various field observations to support the conclusions above have already been presented by Brooks (9)and have been discussed at length (27, 22) and will not be repeated here. (See also Chaps. II and VIII.) However, some recent field data for the Rio Grande River at Bernalillo, New Mexico, were analyzed for comparison with the laboratory results, and will be presented here. The basic data and some computed quantities, such as the shear velocity and the friction factor, are tabulated in Table 10. The measurements were taken by the U. S. Geological Survey and the U. S. Bureau of Reclamation, and were furnished to the writers by a personal communication from Dr. Luna B. Leopold of the U.S.G.S. The column headings in the table follow as nearly as possible those used in the previous tables for the laboratory results; however, since the ratio of the width to depth is of the order of 100 or more, there is essentially no difference between the mean depth and the hydraulic radius. Furthermore, no sidewall corrections were made, inasmuch as they are unnecessary, and so there is no distinction between f and f_b. At Section F, it is presumed that local degradation and elimination of some overbank flow is responsible for the large variations in channel width.

From the tabulated data it is apparent that the friction factor varies considerably, generally being higher when the velocity and suspended-load discharge* are low. To present the data graphically, Fig. 26 has been prepared with discharge per unit width as abscissa and hydraulic radius as ordinate in a manner similar to Fig. 25. Adjacent to each plotted point are numbered the values of the slope, the friction factor, and D_{65}. The arrows in the figure show the progress of time from the earliest to the latest observation.

The loops shown in Fig. 26 are due mainly to variations in the friction factor. At each station neither the slope nor D_{65} changed radically during the passage of the spring floods, although it may be noted that the friction

*Note that the wash load is included in the sediment discharge data given in Table 10; since only the bed-material load has a significant effect on roughness, the relation of f to the total suspended-load discharge is not clear-cut.

TABLE 10

RIO GRANDE RIVER AT BERNALILLO, NEW MEXICO: SUMMARY OF SPECIAL MEASUREMENTS DURING APRIL-JULY, 1952[1]

Section[2]	Date (1952)	Q Discharge cfs	b Width ft	q=Q/b cfs/ft	d = r Depth or Hyd. Rad. ft	S Slope	U* Shear Velocity fps	U Average Velocity fps	f Friction Factor	T[3] Water Temp. °C	Measured Suspended Load Discharge tons/day	Measured Suspended Load Discharge gr/ℓ	Bed Material Analysis D_{35} mm	Bed Material Analysis D_{65} mm	F Froude No.
A-2	Apr 25	2820	272	10.4	2.49	0.00096e	0.277	4.14	0.036	12	25,300	3.33	0.19	0.28	0.46
	May 12	6440	272	23.7	3.55	0.00096	0.331	6.52	0.026	18	64,500	3.72	0.33	0.47	0.61
	June 17	6120	272	22.5	3.72	0.00086	0.321	5.95	0.023	18	38,700	2.34	0.25	0.33	0.54
	June 20	4775	272	17.6	3.44	0.00084	0.304	5.04	0.029	18	21,250	1.65	0.28	0.37	0.48
	June 26	2800	268	10.4	2.75	0.00079	0.264	3.74	0.040	18	7,070	0.94	0.25	0.36	0.40
	July 24	2030	270	7.52	2.69	0.00096	0.288	2.77	0.086	20	14,910	2.72	0.22	0.33	0.30
F	Apr 25	2820	640	4.41	1.18	0.00084	0.178	3.72	0.018	12	21,600	2.84	0.25	0.35	0.60
	May 12	6440	570	11.3	2.09	0.00086	0.240	5.40	0.016	18	49,400	2.84	0.30	0.44	0.66
	June 17	6120	497	12.3	2.18	0.00075	0.230	5.73	0.013	18	28,700	1.74	0.26	0.36	0.68
	June 20	4775	350	13.6	2.51	0.00086	0.264	5.43	0.019	18	20,100	1.56	0.27	0.40	0.60
	June 26	2800	370	7.57	2.42	0.00100	0.279	3.11	0.064	18	7,090	0.94	0.26	0.36	0.35
	July 24	2030	581	3.49	1.58	0.00093	0.217	2.20	0.078	20	10,560	1.93	0.27	0.35	0.31

Footnotes: 1. Dr. Luna B. Leopold, personal communication. Measurements by U. S. Geological Survey and U. S. Bureau of Reclamation.

2. Section A-2 is located at the cable where discharge measurements are usually taken by U. S. G. S.; Section F is located approximately 1 1/2 miles downstream from Section A-2.

3. Temperatures from Water Supply Paper 1252, U. S. G. S., p. 379.

e Estimated.

factor does change substantially. This would appear to indicate that the cause of the variation in f is the change in the bed configuration and that this change happens to be of about the right order of magnitude to keep the slope nearly the same in spite of the other variations. It appears from Fig. 26 that it is possible to get two different velocities or discharges for the same hydraulic radius and slope, thus confirming similar observations from the flume data to the effect that the velocity (or unit discharge) need not be a unique function of r and S. In fact, for Section F between June 20 and 26, with r nearly constant at 2.5 ft, the slope actually increased from 0.00086 to 0.00100 at the same time the velocity dropped from 5.4 to 3.1 fps; this was possible only because f increased from 0.019 to 0.064.

When an alluvial stream will flow at two different velocities on two different occasions, even with the same r and S, it may only be presumed that the change in f comes about because of a change in the sediment load entering the reach (f being higher when the sediment discharge is lower). From Fig. 26, it also appears possible that for a given unit discharge q there may be more than one equilibrium depth, depending again on the character of the sediment load. The fact that these changes can come about without significant change in the grain size of the bed material seems to contradict a suggestion by Einstein (27) to the effect that they occur as the response to significant changes in the size of the bed material during the passage of a flood.

Although the field data for the Rio Grande River (Table 10) are somewhat limited, nevertheless it is hoped that they will help to point the way for future study. Much information is available on the behavior of natural rivers, but very little of it is complete in the sense that all necessary quantities were measured, including items such as slope, grain size distribution of the bed material, and sediment discharge and its size distribution.

Carey and Keller (14) have shown a similar rating curve with a loop in it, with the rising stage being on the lower part of the loop and the falling stage on the upper part. They have explained this as a lag in the adjustment of the sand waves on the bed to the changing of the rate of discharge, so that on the rising stage the bed is not as rough as it should be, and on the falling stage it is rougher than it should be. This, however, presumes

that the sand waves are the largest at the maximum rate of flow, whereas in the flume it has been found that at the highest rate of flow the bed is smoothest. The velocities in the Mississippi River may never get high enough to produce a flat bed. The bed of the Mississippi may also not become as smooth as that of a flume because of armoring, or other effects resulting from its larger range of particle sizes in the bed.

On the other hand, the observed loop may be explained on the basis of higher bed-material load to be carried on the rising stage, so that a smaller stage and friction factor at given Q may be an equilibrium condition. On the basis of observations of rapid bed changes in the flumes, it is believed that beds of rivers may readjust themselves more rapidly than is sometimes believed, i.e., perhaps in a few days instead of a few months.

C. Analysis of Channel Friction

In the previous section it has been shown how variable the hydraulic roughness of a channel may be. Consequently, no theory for the hydraulics of channels with highly movable beds is adequate without a means for predicting the roughness from other known properties of a stream.

Only very recently have any attempts at this been made. One of the most significant is an analysis proposed by Einstein and Barbarossa. They consider that the bed shear stress τ_o may be divided into two parts

$$\tau_o = \tau'_o + \tau''_o \tag{5}$$

wherein τ'_o is the shear stress which would result from grain resistance only on a flat bed, and τ''_o is the additional shear stress due to irregularities in bed and banks such as dunes and bars. In using the term "shear" it should, of course, be recognized that the resistance of the dunes is actually form drag resulting from pressure differentials on the front and back sides of the dunes, and is expressed as an equivalent shear strees (τ''_o) for convenience.

With the shear thus divided, they then divide the hydraulic radius r into two parts r' and r'' in a corresponding way:

$$\tau_o = \gamma r S = \gamma S(r' + r'') \tag{6}$$

or $$\tau_o' = \gamma S r' \quad (7)$$

$$\tau_o'' = \gamma S r'' \quad (8)$$

Furthermore, corresponding shear velocities u_*' and u_*'' are defined as follows:

$$u_*' = \sqrt{g\, r' S} \quad (9)$$

$$u_*'' = \sqrt{g\, r'' S} \quad (10)$$

where $$U_*^2 = u_*'^2 + u_*''^2 \quad (11)$$

The quantity r' is the hydraulic radius which the stream must have in order to flow at the same velocity and slope without dune resistance. A relation between velocity U and r' is given by the Prandtl-von Karman logarithmic resistance law for fixed channels with constants as given by Keulegan (28)

$$\frac{U}{u_*'} = 5.75 \log_{10}(12.27\, \frac{r'}{K_s}\, x) \quad (12)$$

where $K_s = D_{65}$ is the grain roughness of the bed, and x is a correction factor for channels which are not hydrodynamically rough expressed in the form (16, Fig. 2)

$$x = f(\frac{K_s}{\delta'}) = f\ (\frac{K_s\, u_*'}{11.6\, \nu}) \quad (13)$$

with δ' being the thickness of the laminar sublayer. As long as $K_s/\delta' > 5$, $x = 1.00$ for all practical purposes.

Using these equations, r' and u_*' can be determined by trial and error for any set of hydraulic measurements. The shear velocity for the dune resistance may then be found by Eq. 11 with U_* and u_*' known. Considering that the resistance is intimately related to the sediment transport along the bed, Einstein and Barbarossa express the dimensionless ratio U/u_*'' as a function of Einstein's flow intensity parameter ψ' which is

$$\psi' = \frac{\rho_s - \rho}{\rho}\ \frac{D_{35}}{r' S} \quad (14)$$

The quantities ρ_s and ρ are the mass densities of sediment and fluid, respectively, and D_{35} is considered the representative grain size of the bed material for the purpose of this analysis. The transport of sand grains is considered a function of the grain shear τ_o' alone, so that r' appears in the above formula instead of r. In case a sidewall correction is made, r, r', and r'' in all the foregoing equations are replaced by r_b, r_b', and r_b'', which apply to the bed section only.

From data for a number of large rivers they prepared a graph of U/u_*'' versus ψ' (16, Fig. 3). Although there is a consistent trend in the points, the zone of scatter is so great that the solution to roughness problems, using their curve of best fit, is subject to large errors (22).

For comparison of laboratory with field data, values of ψ' and U/u_*'' were computed for all the runs with sediment listed in this report (Tables 6, 7, 15, 16) and were plotted in Figs. 27 and 28. To facilitate the computations, a special graphical procedure, described in Appendix C, was evolved to avoid trial-and-error solutions. The array of points for the Caltech data (Fig. 27) deviates substantially from the curve given by Einstein and Barbarossa, especially for the smaller values of ψ'. When the flume data show higher values of U/u_*'' for the same ψ', it means that the bed of the flume is smoother than would be predicted from the curve. Since ψ' decreases as U and $r'S$ increase, it may be said that with increasing velocity the "flume rivers" get smooth faster than natural rivers. Although it has been suggested (27) that this discrepancy is due to differences in σ_g (or in the uniformity of bed material), this is not the case inasmuch as the data points in Fig. 27 align themselves practically independently of σ_g which covers the wide range from 1.11 to 1.76 with D_g nearly constant.

On the other hand, Barton and Lin's data* (Fig. 28) show much better agreement with the bar-resistance curve. A curve of best fit for these points would be nearly parallel to the Einstein curve and slightly above it, whereas in Fig. 27 a curve fitting the data would cross it at a considerable angle. The apparent difference in results is not understood; however, since the 4-foot-wide flume used by Barton and Lin is larger than either of the

---

*Sidewall corrections were made (Table 16) before the values of ψ' and U/u_*'' were calculated.

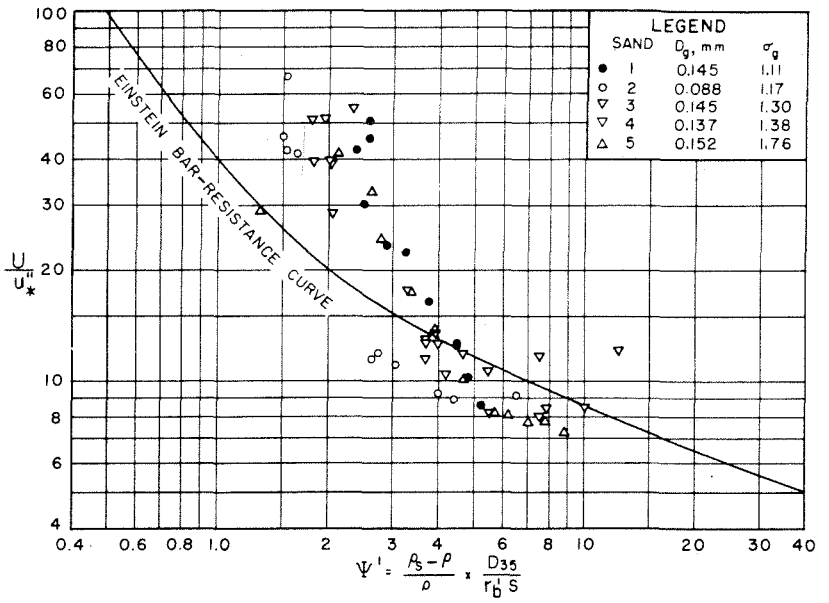

Fig. 27. Resistance data for flume experiments listed in Tables 6, 7 and 15 compared with Einstein-Barbarossa bar-resistance curve for natural channels.

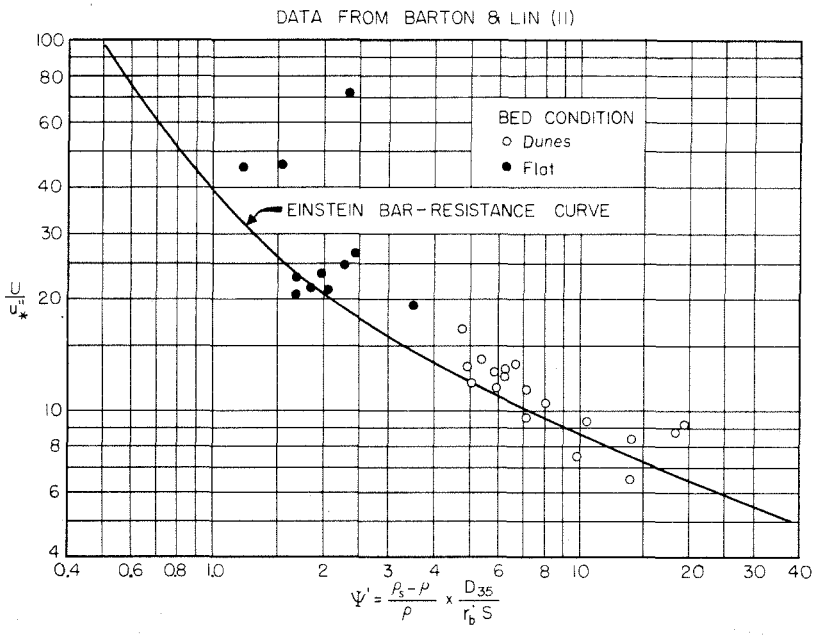

Fig. 28. Resistance data for flume experiments by Barton and Lin (Table 16) compared with Einstein-Barbarossa bar-resistance curve for natural channels.

flumes used by the writers, there may be a scale effect which is not accounted for by the analysis of bar and dune resistance by Einstein and Barbarossa.

Another possible explanation for the apparent inconsistency between some of the flume and river data is the wall effect. Whereas, in the laboratory flumes the maximum width-to-depth ratio was only about 12, natural rivers commonly have width-depth ratios of the order of 100. In the laboratory, the stream is confined to a straight channel and the walls are usually smooth. The sidewall correction procedure (Appendix A) is supposed to eliminate the wall effect as far as the calculation of the bed friction is concerned, but there is no known correction for the effect of the walls on the sediment transportation and dune configuration.

Figure 29 shows the computed values of ψ' and U/u''_* for the Rio Grande River data presented in Table 10. The time sequence of points does not lend confidence to the bar-resistance curve, and one is led to believe that the scatter is not entirely random but that the roughness problem has not yet been solved satisfactorily.

A simpler approach to the roughness problem is to divide the slope S into two parts, S' and S'', (as suggested by Meyer-Peter and Muller (29)). Thus in place of Eqs. 7 and 8, we would have

$$\tau'_o = \gamma S' r \tag{15}$$

$$\tau''_o = \gamma S'' r \tag{16}$$

In this sense S' is the slope that the stream would have if it were to flow at the same velocity and depth without any form resistance due to dunes and bars; S'' is the additional slope (or energy) required to overcome dune resistance. The advantage of this point of view is that r' in Eq. 12 is replaced by r, and S' (in $U'_* = \sqrt{gS'r}$) is simply determined without trial and error. (An ordinary pipe friction diagram may also be used instead of Eq. 12, using 4r in place of the pipe diameter). Furthermore, in comparing the roughness of a stream with and without dunes, it seems logical to keep the velocity, cross section and discharge the same with all the variation in the slope. On the other hand, it is not clear what the significance is of comparing a stream with dunes having hydraulic radius r with one

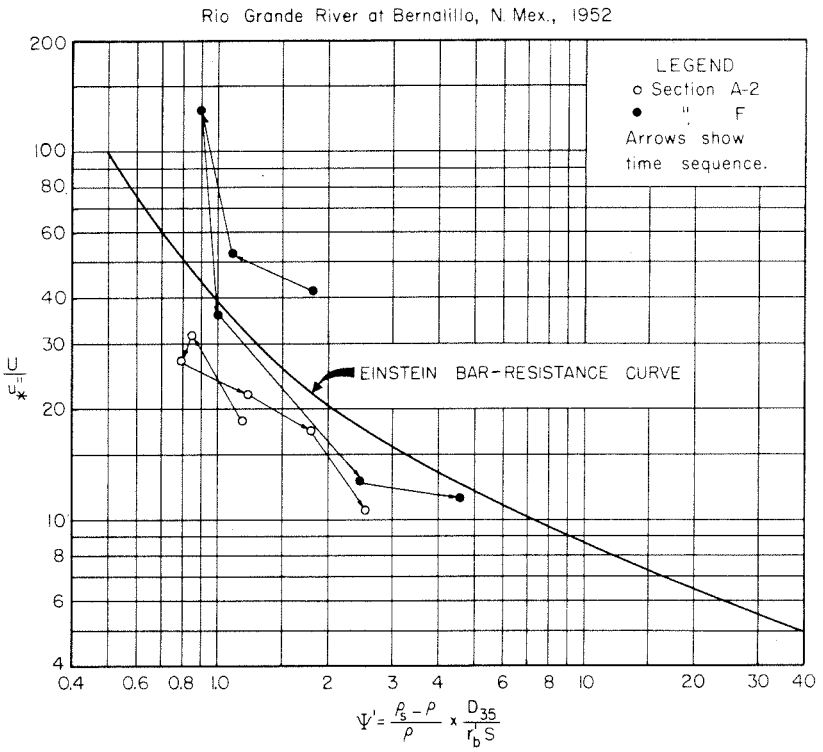

Fig. 29. Resistance data for Rio Grande River at Bernalillo, New Mexico, April-July, 1952, compared with Einstein-Barbarossa bar-resistance curve.

without dunes having a much smaller hydraulic radius r' (and hence smaller discharge) as implied by the Einstein-Barbarossa analysis; for example, it appears unreasonable to represent the relative grain roughness in Eq. 12 by r'/K_s, based on the fictitious hydraulic radius r', instead of by r/K_s, which may be much larger.

The proportionality between the friction factor f and the slope S makes the interpretation of the divided slope $S = S' + S''$ simple. By definition

$$f = \frac{8grS}{U^2} = \frac{8gr}{U^2}(S' + S'') \tag{17}$$

Thence we may easily define f' and f'' as

$$f' = \frac{8grS'}{U^2} \tag{18}$$

$$f'' = \frac{8grS''}{U^2} \tag{19}$$

and

$$f = f' + f''. \tag{20}$$

The friction factor is thereby divided into two parts: f', which would obtain in the absence of dune resistance, and f'', the coefficient for the additional friction due to dunes. As mentioned above, f' can be determined in a straightforward way from a pipe friction diagram; however, a universal method or graph for determining f'' has not yet been evolved, although research is continuing. It may be noted that for the flume experiments the ratio f''/f' was sometimes as high as seven.

A wholly different procedure has been suggested by Ali and Albertson (10). They have attempted to define a relation of the type

$$\frac{C}{\sqrt{g}} = \sqrt{\frac{8}{f}} = \varphi\left(R, \frac{r}{D}\right)$$

where R is the Reynolds number (Ur/ν), C is the Chezy coefficient and D is the representative size of the bed material. The laboratory data for the 10.5- and 33.5-inch flumes were plotted on the graph presented by Ali

and Albertson ($\sqrt{8/f}$ vs. R with curves for different r/D), but the agreement between their curves for various values of r/D and the plotted points was not good. In particular, it appeared that the friction factor did not change fast enough with changes in velocity or Reynolds number. For example, the runs in the 10.5-inch flume with Sand 5 (Table 7) show a change in $\sqrt{8/f_b}$ from 7 to 18 (f_b from 0.16 to 0.025) when R increases only from 20,000 to 35,000 at $r_b/D_g \doteq 400$. On the other hand, by interpolation on the Ali and Albertson graph (10, Fig. 1) one would expect only a change of $\sqrt{8/f}$ from 7 to 9 (f_b from 0.16 to 0.10) for the same range in Reynolds numbers. It seems probable that the dune roughness cannot be represented as a function of only R and r/D as with channels of fixed roughness. By separating f into two parts, f' and f'', as suggested above, it is possible to use the wealth of information already available for f' and to work out f'' in terms of factors pertinent only to the dune resistance, whatever they may be.

D. Suspended Sediment Load - Experimental Observations

The suspended load of a natural stream includes both bed-material load and wash load. The wash load consists of fine particles, usually of the silt and clay sizes, of which there is very little in the stream bed. Although in streams the concentration of bed-material load is often much smaller than that of the wash load, nevertheless the bed-material load is the more important in the regimen of a river, for it is the changes in bed-material load which produce local aggradation, degradation, or changes in channel roughness. Whereas the amount of bed-material load is intimately related to the hydraulic characteristics because of the abundance of material on the bed, the wash load is relatively independent of the stream characteristics and depends primarily on the rate at which fine material is fed into the stream system by watershed erosion and bank caving. Consequently, suspended sediment transportation theory can deal only with the bed-material load as pointed out by Chien (30).

Since the suspended load in the flume is derived entirely from the bed, it is all bed-material load. It is not necessary to include any wash load in the laboratory experiments, and indeed it would be a hindrance anyway because of the high turbidity it produces.

The suspended load discharge in each flume was measured, together with the bed-load discharge, in the return circuit as described in Chapter IV. The sediment discharge concentrations ($\overline{C}$), thus measured, are listed in Tables 6, 7, and 8, and plotted as a function of velocity U in Fig. 23 (page 52). This figure shows, as would be expected, a consistent increase in $\overline{C}$ with increasing U until the sand waves develop, and thereafter a leveling off except for another substantial rise for the single run with the highest velocity for Sand 5. Even if $\overline{C}$ reached a stable value, the transportation rate ($G = \overline{C}Q$) would still increase steadily with Q.

Because of the inflections in the curves for bed-shear velocity (U_{*b}) versus mean velocity (U) in Figs. 20, 21 and 22, $\overline{C}$ cannot be plotted as a unique function of U_{*b} for given depth and bed material. The $\overline{C}$-curves in Fig. 23 also have inflections, but they are at different velocity values. Likewise the total transportation rate, $G = \overline{C}Q$, cannot be expressed uniquely in terms of U_{*b} and the properties of the sediment, because neither $\overline{C}$ nor Q can be so expressed.

Figure 24 (page 53) shows how q and q_s, the water and sediment discharges per unit width, respectively, can be used as independent variables for the laboratory stream. Contours of equal depth have been plotted for different sands. As indicated in Chap. VI, Sec. A, this figure shows that for a given bed material: (1) an increase in depth d with q constant causes a decrease in q_s, (2) an increase in q at constant d results in an increase in q_s, and (3) an increase in q with q_s constant means an increase in d (although proportionately less than in q).

The effect of the geometric standard deviation of sand grain sizes is also apparent from Fig. 24. Other things being equal, an increase in σ_g means an increase in q_s, primarily because more fine material is available for transport, as may be seen from Fig. 14 showing the sand size distributions. For example, the following quantities may be read from the curves in Fig. 24:

q cfs/ft	d ft	D_g mm	σ_g	q_s lbs/ft. min.
0.3	0.24	0.145	1.11	1.0
0.3	0.24	0.145 0.137	1.30 1.38	1.7
0.3	0.24	0.152	1.76	3.0

Since the mean size D_g changes very little, the change in q_s from 1.0 to 3.0 lbs/min. ft may be attributed almost entirely to the increase in σ_g from 1.11 to 1.76.

For each run, a sieve analysis was made of the sand obtained in the samples, and the values of D_g and σ_g determined from the analysis are given in two columns in Tables 7 and 8. It is apparent that D_g for the sediment load is substantially smaller than the bed material (with the exception of Run 9, Table 7), and σ_g is usually larger. For example, an examination of Table 6 shows the following comparison between the average D_g and σ_g for the sediment load and for the bed material:

	D_g mm	σ_g
Average for sed. load for Runs 2-1 to 2-17	0.092	1.53
Bed material	0.137	1.38

Since the fine particles in the bed are more readily transported than the coarser ones, the observed decrease in D_g is logical. The amount of decrease in D_g also increases as σ_g of the bed material increases.

Temperature is also a factor which affects the suspended load. As the temperature rises the settling velocity of the sand grains increases owing to the reduced viscosity of the water; consequently the sand is less easily suspended and the transportation rate drops when the temperature increases. This effect was demonstrated by Nomicos with some special runs in the 10.5-inch flume for which the essential data are tabulated in Table 8. The temperature effect described is clearly demonstrated by the following abbreviated tabulation for depth d = 0.240-0.242 ft, and Sand 3:

Run No.	Q cfs	Temp. °C	f_b	$\overline{C}$ gr/ℓ	Bed Condition
D_1	0.435	15.3	0.025	3.24	Flat
A	"	25.0	0.021	1.87	"
D	"	25.0	0.024	2.14	"
D_2	"	38.0	0.023	1.66	"
G_1	0.193	15.0	0.162	0.31	Dunes
C	"	25.0	0.141	0.23	"
G	"	25.0	0.142	0.22	"
G_2	"	35.6	0.126	0.11	"

Runs A and D, and Runs C and G are bracketed together because they are supposed to be identical; Runs A and C also appear in Table 7. The concentration $\overline{C}$ clearly drops with temperature increase for both flat and dune-covered bed, but the bed friction factor f_b decreases significantly only for the dune case. Since the dune resistance is primarily form drag, it is surprising that f_b should respond so sensitively to a change in viscosity; rather than being a direct effect, it is more likely that the bed configuration itself changed in response to change in $\overline{C}$.

The effect of temperature on the suspended load has previously been noted by Straub (31) in the laboratory and by Lane, Carlson and Hanson (32) in the field. For the Colorado River below Parker Dam, the latter report that the concentration is about 2.5 times as great in the winter when the water temperature is about 50° F (10°C) than it is in the summer when the temperature is about 85°F (29°C). Since other conditions are nearly constant owing to the regulation of the river by Hoover Dam, there is no doubt that this is mainly a temperature effect. The order of magnitude of the change in $\overline{C}$ agrees well with the flume observations reported above.

E. Evaluation of Theories for Suspended-Load Discharge

The analysis of suspended load can deal either directly with the total sediment transportation rate or with parameters in the equation for the concentration profile. If this concentration distribution is denoted by $c(y)$ and the velocity distribution by $u(y)$, then the sediment discharge per unit width for two-dimensional flow is given by the integral

$$q_s = \int_o^d c(y)\, u(y)\, dy \qquad (21)$$

where y is the distance up from the bed. However, because of the complex nature of the flow near the bed, and steep concentration gradients there, it is very difficult to analyze the suspended load even with the use of Eq. 21.

The equation for the concentration distribution (often called the suspended load equation) may be derived by considering the balance between the turbulent diffusion of material upward from the bed and the gravity settling back toward the bed.

Assuming similarity between the turbulent diffusion of sediment and momentum, and using von Karman's logarithmic velocity law (Eq. 1) to obtain the distribution of the diffusion coefficient, one may derive the well-known equation (33, 21) for two-dimensional flow:

$$c = c_a \left(\frac{d-y}{y} \quad \frac{a}{d-a}\right)^z \tag{22}$$

wherein c_a is the point concentration at a reference level $y = a$, d is the total depth, and the exponent z is given by

$$z = \frac{w}{\beta k u_*} . \tag{23}$$

Here w is the settling velocity of the particles, β is the ratio of the diffusion coefficient for sediment to the kinematic eddy viscosity (usually close to 1), k is the von Karman universal constant and u_* is the shear or friction velocity. Equation 22 has been verified for streams with flat beds by Vanoni (7), and for those with dune-covered beds by Barton and Lin (11) and Nomicos (Run 1, Table 13 and Fig. 35).

This suspended load equation is satisfactory except near the boundaries where the assumptions under which the equation was derived break down. Indeed, from the equation itself it is easily seen that as $y \longrightarrow 0$, $c \longrightarrow \infty$, a physically impossible situation. Consequently, it is not a simple matter to supply a boundary condition, and Eq. 22 of necessity contains an unpredictable quantity c_a at an arbitrary reference level $y = a$. Thus Eq. 22 yields only the relative distribution within the stream, whereas the absolute concentrations depend on the diffusion mechanisms right at the sand bed, i.e., the source of the suspended material. To date, little is known about the precise interactions between a turbulent stream and its movable sand bed. Obviously, if only the relative concentrations are known, it is impossible to find the sediment discharge by the integral of Eq. 21.

Therefore, to make full use of Eq. 22 it is necessary to know c_a. Since a is arbitrary, it is conveniently chosen as $a = d/2$ to make Eq. 22 read

$$c = c_{md} \left(\frac{d-y}{y}\right)^z \tag{24}$$

where c_{md}, the concentration at mid-depth, replaces c_a. When adequate laboratory and field data become available, it should be possible to find a rational relationship between c_{md} and the velocity, depth, z-value and other pertinent variables for an alluvial stream.

To find the suspended sediment discharge from Eq. 21, it is necessary to know not only z and c_{md} in Eq. 24, but also the friction factor f, the von Karman k, and shear velocity u_* which are required to evaluate $u(y)$ by Eq. 1. Moreover, there is a difficulty with the lower limit of the integral (Eq. 21) because both the functions $c(y)$ and $u(y)$ cease to apply at small, but finite, distances from the bed, and mathematically both functions become infinite as y approaches zero. Brooks (18) has discussed this problem at some length, comparing different possible choices of the lower limit in place of 0, and presents an approximate graph for quickly determining $\overline{C}/c_{md} = q_s/q\, c_{md}$ from the parameters z, k, and f.

To date there have been few published theories dealing with the evaluation of the suspended-load discharge of streams. Lane and Kalinske (34) first advanced a bed pickup theory in 1939 which is unsatisfactory because it dealt only with the pickup mechanism from a flat bed and did not recognize the importance of dunes in the entrainment process. Furthermore their analysis and subsequent modifications thereof (24) were based on the common, but erroneous, supposition that the total shear could be used as an independent variable.

In 1950, Einstein (23) made a substantial contribution to the theory by relating suspended load to bed load. His theory involves his and Barbarossa's roughness analysis (16) (discussed in Sec. C),and thus does take account of the changing bed configuration. Nevertheless, an examination of his theory will reveal that for a given bed material there is only one equilibrium rate of flow and sediment transportation rate corresponding to each combination of bed hydraulic radius and slope. Experiments presented in this report indicate that this is certainly not true for fine sand in the laboratory flume, and it is the opinion of the writers, with some substantiating evidence from Leopold and Maddock (12, 35) that this presumption is not always correct for natural rivers either.

A number of assumptions in Einstein's theory which are subject to

doubt will be reviewed briefly here. Among them are the following:

1. The concentration of suspended material at a distance equal to two grain diameters above the bed ($y = 2D$) may be considered a boundary condition for the suspended load equation (Eq. 1). This concentration is found by dividing the bed-load transport by $2D(11.6\, u_*')$ in which u_*' is the shear velocity associated with the grain resistance only.

2. The velocity distribution is expressed in terms of $u_*'/0.40$, thus implying (a) that the von Karman constant $k = 0.40$ and (b) that only the shear due to grain resistance affects the velocity distribution in the vertical.*

3. The exponent z of the suspended load equation (Eq. 22) is given by

$$z = \frac{w}{0.40\, u_*'}$$

where w is the settling velocity and 0.40 is βk (see Eq. 23). It is implied by this relation that the upward diffusion of the suspended load depends only on u_*', and not the over-all shear velocity u_* (or U_{*b}).

Using these assumptions, the product of concentration and velocity is integrated from $y = 2D$ to $y = d$ to yield the rate of suspended-load transport as a certain multiple of the bed-load transport, which in turn is determined by Einstein's basic bed-load formula (23).

Now each one of the three basic assumptions above is open to serious question, especially for runs with dune-covered beds. In the first place, it is unreasonable to apply the suspended-load equation down to an elevation of two grain diameters when the height of the dunes is of the order of several hundred grain diameters. In the second place, it should be noted that many investigators (Chien, 36) have shown that the von Karman constant

---

* Actually u_*' introduced by assumption (1) cancels the same quantity arising from assumption (2) in the final computations in Einstein's method.

k for sediment-laden streams is substantially less than the assumed value 0.40; data reported by Barton and Lin (11) and Run 1 (Table 13, Fig. 34) also show that assumption No. 2, above, is poorly supported in fact for runs with dune-covered beds. In regard to assumption No. 3, these same experiments indicate that values of the exponent z based on u_*' instead of u_* are much too large; even when u_* is used the computed z-value is still too large compared with the measured exponent when the bed is covered with dunes. Since it is not uncommon to have $u_*' < 0.5\ u_*$, the error in the shape of the suspended load distribution can be considerable as the result of using u_*' instead of u_* to compute a value of z which may be more than twice the actual value.

Although the gross errors in each of the above mentioned assumptions may tend to cancel out in the interlocking of the assumptions in the computations, the writers still believe that improvements can be made in the theory as the mechanics of sediment transportation become better understood from new laboratory and field data. Unfortunately, even in the present investigation it was not feasible to make extensive measurements of concentration profiles. Since little experimental or field data were available at the time when Einstein's theory was published, his analysis was of necessity quite theoretical.

A very recent contribution to the field has been made by Laursen (26) whose analysis is largely empirical and deals only with the sediment discharge concentration $\overline{C}$, in contrast to the theories of Lane and Kalinske, and Einstein, which each involve an equation for the concentration profile. Since Laursen's report became available just before the publication of this report, a detailed discussion of his laboratory data and proposed transportation formulas could not be included here.

A summary of the conclusions of the General Studies presented in Chapter V and discussed in Chapter VI may be found in Chapter IX.

VII. SPECIAL STUDIES *

A. Objective

As stated in the introduction, the objective of these experiments was to determine directly the effect of moving sediment on the friction factor of a stream apart from the effects of the changing dune pattern. To accomplish this, uniform flow was first established in the 10.5-inch flume with a bed covered with loose sand, and measurements were made of slope, discharge, depth and sediment transport. The flume was then drained slowly without disturbing the bed, and the sand was solidified chemically. A uniform flow of clear water with the same depth and discharge as previously obtained was then established and the slope observed. From such sets of experiments friction factors and other data for the sediment-laden and clear flows were obtained. By comparing these data, the effect of the moving sediment on the various characteristics was observed directly.

B. Apparatus and Procedure

The experiments for the special studies described in this section of the report were all made in the 10.5-inch wide flume described in Chap. III, by the procedures outlined in Chap . IV, except for the special procedures discussed below:

1. Special procedure for stabilized bed experiments. A run with uniform flow was first established by the usual techniques with determinations of depth, discharge, sediment discharge and slope. After the final determination of the bed profile by the leveling process, the flow was again started in order to regenerate the bed configuration which was, of course, destroyed when the bed profile was taken. When the bed was reestablished the flow was stopped and the water carefully drained off. The bed was then solidified by spraying with chemicals, as explained in detail in the following section. After the chemicals had set, experiments with the stable bed were made, first using clear water and then with varying small amounts of sediment added to the system. The first series of experiments in the Special Studies (Sets I, II, III, IV) was made in this way.

In the second series, some experiments (Set V) in which the bed of the flume was painted smooth were made first with clear water and then

* This chapter is based largely on a Ph. D. thesis by Nomicos (40).

with small amounts of sediment added to the flow. Others (Sets VI, VII) were made with the bed coated with the same sand that was being transported. In this case the sand was applied to the steel bottom by sifting a generous amount of it on the freshly painted bed while the paint was still wet. After the paint dried all of the loose sand was brushed off, leaving a surface much like sand paper.

2. Stabilization of sand bed. The method of stabilizing the sand bed was developed by tests of samples in trays and in actual flume tests. The most satisfactory method involved the use of sodium aluminate and sodium silicate as stabilizing chemicals. The steps followed in the stabilizing process are as follows:

(a) Drain the water from the flume and allow the sand to dry for 24 to 48 hours so that the moisture content is about 10% by weight.

(b) Spray the sand with a mixture of the following three materials:

1. 68% by volume of a 2% solution of sodium aluminate,
2. 22% by volume of a solution of sodium silicate of specific gravity 1.2,
3. 10% by volume of pure water.

This mixture was applied to the bed with a paint sprayer until the sand showed signs of saturation. This required an amount of the mixture about equal to 10% by weight of the sand being treated.

(c) After drying for about 12 hours, the sand was sprayed with a light application of a calcium chloride solution with specific gravity 1.2.

(d) Finally, a thin coat of synthetic varnish manufactured by Krylon, Inc., and sold under the trade name "Krylon Acrylic", was sprayed on the sand to form a waterproof surface.

One of the most difficult problems in the stabilization process was the preservation of the proper grain roughness of the surface of the bed. To disturb the surface characteristics as little as possible, care was taken not to apply an excess of chemicals which would flood the surface, and the solutions were applied gently with a paint sprayer aimed parallel to the bed instead of at the bed. Although the results appeared satisfactory visually,

TABLE 11

Summary of Characteristics of Sand Used for Special Studies

Sand No.	Experiments used in Set No.	D_g Geom. mean diameter mm	σ_g Geom. std. deviation	D_s Mean sed. diameter mm	w Mean fall velocity at 25° C. ft/sec
6	I, II, III, V, VI	0.091	1.16	0.105	0.031
7	IV, VII	0.148	1.16	0.161	0.062

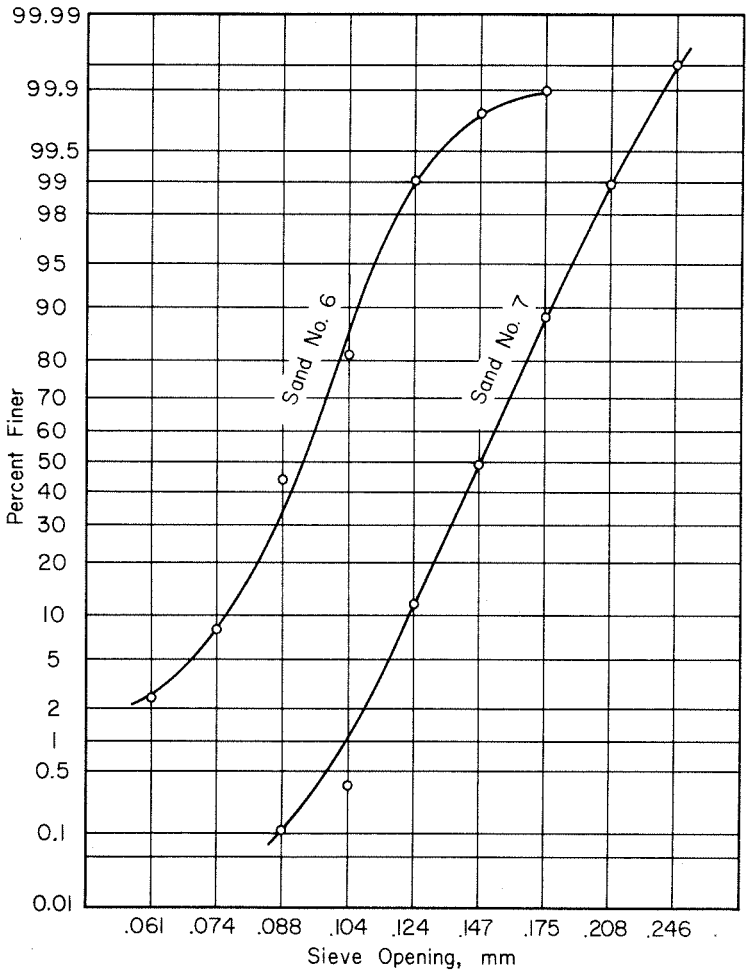

Fig. 30. Sieve analyses of the sands used in the Special Studies.

TABLE 12

Relation between sedimentation diameter and sieve diameter based on Vanoni (17) for Nevada white sand

Tyler sieve No. retained on	Sieve opening next above mm	Sieve opening retained on mm	Mean sieve diam. mm	D_{si} Mean sediment. diam. mm	w_i Fall velocity at 20° C fps	w_i Fall velocity at 25° C fps
80	0.208	0.175	0.191	0.198	0.078	0.083
100	0.175	0.147	0.161	0.168	0.061	0.066
115	0.147	0.124	0.135	0.153	0.053	0.058
150	0.124	0.104	0.114	0.128	0.038	0.042
170	0.104	0.088	0.096	0.107	0.029	0.032
200	0.088	0.074	0.081	0.096	0.024	0.027
250	0.074	0.061	0.0675	0.086	0.020	0.022

there was, unfortunately, no method of testing whether the grain roughness of the finished surface was exactly the same as that of the loose sand itself.

C. Sand Characteristics

Cumulative size frequency curves for the two sands used in these experiments are shown in Fig. 30, and the size characteristics are summarized in Table 11. These sands were prepared from white foundry sands with well-rounded grains. The material was almost entirely silica, so that the mean specific gravity of the grains was 2.65. The mean settling velocity of the various sands used was determined from sedimentation diameters of sieve fractions obtained by Vanoni (17) with a nest of sieves with openings of adjacent sieves in the ratio $\sqrt[4]{2}$. These sedimentation diameters are shown in Table 12.

D. Results

1. Outline of experiments. The general plan of the experiments may be seen from Table 13, which shows some of the principal quantities

TABLE 13

SUMMARY OF EXPERIMENTS BY NOMICOS IN 10.5-INCH FLUME, 1954-55

Set No.	Run No.	Q Discharge cfs	d Depth ft	r Hydr. Radius ft	S Slope	U_* Shear Velocity fps	U Average Velocity fps	f Friction Factor	f_b Bed Friction Factor	u_{*cl} Shear Vel. at Center Line fps	k_{cl} von Karman const. at Center Line	$\bar{C}$ Sed. Discharge Conc. gm/l	F Froude No.	Bed Condition See Footnotes	Bed Treatment See Footnotes	Amount of Loose Sand in System Kilograms
Series I, Sand No. 6, D_g = 0.091 mm, σ_g = 1.16																
I	1	0.306	0.284	0.172	0.0025	0.118	1.23	0.074	0.106	0.151	0.369	3.64	0.41	(1)	(a)	90
	1A	0.306	0.284	0.172	0.00245	0.117	1.23	0.073	0.104	0.150	0.367	3.38	0.41	(1)	(a)	90
	2	0.306	0.284	0.172	0.0026	0.121	1.23	0.077	0.112	0.155		0.00	0.41	(1)	(b)	0
	2a	0.306	0.284	0.172	0.00255	0.119	1.23	0.076	0.109	0.153		0.31	0.41	(1)	(c)	**
	2b	0.306	0.284	0.172	0.00255	0.119	1.23	0.074	0.107	0.152		0.47	0.41	(1)	(c)	**
	2c	0.306	0.284	0.172	0.0025	0.118	1.23	0.073	0.105	0.151		0.60	0.41	(1)	(c)	**
	2d	0.306	0.284	0.172	0.00245	0.117	1.23	0.073	0.104	0.150		0.83	0.41	(1)	(c)	**
II	3	0.433	0.244	0.157	0.0020	0.101	2.02	0.0198	0.0211	0.110	0.265	4.60	0.72	(2)	(a)	85
	4	0.433	0.244	0.157	0.0025	0.112	2.02	0.0246	0.0283			0.00	0.72	(2)	(b)	0
	4a	0.433	0.244	0.157	0.0023	0.108	2.02	0.0226	0.0253			1.71	0.72	(2)	(c)	**
	4b	0.433	0.244	0.157	0.0021	0.103	2.02	0.0207	0.0225			3.44	0.72	(2)	(c)	**
	4c	0.433	0.244	0.157	0.0020	0.101	2.02	0.0198	0.0211			3.63	0.72	(2)	(c)	**
III	5	0.509	0.257	0.162	0.00206	0.104	2.26	0.0169	0.0170	0.111	0.283	6.92	0.78	(4)	(a)	55
	5A	0.509	0.255	0.161	0.00206	0.104	2.28	0.0165	0.0165	0.109	0.219	8.08	0.79	(4)	(a)	55
	6	0.509	0.255	0.161	0.00251	0.114	2.28	0.0208	0.0229	0.136	0.384	0.00	0.79	(4)	(b)	0
	6a	0.509	0.255	0.161	0.00227	0.108	2.28	0.0182	0.0189	0.116	0.255	3.99	0.79	(4)	(c)	3.00
	6b	0.509	0.254	0.161	0.00227	0.108	2.28	0.0180	0.0187	0.116	0.236	5.71	0.80	(4)	(c)	5.00
	6c	0.509	0.252	0.160	0.00210	0.104	2.30	0.0163	0.0164	0.114	0.209	6.82	0.81	(4)	(c)	9.00
Series I, Sand No. 7, D_g = 0.148 mm, σ_g = 1.16																
IV	7	0.509	0.255	0.161	0.00258	0.116	2.28	0.0207	0.0227	0.135	0.299	3.61	0.79	(4)	(a)	55
	8	0.509	0.253	0.160	0.00293	0.123	2.29	0.0230	0.0262	0.150	0.364	0.00	0.80	(4)	(b)	0
	8B	0.509	0.253	0.160	0.00259	0.116	2.29	0.0203	0.0222	0.134	0.355	0.00	0.80	(4)	(b)	0
	8a	0.509	0.254	0.161	0.00259	0.116	2.28	0.0206	0.0225	0.135	0.345	0.51	0.80	(4)	(c)	0.50
	8b	0.509	0.253	0.160	0.00257	0.116	2.29	0.0202	0.0219	0.133	0.330	1.41	0.80	(4)	(c)	1.50
	8c	0.509	0.253	0.160	0.00257	0.116	2.29	0.0202	0.0219	0.133	0.319	2.43	0.80	(4)	(c)	3.00
	8d	0.509	0.253	0.160	0.00259	0.116	2.29	0.0203	0.0222	0.134	0.310	3.27	0.80	(4)	(c)	4.00
Series II, Sand No. 6, D_g = 0.091 mm, σ_g = 1.16																
V	9	0.509	0.255	0.161	0.0020	0.102	2.28	0.0160	0.0162	0.113	0.364	0.005	0.79	(6)	(d)	0.005
	9a	0.509	0.255	0.161	0.0020	0.102	2.28	0.0160	0.0162	0.113	0.360	0.05	0.79	(5)	(e)	0.040
	9b	0.509	0.255	0.161	0.0020	0.102	2.28	0.0160	0.0162	0.112	0.354	0.13	0.79	(5)	(e)	0.12
	9c	0.509	0.255	0.161	0.0020	0.102	2.28	0.0160	0.0162	0.112	0.348	0.42	0.79	(5)	(e)	0.30
	9d	0.509	0.254	0.161	0.00205	0.103	2.28	0.0163	0.0164	0.113	0.319	1.02	0.80	(3)	(e)	1.10
	9e	0.509	0.253	0.160	0.00207	0.104	2.29	0.0163	0.0164	0.114	0.284	2.10	0.80	(3)	(e)	2.20
	9f	0.509	0.252	0.160	0.0021	0.104	2.30	0.0163	0.0164	0.116	0.258	3.46	0.81	(4)	(e)	4.00
	9g	0.509	0.250	0.159	0.0022	0.106	2.32	0.0167	0.0169	0.119	0.227	8.06	0.82	(4)	(e)	8.00
VI	10	0.509	0.255	0.161	0.0021	0.104	2.28	0.0168	0.0170	0.113	0.348	0.00	0.79	(6)	(f)	0
	10a	0.509	0.255	0.161	0.0021	0.104	2.28	0.0168	0.0170	0.113	0.326	0.75	0.79	(5)	(g)	0.50
	10b	0.509	0.255	0.161	0.0021	0.104	2.28	0.0168	0.0170	0.113	0.307	2.33	0.79	(3)	(g)	1.50
	10c	0.509	0.255	0.161	0.0021	0.104	2.28	0.0168	0.0170	0.113	0.275	5.56	0.79	(4)	(g)	3.50
	10d	0.509	0.255	0.161	0.0021	0.104	2.28	0.0168	0.0170	0.113	0.242	6.28	0.79	(4)	(g)	7.00
Series II, Sand No. 7, D_g = 0.148 mm, σ_g = 1.16																
VII	12	0.509	0.255	0.161	0.00222	0.107	2.28	0.0178	0.0184	0.119	0.359	0.00	0.79	(6)	(f)	0
	12a	0.509	0.255	0.161	0.00222	0.107	2.28	0.0178	0.0184	0.120	0.335	0.51	0.79	(5)	(g)	0.50
	12b	0.509	0.254	0.161	0.00243	0.112	2.28	0.0193	0.0206	0.127	0.328	1.65	0.80	(3)	(g)	2.00
	12c	0.509	0.254	0.161	0.00253	0.114	2.28	0.0201	0.0218	0.131	0.314	2.83	0.80	(4)	(g)	3.50
	12d	0.509	0.255	0.161	0.00255	0.115	2.28	0.0204	0.0223	0.134	0.299	3.26	0.79	(4)	(g)	7.00

Notes: 1. Temperature for all runs: 25.0°C.

2. ** Not measured.

Key for Bed Condition:

(1) Dunes

(2) Dunes, largest at walls tapering down to nearly flat in center of flume.

(3) Ripples near walls, flat in center.

(4) Flat except for slight ripples extending about 2 inches out from walls.

(5) Flat or streaks, very little sand in system.

(6) No loose sand.

Key for Bed Treatment:

(a) Bed of loose sand covering bottom of flume.

(b) Sand bed stabilized in natural configuration with no loose sand.

(c) Sand bed stabilized in natural configurations with loose sand added.

(d) No sand, bed of flume painted (smooth).

(e) Small amounts of sand added, starting with bed of flume painted (smooth).

(f) No loose sand, bed of flume painted and coated with sand grains (of size to be transported).

(g) Small amounts of sand added, starting with bed of flume coated with size of sand being transported.

measured. The experiments are divided into series, sets and individual experiments. The first four sets of experiments comprise the first series, and the remaining three sets comprise the second. The flow depth, discharge and mean velocity are kept the same in each set of experiments, but the slope is varied. In Sets III to VII the depth, discharge and velocity are kept constant throughout.

Each set in the first series contains runs with (i) movable bed, (ii) stabilized bed and clear water, and (iii) stabilized bed with varying amounts of loose sand added to the system where the material added is the same as that in the bed. In Runs 2, 4, 6 and 8 of the first series, the bed was stabilized and no sediment was being transported by the flow, i.e., the flow consisted only of clear water.

Table 13 shows the most important measured and calculated quantities obtained in the experiments. Where blank spaces occur in the table, the items were either not measured or not calculated. Measured values of the exponent z in the suspended load equation (Eq. 22) are listed in Fig. 35 for Runs 1, 3, 5 and 7.

2. Bed configuration. Observations of the bed configuration and the movement of the configuration were made visually and by means of systematic photographs during the experiments. Figure 31 shows a side view of the bed for Run 1 and a plan view for Run 2, where the bed configuration for Run 2 is the same as that for Run 1 except that it has been stabilized by the method described previously. Figure 32 shows a similar set of pictures for Runs 3 and 4. The pictures of Figs. 31 and 32 illustrate the meaning of the terms used to describe the bed condition in the 15th column of Table 13. Figure 33 shows the side view and plan view of the bed in Run 5, which has been described as "flat" in Table 13. It will be seen that the bed is actually not entirely flat but that there are small ripples near the wall.

3. Velocity profiles. Velocity profile measurements were made at the centerline of the flume at Station 24, i.e., 24 feet downstream from the inlet to the flume. These measurements fitted the logarithmic law very well, as may be seen in Fig. 34 which shows the profiles for some of the runs (Nos. 1, 3, 5 and 6). The quantity m noted on the figure is the slope

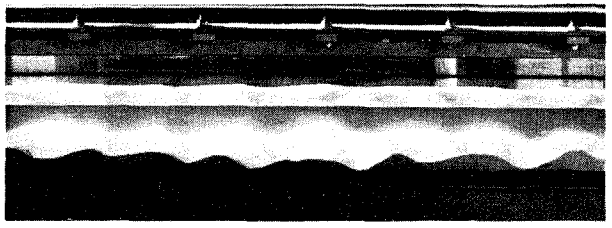

Fig. 31 (a). Run 1, side view, loose sand, during flow.

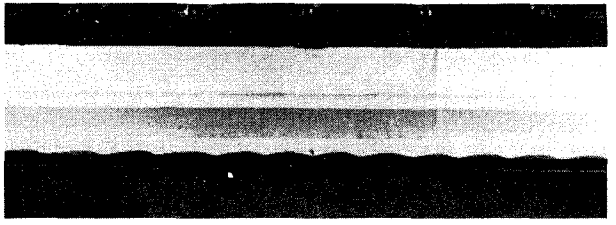

Fig. 32 (a). Run 3, side view, loose sand, during flow.

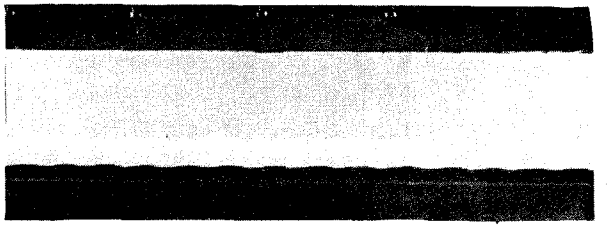

Fig. 33 (a). Run 5, side view, loose sand, without flow.

Fig. 31 (b). Run 2, plan view, stabilized bed, looking upstream, without flow.

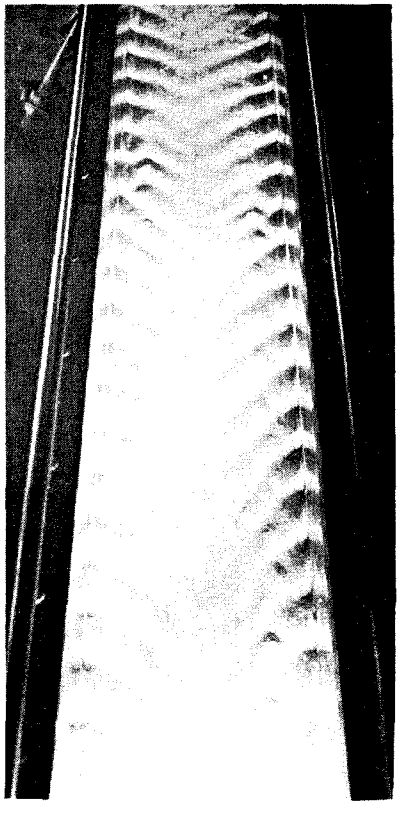

Fig. 32 (b). Run 4, plan view, stabilized bed, looking upstream, without flow.

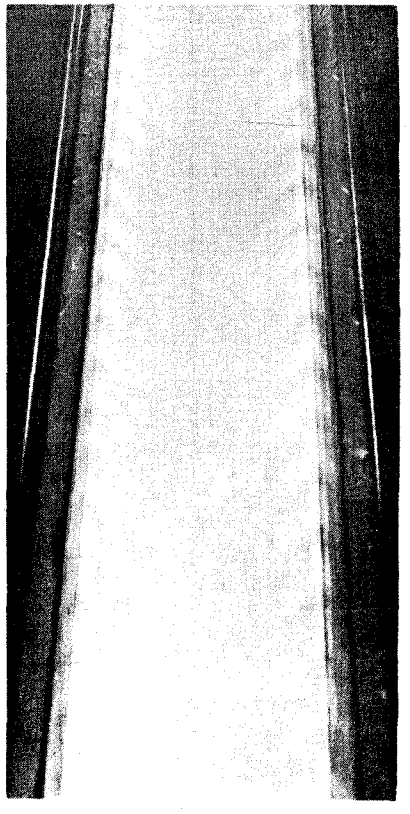

Fig. 33 (b). Run 5, plan view, looking upstream, loose sand.

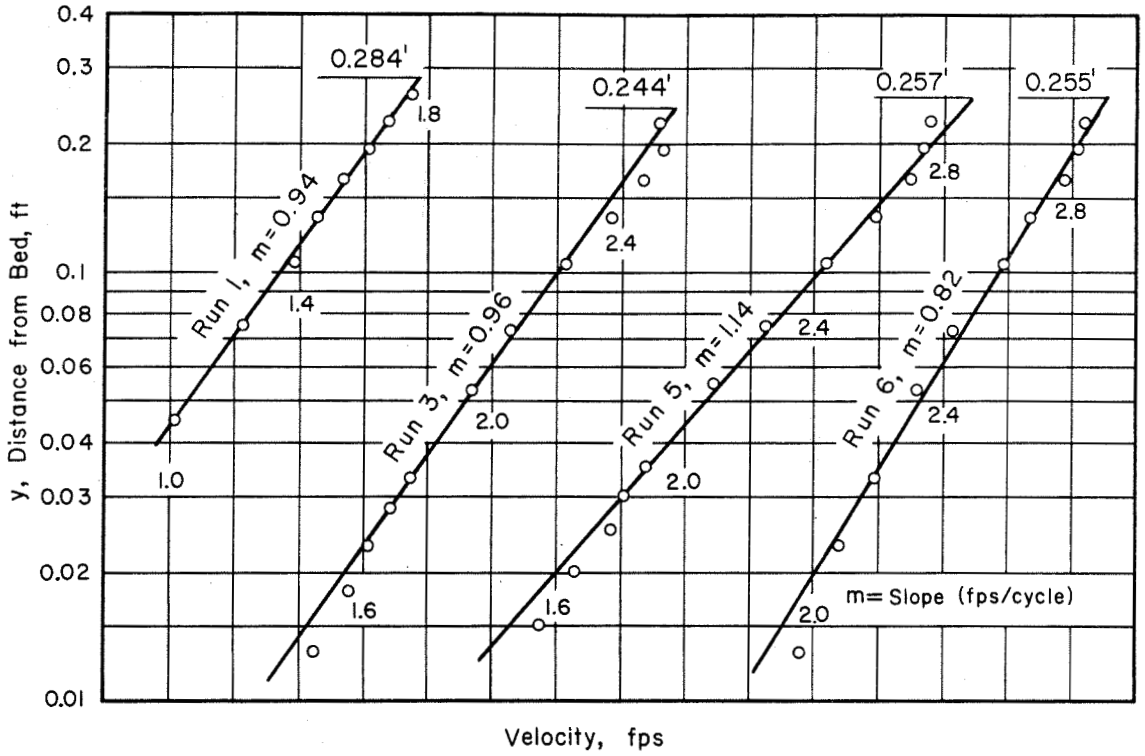

Fig. 34. Measured velocity profiles at the centerline of the flume at Station 24 for Runs 1, 3, 5, 6.

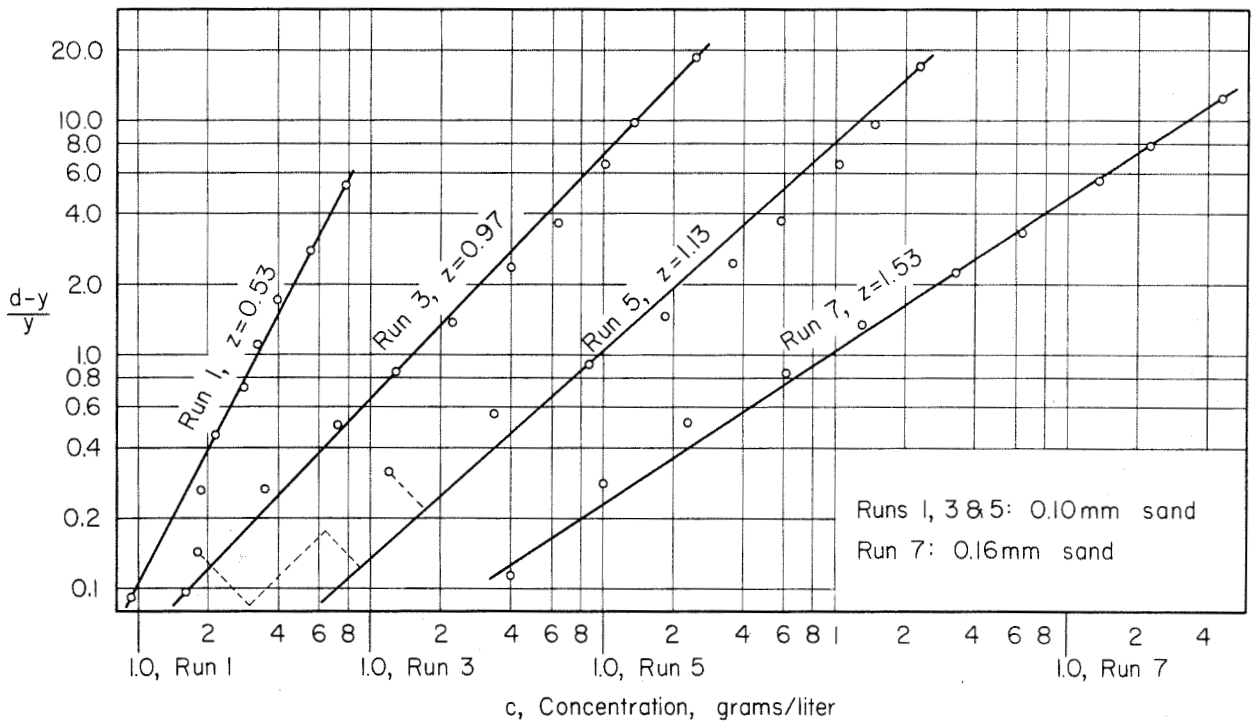

Fig. 35. Measured concentration profiles on centerline of the flume at Station 24 for Runs 1, 3, 5, 7.

of the lines fitted to the points in fps per cycle. The von Karman constant k is determined from Eq. 3 using the centerline shear from Eq. 4 and m as determined from the graphs. The values of k, which are listed in Table 13, consistently decrease as the concentration $\overline{C}$ increases.

4. Sediment concentration profiles. Figure 35 shows logarithmic graphs of $(d - y)/y$ versus c for measurements made on the longitudinal centerline of the flume. It is seen that these sediment profiles follow Eq. 22 (or 24) which is the well-established equation for distribution of suspended load. The values of the exponent z calculated by Eq. 23 using $k_{c\ell}$ from Table 13, $\beta = 1$, and $u_* = u_{*c\ell}$, (the centerline value defined by Eq. 4) are very close to those determined from the slope of the lines in Fig. 35. It is of interest to note that the profile for Run 1 agrees with the theory as well as the other runs in spite of the fact that it is the only one of the four for which the bed was covered with dunes.

5. Friction factor. From Table 13 it is seen that the bed friction factor f_b for sediment-laden flow over loose sand beds is less then f_b for comparable clear flow over fixed beds of the same configuration. The f_b-values for comparable sediment-laden and clear-water flows are summarized in Table 14. This shows clearly the effect of moving sediment in reducing the friction factor from 5 to 28 percent. The results shown in Tables 13 and 14 also indicate roughly that the larger decreases in the friction factor f are associated with larger mean concentrations $\overline{C}$.

Attention is called to the fact that f_b-values for the identical runs, Runs 8 and 8B, with clear water and stabilized bed are not the same. Run 8 was made once and then repeated on the following day, and the results agreed closely. However, when the water had been in the flume for longer than a total time of about ten hours, the flow characteristics changed slightly, giving the results of Run 8B. To further investigate this problem Run 8B was repeated three times, once on each of three days, drying the sand bed after each experiment. On the first day the water was run continuously.

TABLE 14

Comparison of friction factors for sediment-laden streams with those for clear water flows over stabilized sand beds

Set No.	Run No.	Depth ft	Bed Cond.	Sed. Disch. Concent. $\overline{C}$ grms/liter	Friction Factors f	Friction Factors For Bed f_b	Decrease Δf_b	Decrease %
I	1	0.284	Dunes	3.64	0.074	0.106	.006	5
	2	0.284	Dunes	0	0.077	0.112		
II	3	0.244	Small dunes	4.60	0.0198	0.0211	.0072	25
	4	0.244	"	0	0.0246	0.0283		
III	5A	0.255	Flat	8.08	0.0165	0.0165	.0064	28
	6	0.255	Flat	0	0.0208	0.0229		
IV	7	0.255	Flat	3.61	0.0207	0.0227	.0035	13.5
	8	0.253	Flat	0	0.0230	0.0262		

Cn the second day the experiment was completed in as short a time as possible and the pump stopped, leaving the water in the flume. After about three hours the run was repeated. The flow characteristics and friction factor of the flow were changed by approximately the same amount as they would have been if the water had been running continuously. The run for the third day was a repetition of that for the first, with approximately the same results. From this it was concluded that the water was in some way affecting the varnish coat applied to the sand when the water remained in the flume for long periods. Run 8 is considered to give the valid results, with Run 8B being affected by swelling of the varnish between grains.

Table 13 shows for Set V that f_b changes very little as concentration changes, and in Set VI no change occurred despite the development of ripples on the bed. These two sets of experiments were made with 0.1 mm sand. In Set V the flume bottom was smooth painted steel, and in Set VI the bed was roughened with the same sand as was being transported, i.e., 0.10 mm sand. Cn the other hand, in Set VII where 0.16 mm sand was used, f_b increased continuously as the load increased. In this set the mean concentration was less, and more ripples developed on the bed than in Sets V and VI.

The results are discussed further in Chap. VIII, with some possible explanations for the observations.

VIII. DISCUSSION OF RESULTS OF SPECIAL STUDIES

A. Effect of Sediment Load on the Friction Factor

The effect of the sediment load on the friction factor may be seen in Table 14 by comparing the results of clear and sediment-laden water for each set of runs. Sets I, II and III were made with the same sediment, so the results are directly comparable. Set IV was made with a coarser material. It is clear that by adding a sediment load to a flow the friction factor is decreased, since in all four sets of experiments the sediment-laden flows had smaller friction factors than the comparable clear flows. The relative magnitude of the reduction in friction factor seems to vary with concentration, the values with highest concentration producing the largest change. Referring again to Table 14, it is seen that in Set I the friction factor f_b for a flow with a concentration of 3.64 grams per liter was 5 percent lower than the comparable clear flow. In Series II and III the reductions in f_b were 25 percent and 28 percent with concentrations of 4.60 and 8.08 grams per liter, respectively. From these figures it

appears that rate of change in f_b with concentration decreases at high values of the concentration.

The fact that the friction factor in Sets V and VI did not change appreciably seems to be a coincidence. To begin with, the two sets of runs are alike for all practical purposes, since the same bed material was used with the same discharge and depth. The fact that some ripples developed during the run means that the roughness of the bed must have increased. However, f_b did not change, which means that the damping effect offset the increase in bed roughness due to the formation of ripples. By contrast, the fact that f_b increased continuously with increasing $\overline{C}$ in Set VII, indicates that the increased roughness due to the slight ripples overshadowed the tendency for the sediment in suspension to decrease f_b.

The reduction in f_b may be attributed to alterations of the turbulent structure of the flow by the suspended load. The mechanism of this process is discussed in more detail in Section C below.

B. Effect of Bed Configuration on the Friction Factor

The effect of dunes and ripples on the friction factor agrees with the data presented in Chap. V. For example, the large dunes in Set I cause f_b to attain the high value of 0.106 in Run 1, compared with the values for all other runs which were less than 0.030 because of predominantly flat beds. From these data one can conclude that in flume experiments changes in friction factor due to dunes can greatly exceed changes due directly to the moving sediment.

In a study of the Mississippi River, Eden (13) observed that at Vicksburg the largest dunes occurred at the highest stage. At Memphis, he observed bed irregularities only on the rising part of the highest stage. The largest of these had heights as much as 34 feet. Carey and Keller (14) observed bed configurations of the Mississippi River near Baton Rouge by means of a sonic fathometer. They also found that the largest dunes occurred at the highest stages. There were several systems of dunes of varying wavelengths, the largest of which had lengths of as much as two miles and heights of the order of 30 feet. The shorter dunes were superposed on the larger ones. A study of these profiles showed that at low stage the long waves disappeared but that short waves of the order of 20 to

50 feet in length and 1 to 5 feet in height remained. Figure 36, reproduced from the work of Carey and Keller, shows profiles at Donaldsonville gage for two stages. For the high stage which occurred on April 10, 1956, it is seen that there are waves of considerable length. For the lower stage which occurred in July, the long waves are no longer present. Despite the increase in dune height with stage, Eden (13) found that the Manning coefficient n decreased as the stage increased. The sediment load also increases with stage, and can account for some reduction in the roughness factor but not necessarily for all of it. It is possible that the long waves actually do not contribute much to the bed roughness and that the shorter, steeper ones, which seem to predominate at the low stages, may actually result in a higher roughness than the larger ones which have been observed at the highest stages.

Data presented by Leopold and Maddock (12, 35), an example of which is Fig. 37, for the spring flood of the Colorado River at the Grand Canyon (1941), show that for a given discharge the velocity is higher on the rising flood when the concentration is high than on the falling flood when the concentration is considerably lower. The fact that the depth is less on the rising than on the falling flood means that the friction factor is lower on the rising flood, assuming insignificant changes in slope and slow rate of change of stage. This follows the same pattern as observed in flume experiments where flows with the higher velocities and sediment concentration tend to have lower friction factors, although it is not clear from the field data whether the damping effect of suspended sediment or change in the bed configuration is the predominate factor.

Leopold and Wolman (37) report that in degrading portions of the Rio Grande the river channel characteristics follow a pattern similar to that of the Colorado River shown in Fig. 37. In the lower reaches of the river where the bed was aggrading, the velocity and sediment concentration were lower on the rising than on the falling flood, so that the friction factor was now highest on the rising flood. The lower friction factor is still associated with high concentration, but for some reason the sequence of change has been reversed. These same authors (37) also report that the characteristics of streams in the sub-humid areas, such as in the eastern United States, are much more stable than those of the arid western part. The sediment loads are much lower and the beds apparently much more stable,

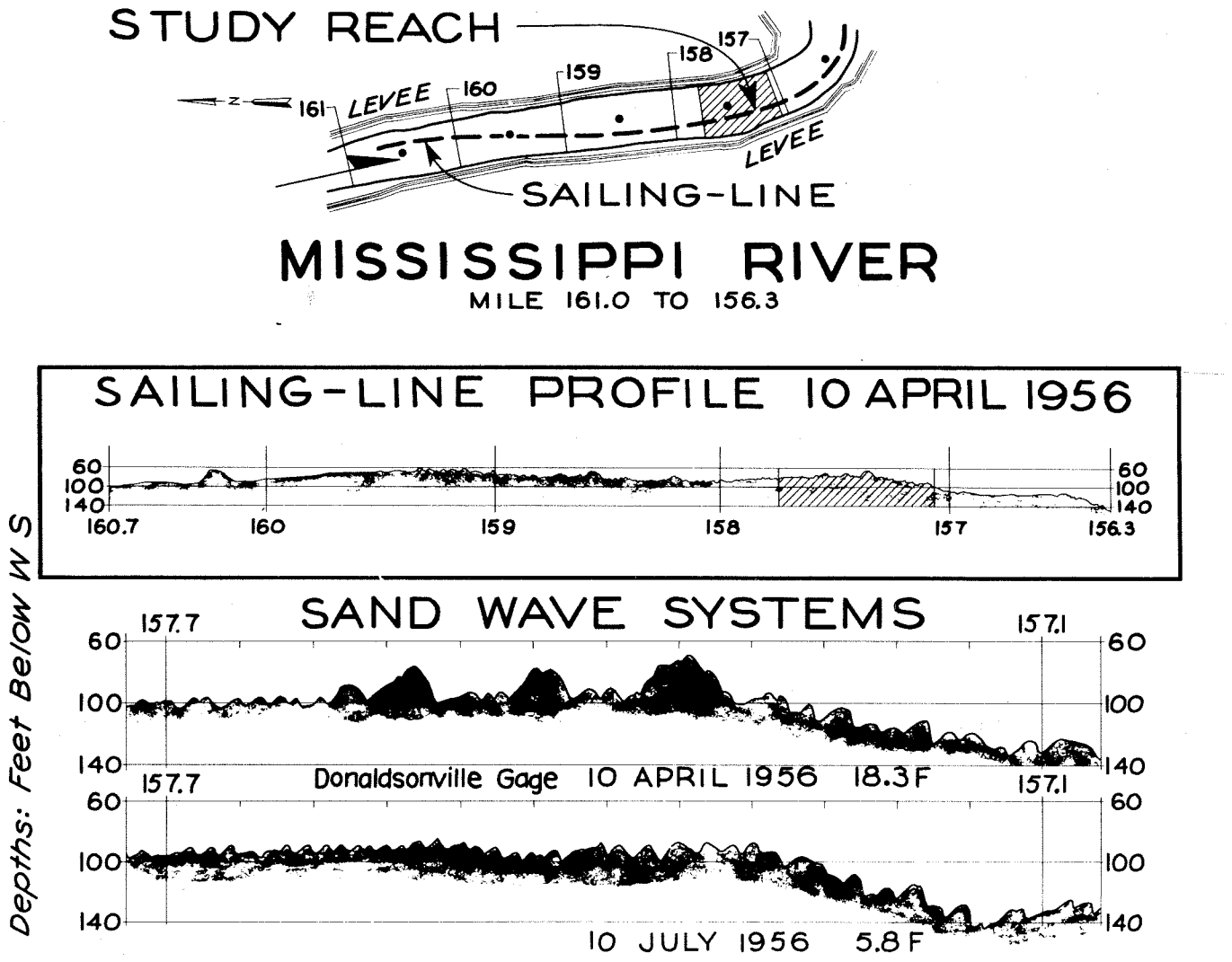

Fig. 36. Bed profiles for lower Mississippi River (Louisiana) from Carey and Keller (14).

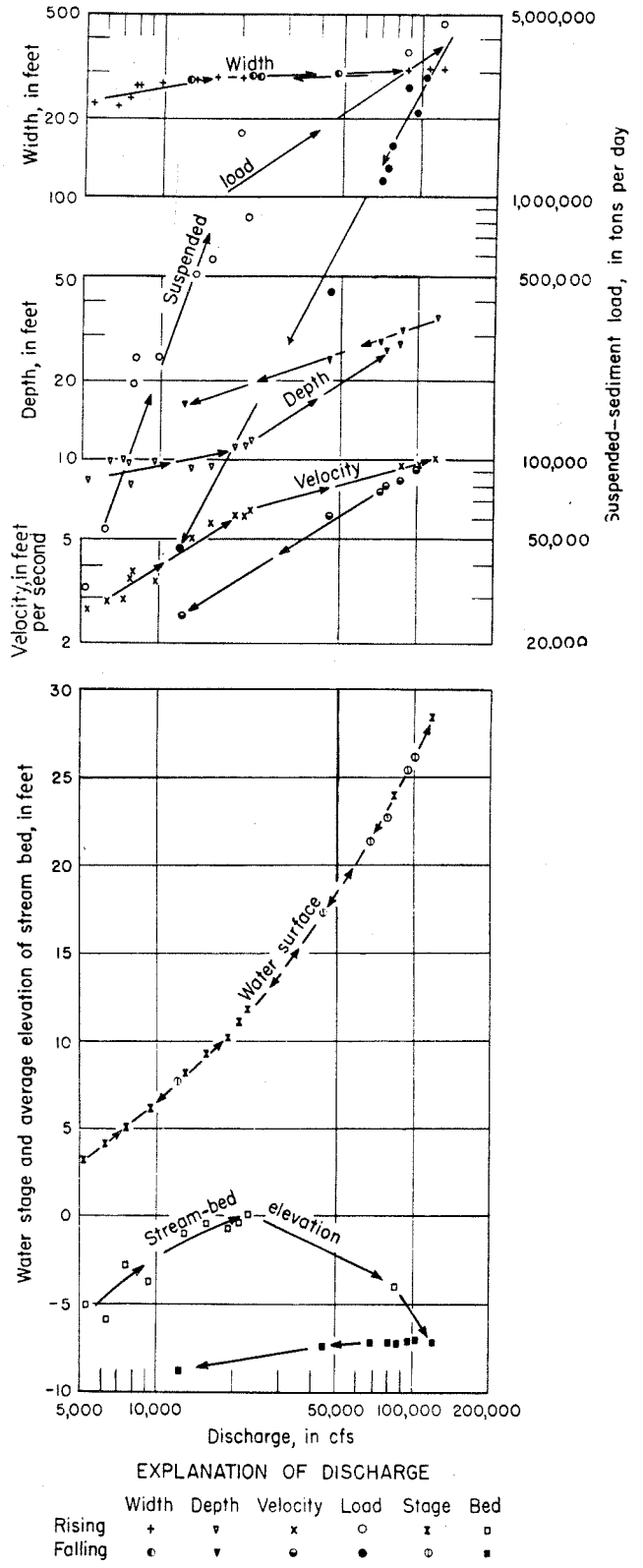

Fig. 37. Changes in width, depth, velocity, stage, and stream-bed elevation with discharge during flood of December 1940-June 1941, Colorado River at Grand Canyon, Arizona (from Leopold and Maddock (35)).

so that the changes in the bed are probably much smaller than in streams whose beds are easily eroded.

C. Effect of Sediment Load on the Velocity Profile

The effect of suspended sediment on the velocity profile of a stream is illustrated by Fig. 2, which shows profiles for a clear flow and sediment-laden flow with the same depth and slope. It is clear that in addition to having the higher velocity at any level, the sediment-laden flow also has a higher velocity gradient. Figure 2 shows that very near the bed the velocity of the two flows is about the same, so that some distance from the bed the flow with the higher velocity gradient will have the higher velocity. By differentiating the equation for the velocity distribution, Eq. 1, with respect to y, one obtains

$$\frac{du}{dy} = \frac{1}{ky}\sqrt{\frac{\tau_o}{\rho}} = \frac{u_*}{ky} \tag{25}$$

Since in the two flows the shear velocity u_* is the same, the gradient for any value of y is inversely proportional to k, and since the gradient is seen to increase with load, k must decrease with the load. Thus it can be seen that the effect of sediment on the velocity gradient can be studied by observing k.

The fact that suspended sediment increases the velocity gradient was observed by Gilbert (1, page 229), although the full significance of this was apparently not realized. Flume experiments (7, 8) have shown that this is a systematic effect, and observations on the Missouri River by the Corps of Engineers (38) showed that this effect was also present in natural streams. The mechanism by which the sediment increases the gradient, and hence the mean velocity, has been explained in terms of the damping effect of suspended material on the turbulence (7).

To keep sediment in suspension, i.e., to prevent it from settling due to gravitational force, work must be done on the sediment grains. This work must come from the vertical components of turbulence fluctuations and must result in damping of the turbulent motion. To investigate this problem, Einstein and Chien (39) correlated k with the ratio of the power, P_s, to suspend sediment to the power, P_f, to overcome hydraulic resistance

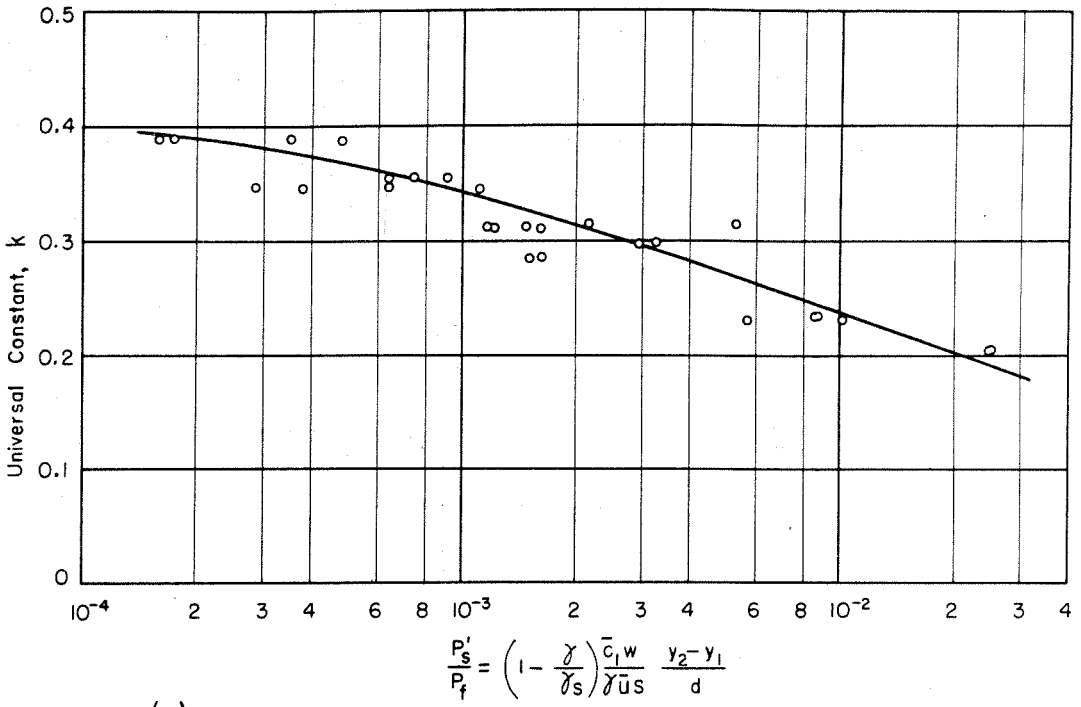

(a)

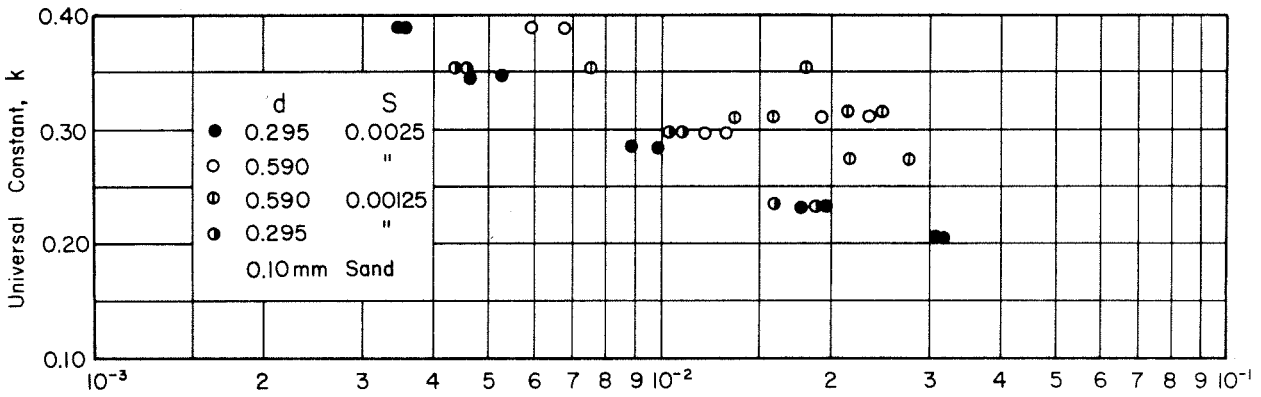

(b)

Fig. 38. Reduction of the von Karman constant for sediment-laden flow.

Note: $\bar{c}$ = mean concentration over depth

$\bar{c}_1$ = mean concentration over interval $y_1/d = 0.001$ to $y_2/d = 0.01$

P_f = power to overcome friction of prism of water of unit width and height equal to flow depth

P_s = power to suspend sediment contained in water prism

P_s' = power to suspend sediment contained in water prism between levels y_1 and y_2.

to the flow, using data obtained from measurements on the Missouri River and from laboratory experiments by Ismail (21). A similar graph was presented (8) for flume experiments made with 0.1 mm sand. Buckley (6) and Chien (36), in discussing the effect of sediment on the flow, postulated that the main damping effect of the sediment on turbulence occurred near the bed where the concentration was highest. This appears reasonable since it is in this zone that the shear rate is highest and most of the turbulence is produced. With this idea in mind, k was correlated against the ratio of the power P_s' to suspend the sediment in a thin layer near the bed to the power P_f required to overcome the frictional resistance. Figure 38a shows such a graph for flume data obtained with uniform sand of 0.1 mm size. Figure 38b shows a graph of the same data (8) plotted according to the method of Einstein and Chien (39), i.e., k is plotted against P_s/P_f. It is seen that the correlation of the data in Fig. 38a is better than in 38b. This tends to support the ideas of Buckley and Chien and may also explain why the velocity remains logarithmic, as seen in Fig. 2, even though the turbulence has been modified considerably. If significant damping of the turbulence occurred over the entire depth, one would expect a distortion in the distribution of the turbulence, and hence in the shape of the velocity profile. However, if the principal interference with the turbulence occurs near the bed, the turbulence energy will be reduced but it may still follow the same laws in diffusion through the section, and one might expect the same shape of velocity distribution.

Referring again to Fig. 2, it is seen that the two flows have the same depth and hence hydraulic radius, and the same slope. The one with the higher mean velocity, i.e., the sediment-laden flow, will have the lower friction factor. The decrease in f, shown in Table 14 for the sediment-laden flows, results from the damping phenomenon discussed above. A comparison of the k-values listed in Table 13 will show that the turbid flows have much the lower values, thus indicating that damping has occurred.

D. General Discussion

The present experiments have shown that a sediment-laden stream acts in two ways to change its roughness coefficient: (1) a change in the bed configuration tends to reduce the coefficient as the velocity increases; (2) damping of the turbulence by suspended sediment tends to increase the

velocity gradient so that the difference between the velocity near the bed and near the surface increases along with the mean velocity. In the laboratory experiments with 0.1 mm sand, the change in the bed friction factor f_b resulting from change in bed configuration alone was as much as 5-fold in going from a dune-covered bed to a flat bed. On the other hand, the maximum reduction in f_b due to the sediment load was only 28 percent (Run 5A). Since the Manning roughness coefficient n is approximately proportional to $\sqrt{f_b}$, the corresponding changes in n are about 2-fold and 13 percent, respectively. It is significant that the run which showed the maximum damping effect, i.e., Run 5A also had the lowest value of k as determined from the centerline velocity profile. From these few data, it appears that the change in bed configuration has a much larger influence on the roughness coefficient than the damping effect. From this one would judge that the large reductions in roughness coefficients reported by Buckley for the Nile, Eden for the Mississippi, and Lindley for the Indus River, could not be the result only of damping, but must have been also affected by significant changes in dunes on the bed. Judging from the flume experiments one would expect the dunes to diminish as the velocity increased, while, at the same time the load increased. Since both of these effects tend to reduce the roughness coefficient, the field observations are in agreement with flume studies and the process can be explained at least qualitatively by the combination of the two effects.

The explanation of the observations that for the same discharge the roughness coefficient of a stream on a rising flood is smaller than on a falling flood presents some difficulties. Buckley and Lindley noted that during the rising flood the concentration was higher, and explained the reduction in roughness by the effect of the higher load. Judging from the results of the present experiments as shown by Table 14, the changes in roughness factor observed in the field are too large to be accounted for by damping effect alone, and some readjustment of the bed must be involved in order to achieve the changes observed. During the rising stage the stream bed probably becomes smoother because the transportation of a high sediment load requires a lower depth and higher velocity compared with the falling-stage flow for which the transport rate is usually less (cf. Fig. 24); however, since the damping effect also reduces the roughness, it is not possible to determine the relative magnitude of the two effects from

the field data alone. Bottom configuration data of the kind obtained by Carey and Keller, along with stage, slope, discharge and load data, would do much to clarify this problem.

The field data of Buckley, Lindley, Leopold and Maddock on the variation of stream characteristics, report only total sediment concentration and do not give size distribution of the load or division between wash load and bed-material load. As seen from Fig. 38, the effect of concentration on k, and hence upon friction factor, depends on the settling velocity w as well as the concentration, so that for the same $\overline{C}$, coarse material with high settling velocity has a greater effect on k and on the reduction in friction factor. By the same token, fine materials such as silt and clay have low settling velocities, and hence small damping effects even for large concentrations. The loads in streams such as the Indus, Colorado and Rio Grande, which show a correlation between mean concentration and velocity (or friction factor) (6, 12) are predominantly fine sediments which should have small damping effects, yet changes in load are accompanied by substantial changes in friction factor for the same discharge. According to laboratory results it is unlikely that all of this is caused by damping effects.

The discussion thus far has dealt with those observations that show a reduction in friction coefficient as the load increases; however, it will be recalled that Kantlack (6) reported that Swiss engineers found that the velocity was reduced by an increase in the load, and that Latham (3) reported a similar behavior in a storm sewer. The latter might be explained by postulating that dunes formed when sediment was being transported, thus causing a high friction factor, and that during clear flows sediment was cleaned out of the sewer, leaving the water in contact with the smooth walls, which resulted in low friction at low flow. The explanation of the behavior of the Swiss rivers may be associated with the phenomenon observed in the 33.5-inch flume at low transportation rates; as may be seen in Fig. 22 (Chap . VI), there was a tendency at low velocities (i.e., low transportation rates) for the friction factor to increase with the velocity to a maximum, and then to decrease as the velocity increased further. The experiments which yielded the data of Fig. 22 are listed in Table 6. Two similar sets of experiments (Fig. 20, 21) made in the 10.5-inch flume did not yield a maximum for f_b as shown in Fig. 22. Therefore, the explanation offered above, based on this one set of experiments, must be considered as speculative.

IX. SUMMARY AND CONCLUSIONS

This report describes investigations of the roughness and sediment transport in alluvial streams with beds of fine sand. The experiments in the two laboratory flumes have been presented in two parts: General Studies, Chapters V and VI, and Special Studies, Chapters VII and VIII. In the General Studies, 40 runs were performed with the bed of the flume covered with loose sands, all with a median size of about 0.14 mm but with geometric standard deviations ranging from 1.30 to 1.76. Under some conditions the bed of the stream became covered with dunes, while at other times it was relatively flat. The friction factor for the bed varied widely.

While the General Studies represented more or less natural conditions, the Special Studies were aimed at separating the two processes affecting channel roughness by means of some unnatural experiments involving solidification of the fine sand bed. In this way the friction factors were determined for runs with identical bed configurations but with suspended sediment loads ranging from zero to the equilibrium rate. It was found that the reduction in friction factor due to the suspended load directly ranged only from 5 to 28 percent for the experiments conducted, whereas the change in bed configuration may change the friction factor several fold.

Although the General Studies and the Special Studies are complementary, the conclusions from each will be summarized separately below.

A. General Studies

The 51 runs in the General Studies were actually undertaken as an extension of the research by Brooks (9, 18) to consider the basic relationships between depth, velocity, slope, friction factor, sediment discharge and bed configuration. Twenty-five of the runs were made in the 10.5-inch wide flume and 26 in the 33.5-inch flume, 11 of the latter runs being with clear water. For these runs, no velocity or concentration profiles were measured. The principal findings may be summarized as follows:

1. As reported by Brooks (9), the discharge and sediment load may not be expressed as unique functions of the depth, slope, and sand size. This comes about because, at a given depth, there are often two or

three different values of the velocity which yield the same value of slope. The fact that the slope does not always increase with increasing velocity is due to the fact that the roughness decreases tremendously when the velocity becomes high enough to obliterate the dunes.

2. When either velocity and depth or water and sediment discharge are used as the pair of independent variables, no difficulty with multiple solutions was observed. No quantitative formulas are presented, but certain qualitative relationships are described at the end of Section A, Chapter VI, (pages 55-57). These conclusions are essentially the same as those given previously (9, 22).

3. Data from the Rio Grande River at Bernalillo, New Mexico, show behavior which is similar to that observed in the laboratory flume. When discharge is plotted against hydraulic radius, one finds not a unique curve but a loop. It is believed that the cause of this loop is not change in slope, but rather a response of the stream to different incoming sediment loads of bed material. When the bed-material load is high the depth will tend to be smaller and the velocity higher than when the load is smaller; in the latter case dunes are likely to appear and roughen the bed. Similar loops in rating curves have been reported by Carey and Keller (14).

4. An analysis of available roughness data from laboratory flumes and the field are compared to the Einstein bar-resistance curve in Figs. 27, 28, and 29. The agreement is not wholly satisfactory, and no explanation is advanced for the discrepancies.

5. Other things being equal, the sediment transport rate is larger when the geometric standard deviation of the bed material is larger (with the geometric mean size D_g kept fixed). With a greater spread in the sizes, there is more fine material available for transport.

6. In almost all cases, the D_g for the suspended load was considerably less than for the bed material.

7. As previously found by other investigators, the temperature has a significant effect on the transport rate. For example, in one case with dune-covered bed, a change of temperature from 15.0°C to 35.6°C resulted in a decrease of the sediment concentration from 0.31 gr/ℓ to 0.11 gr/ℓ.

B. Special Studies

Seven sets of runs were made in the 10.5-inch flume in an effort to separate the direct effect of suspended sediment on the friction factor from that of the bed configuration. First, a natural run was established over a loose bed of fine sand, and then, after draining the water, the bed

was chemically solidified in its naturally formed configuration. Loose sand was removed from the system then and a flow of clear water was run over the stabilized bed, with the usual measurements being taken. Following that, small increments of sand were added, noting the change in the friction factor which resulted. From these experiments the principal conclusions are as follows:

1. Suspended sediment reduces the friction factor of a flow. The amount, in a limited series of laboratory experiments, varied from 5 to 28 percent.

2. The changes in the friction factor due to variation in bed configuration are much larger than those due to the suspended load itself. A friction factor may change by a factor of 3 to 6 in the laboratory flume between runs of differing velocity at constant depths.

3. Evidence indicates that the suspended load reduces the friction factor by damping the turbulence or interfering with its production near the bed where the sediment concentration is the highest and the rate of turbulence production is the greatest.

4. As observed by previous investigators, the von Karman constant k is also substantially reduced by the suspended sediment.

5. In the field it is impossible to distinguish between the two above-mentioned factors affecting alluvial channel roughness. However, it has been established that the reduction due to the suspended sediment is of importance only for streams carrying a very high suspended load over a flat bed, and can be practically neglected when there are dunes on the bed.

ACKNOWLEDGMENTS

The writers are indebted to Dr. George Nomicos for performing all the experiments in the 10.5-inch flume (Chap. V, Tables 7 and 8, and Chap. VII, Table 13). The data dealing with stabilized-bed experiments (Table 13 and Figs. 31-35) have been previously presented and discussed by Nomicos in his doctoral thesis (40).

The writers also wish to acknowledge Mr. Hugh S. Bell, Jr., for his assistance in building apparatus, making experiments in the 33.5-inch flume, reducing the data, and preparing figures for this report; Mr. Stephen Emanuel for his general aid in the experimental program, Mr. Elton F. Daly for his part in the construction of the new trusses and other flume apparatus, and Miss Ann Rankin for assistance in preparing this final report for reproduction.

In addition, the writers want to thank Dr. Luna B. Leopold of the U. S. Geological Survey for assembling and transmitting the field data presented in Table 10 for the Rio Grande River at Bernalillo, New Mexico.

APPENDIX A

PROCEDURE FCR SIDE-WALL CORRECTICN

Introduction

If the wall surface is not as rough as the bed, as was the case in all the experimental runs with a sand bed, then the distribution of shear is nonuniform. As the bed becomes rougher, the shear on the bed increases and the shear on the wall decreases relative to the bed shear, because the bed offers more resistance to flow. In the central region the flow becomes more nearly two-dimensional, and the effect of the walls diminishes. Because of the variable effect of the walls caused by the changing bed roughness, a wall correction is needed to unify the results.

Several methods of side-wall correction are available. Einstein (41) has given a method based on the Manning flow equation, and Johnson (19) has presented one based on the Darcy-Weisbach formula. The Darcy-Weisbach friction factor has a sounder basis in modern fluid mechanics, and takes account of temperature. Johnson's method has been followed here, with some modifications to facilitate solution of the equations. An explanation of this method, as used, is presented below with an example.

Derivation of Equations for Side-Wall Correction

First, it will be convenient to define here a few new terms and to recapitulate some definitions and formulas already given.

S = slope of the energy line
ν = kinematic viscosity
g = acceleration of gravity
U = mean velocity

These quantities apply to either the entire flow, the bed section, or the wall section.

Each of the following quantities and formulas may be used either with subscript b for the bed section or subscript w for the wall section, or without any subscript for the whole channel:

A = area of cross section
p = wetted perimeter

$$r = A/p = \text{hydraulic radius} \qquad (A\text{-}1)$$

$$U_* = \sqrt{grS} = \text{shear or friction velocity} \qquad (A\text{-}2)$$

$$f = 8(U_*/U)^2 = \text{Darcy-Weisbach friction factor} \qquad (A\text{-}3)$$

$$R = 4\,Ur/\nu = \text{Reynolds number} \qquad (A\text{-}4)$$

The following assumptions are made:

1. The cross section can be divided into two sections, one producing shear on the bed and the other shear on the walls. The boundaries between the bed and wall sections are considered surfaces of zero shear, and are not included in the wetted perimeters p_b and p_w.

2. The velocity in the wall section, U_w, equals the velocity in the bed section, U_b.

3. The formulas above for r, U_*, f, and R can be applied to each section as if it were a channel by itself.

4. The roughnesses of the walls and bed are each homogeneous, although different.

The derivation which follows applies to any reasonable shape of open channel section. It may also be extended to cases with more than two types of roughness.

The following fundamental quantities are taken as known variables: U, S, g, ν, p_w, p_b and A. In addition, the quantities r, U_*, f, and R, for the whole section, may be determined directly by Eqs. A-1 to A-4. The principal unknowns of interest are U_{*b}, the friction velocity for the bed, r_b, the bed hydraulic radius, and f_b, the bed friction factor.

To solve the problem, f_w must also be known. If the equivalent sand roughness of the side walls is known, then the value of f_w can be determined with some auxiliary calculations from a generalized pipe resistance or Stanton diagram, such as the one given by Rouse (42). Since the side walls were practically hydrodynamically smooth in the present investigations, the procedure for finding f_w will be somewhat simplified by the elimination of the relative roughness as one of the variables. However, the general case can be solved with the same type of approach.

For smooth walls, f_w will be a function only of the Reynolds number for the wall which is:

$$R_w = \frac{4\,U_w r_w}{\nu} = \frac{4U\,r_w}{\nu}$$

Inasmuch as r_w is still unknown, rewrite R_w as

$$R_w = R\,\frac{r_w}{r} \qquad \text{(A-5)}$$

By Eqs. A-2 and A-3,

$$g\,r_w\,S = \frac{f_w}{8}\,U^2 \qquad \text{(A-6)}$$

and

$$g\,r\,S = \frac{f}{8}\,U^2\,. \qquad \text{(A-7)}$$

Hence

$$\frac{r_w}{r} = \frac{f_w}{f}\,, \qquad \text{(A-8)}$$

and Eq. A-5 becomes

$$\frac{R_w}{f_w} = \frac{R}{f}\,. \qquad \text{(A-9)}$$

Thus the quantity $\frac{R_w}{f_w}$ can be found directly, but neither R_w nor f_w individually. Consequently, it was necessary to construct a special curve, Fig. 39, giving f as a function of R/f for smooth-walled channels. Fig. 39 is based on the graph of f vs. R given by Rouse for the Karman-Prandtl resistance equation for turbulent flow in smooth pipes. Hence, knowing f and R, it was possible to find f_w by Eq. A-9 and Fig. 39.

Now the geometry requires that

$$A = A_b + A_w\,. \qquad \text{(A-10)}$$

If $r = A/p$ is substituted into Eq. A-7,

$$A = \frac{p\,f\,U^2}{8\,gS}\,.$$

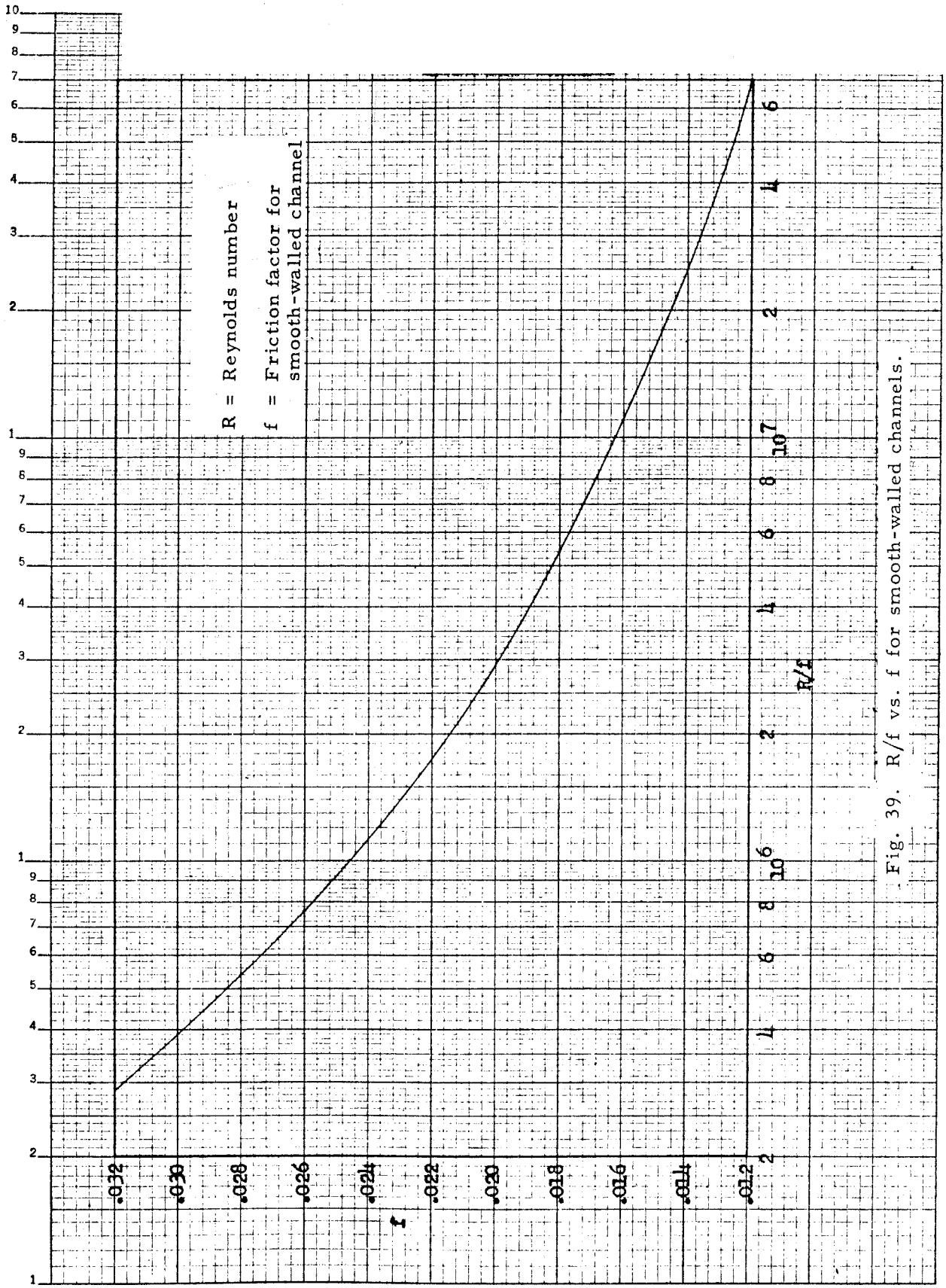

Fig. 39. R/f vs. f for smooth-walled channels.

Similarly, $$A_b = \frac{p_b f_b U^2}{8gS}$$

and $$A_w = \frac{p_s f_w U^2}{8gS} .$$

Putting these expressions for the area into Eq. A-10 and cancelling the common factor $U^2/2gS$, the result is

$$pf = p_b f_b + p_w f_w \qquad (A-11)$$

Since f_b is the only unknown, the solution is

$$f_b = \frac{p}{p_b} f - \frac{p_w}{p_b} f_w . \qquad (A-12)$$

For rectangular channels of width b and depth d, where

$$p = b + 2d,$$

$$p_b = b,$$

and $$p_w = 2d,$$

Eq. A-12 may be further similified to

$$f_b = f + \frac{2d}{b}(f - f_w) \qquad (A-13)$$

By analogy with Eq. A-8,

$$r_b = r \frac{f_b}{f} . \qquad (A-14)$$

To complete the solution, U_{*b} may be found from its definition, Eq. A-2:

$$U_{*b} = \sqrt{gr_b S} . \qquad (A-15)$$

Any other desired quantities, such as r_w, A_w, and A_b may be readily found from the fundamental equations.

Sample Calculation

The application of this side-wall correction method will be illustrated for Run 2-1, for which the bed is covered with dunes. The pertinent

quantities which were measured directly, by methods outlined in Chap. IV, are as follows:

$$Q = 0.855 \text{ cfs}$$
$$d = 0.240 \text{ ft}$$
$$b = 2.79 \text{ ft}$$
$$S = 0.00278$$
$$T = 25.5^{\circ}C$$

From these, the following quantities are calculated using Eqs. A-1 to A-4:

$$A = bd = (2.79)(0.240) = 0.670 \text{ sq ft}$$

$$U = Q/A = \frac{0.855}{0.670} = 1.28 \text{ ft/sec}$$

$$p = b + 2d = 2.79 + 2(0.240) = 3.27 \text{ ft}$$

$$r = A/p = \frac{0.67}{3.27} = 0.205 \text{ ft}$$

$$U_* = \sqrt{grS} = \sqrt{(32.2)(0.205)(.00278)} = 0.135 \text{ ft/sec}$$

$$f = 8\left(\frac{U_*}{U}\right)^2 = 8\,\frac{(0.135)^2}{(1.28)^2} = 0.090$$

$$\nu = 0.955 \times 10^{-5} \text{ ft}^2/\text{sec}$$

$$R = \frac{4\,U\,r}{\nu} = \frac{4(1.28)(.205)}{0.955 \times 10^{-5}} = 110,000 \text{ .}$$

The next step is to find f_w, the friction factor for the smooth walls. By Eq. A-9

$$\frac{R_w}{f_w} = \frac{R}{f} = \frac{110,000}{0.090} = 1,220,000 \text{ .}$$

From Fig. 39, the value $f_w = 0.0236$ is read from the curve for $R_w/f_w = 1.22 \times 10^6$.

Now by Eq. A-13

$$f_b = f + \frac{2d}{b}(f - f_w) = 0.090 + \frac{2(0.240)}{2.79}(0.090 - 0.0236)$$

$$f_b = 0.101 \text{ ,}$$

and by Eqs. A-14 and A-15,

$$r_b = r \frac{f_b}{f} = 0.205 \frac{0.101}{0.090} = 0.231 \text{ ft}$$

$$U_{*b} = \sqrt{g r_b S} = \sqrt{(32.2)(0.231)(0.00278)} = 0.144 \text{ ft/sec}$$

The ratio of the mean bed shear stress to the over-all average is

$$\frac{\bar{\tau}_b}{\bar{\tau}_o} = \frac{r_b}{r} = \frac{f_b}{f} = \frac{0.101}{0.090} = 1.12 \ .$$

Similarly for the wall

$$\frac{\bar{\tau}_w}{\bar{\tau}_o} = \frac{r_w}{r} = \frac{f_w}{f} = \frac{0.0236}{0.090} = 0.26 \ .$$

Since the average bed shear is now almost four times the wall shear, it is clear that a very significant redistribution of shear stresses has been caused by the increased roughness of the bed due to the dunes.

A side-wall correction is obviously indispensable; Johnson's method (19) as used here is the simplest and most reliable one. A slight improvement of the method, allowing for different bed and wall section velocities, has been outlined by Brooks (18) but has not been used in reducing the experimental results because the increased labor of computation is not worthwhile.

APPENDIX B

RELATED FLUME DATA BY OTHERS

Some additional flume data for experiments with beds of fine sand are presented here for the convenience of the reader. Table 15 gives the data from Brooks's thesis (18, 9), and Table 16 presents the data from Barton and Lin's report (11). In the latter case the data have been rearranged and some additional calculations, such as side-wall corrections, have been made to put the data in the same form as the other data presented in this report.

TABLE 15

SUMMARY OF EXPERIMENTS BY BROOKS IN 10.5 INCH FLUME (9)

Run No.	Q Discharge cfs	d Depth ft	r Hydr. Radius ft	S Slope	U_* Shear Vel. ft/sec	U Ave. Vel. ft/sec	f Frict. Factor	T Water Temp. °C	r_b Bed Hydr. Radius ft	U_{*b} Bed Shear Vel. ft/sec	f_b Bed Frict. Factor	No. of Sed. Disch. Samples	$\bar{C}$ Sed. Disch. Conc. gr/l	G Sed. Discharge lb/min	F Froude No.	Water Surface Condition	Bed Condition	Run No.
Clear Water																		
C-1	0.695	0.232	0.152	0.0050	0.157	3.44	0.0167	18	0.156	0.159	0.017	-	-	-	1.27	Smooth	No sand	C-1
C-2	0.45e	0.171	0.123	0.0050	0.141	3.0e	-	18.5	-	-	0.0185e	-	-	-	1.3e	Smooth	No sand	C-2
C-3	0.24e	0.115	0.091	0.0050	0.121	2.4e	-	18	-	-	0.0205e	-	-	-	1.3e	Smooth	No sand	C-3
C-4	0.32e	0.225	0.148	0.00125	0.077	1.6e	-	14.5	-	-	0.0195e	-	-	-	0.6e	Smooth	No sand	C-4
C-6	0.47	0.179	0.127	0.0049	0.142	3.00	0.0180	27	0.131	0.145	0.0185	-	-	-	1.25	Smooth	No sand	C-6
C-7	0.435	0.241	0.155	0.00195	0.099	2.06	0.0183	17	0.157	0.099	0.0185	-	-	-	0.74	Small waves	No sand	C-7
Sand Bed, D_s = 0.16 mm																		
2	0.54e	0.284	0.172	0.0018	0.100	2.15e	0.017e	17	0.174e	0.100	0.018e	0	-	-	0.71e	Small waves	Smooth	2
3	0.435	0.243	0.156	0.0025	0.112	2.04	0.024	22	0.178	0.120	0.0275	5*	1.95*	3.1	0.73	Waves	Smooth	3
4	0.43	0.236	0.153	0.0024	0.108	2.08	0.022	12.5	0.164	0.112	0.023	5	2.45	3.9	0.75	Waves	Smooth	4
5	0.28	0.18	0.13	0.0031	0.115	1.8	0.033	26	0.145	0.12	0.038	5	1.9	2.0	0.74	Lge ripples	Meanders	5
6	0.345	0.195	0.135	0.0024	0.103	2.00	0.021	21	0.143	0.106	0.0225	6	2.45	3.1	0.80	Lge waves	Smooth	6
7	0.435	0.243	0.156	0.0021	0.103	2.04	0.020	31.5	0.170	0.107	0.0225	7**	2.15**	3.5	0.73	Waves	Smooth	7
8	0.375	0.24	0.155	0.0023	0.11	1.75	0.030	27.5	0.185	0.12	0.036	6	1.5	2.1	0.63	Ripples	Meanders	8
9	0.285	0.245	0.155	0.0026	0.115	1.35	0.059	27.5	0.21	0.13	0.079	12	1.1	1.2	0.47	Ripples	Dunes	9
10	0.20	0.25	0.16	0.0020	0.10	0.93	0.095	24	0.225	0.12	0.135	4	0.2	0.15	0.33	Smooth	Dunes	10
11	0.205	0.155	0.115	0.0033	0.11	1.5	0.043	26	0.135	0.12	0.050	6	2.7	2.1	0.67	Lge ripples	Meanders	11
12##	0.37	0.30	0.178	0.0022	0.111	1.40	0.050	26	0.248	0.131	0.070	6	0.72	1.0	0.45	Ripples	Dunes	12##
13	0.215	0.197	0.136	0.0035	0.124	1.25	0.078	26.5	0.178	0.142	0.102	15	1.2	0.95	0.50	Lge ripples	Dunes	13
Sand Bed, D_s = 0.10 mm																		
21	0.435	0.236	0.154	0.00225	0.106	2.10	0.0205	25.0	0.166	0.110	0.022	6	4.85	7.9	0.76	Waves	Smooth	21
21a	0.435	0.236	0.154	0.0022	0.104	2.10	0.020	25.0	0.165	0.108	0.0215	6	4.9	8.0	0.76	Lge waves	Smooth	21a
23	0.325	0.189	0.132	0.00245	0.102	1.96	0.0215	25.0	0.141	0.106	0.023	12	5.1	6.2	0.79	Lge waves	Smooth	23
24#	0.265	0.226	0.149	0.0028	0.116	1.34	0.060	25.0	0.197	0.133	0.079	6	4	4	0.50	Ripples	Dunes	24#
24#	0.265	0.17	0.12	-	-	1.8	-	25.0	-	-	-	6	7	7	0.76	Small waves	Low ripples	24#
25	0.20	0.187	0.131	0.0033	0.118	1.23	0.074	25.0	0.168	0.134	0.095	10	5.3	4.0	0.50	Lge ripples	Dunes	25
26	0.20	0.279	0.170	0.0013	0.084	0.82	0.084	25.0	0.245	0.101	0.12	6	0.19	0.14	0.27	Smooth	Dunes	26
27	0.20	0.231	0.151	0.00235	0.107	0.99	0.094	25.0	0.207	0.126	0.13	11	1.35	1.0	0.36	Small ripples	Dunes	27
28	0.33	0.284	0.172	0.0024	0.116	1.32	0.062	25.0	0.244	0.138	0.088	12	3.6	4.45	0.44	Ripples	Dunes	28
29	0.52	0.280	0.171	0.00185	0.101	2.13	0.0180	25.2	0.178	0.103	0.019	15	3.45	6.7	0.71	Smooth	Smooth	29
30	0.265	0.281	0.171	0.00215	0.108	1.08	0.080	25.0	0.246	0.130	0.115	12	1.75	1.7	0.36	Small ripples	Dunes	30

e - estimated

* Also 5 samples at 17.5°C, $\bar{C}$ = 2.1 gr/l; and 5 at 12.5°C, $\bar{C}$ = 2.35 gr/l

** Also 7 samples at 28°C, $\bar{C}$ = 1.8 gr/l; and 10 at 26°C, $\bar{C}$ = 1.6 gr/l

\# Dual equilibrium due to a long flat sand wave. See text.

Long flat sand wave present, but data pertain only to rugged dune section.

Note: See Fig. 14(p.34) for sieve analyses of sands.

TABLE 16

SUMMARY OF EXPERIMENTS BY BARTON AND LIN IN 4-FOOT FLUME AT COLORADO A & M COLLEGE IN 1955

Sand Size: D = 0.18 mm, # σ = 0.041 mm ##

* Run No.	Q Discharge cfs	d Depth ft	r Hydr. Radius ft	S Slope	U_* Shear Vel. ft/sec	U Ave. Vel. ft/sec	f Frict. Factor	**T Water Temp. °C	r_b Bed Hydr. Radius ft	U_{*_b} Bed Shear Vel. ft/sec	f_b Bed. Frict. Factor	$\bar{C}$ Sed. Disch. Conc. gr/ℓ	G Sed. Discharge lb/min	F Froude No.	Bed Condition	Run No.
13	1.53	0.54	0.425	0.00045	0.0785	0.71	0.099	22.3	0.512	0.086	0.119	0.28	1.60	0.216	Dunes	13
12	1.96	0.66	0.496	0.00044	0.084	0.74	0.103	22.2	0.619	0.094	0.128	0.019	0.14	0.202	Dunes	12
21	0.90	0.30	0.261	0.00160	0.116	0.75	0.192	22.9	0.296	0.123	0.216	0.011	0.38	0.277	Dunes	21
11	1.5	0.46	0.374	0.00087	0.102	0.815	0.126	20.2	0.412	0.107	0.139	0.065	0.37	0.257	Dunes	11
17	1.34	0.36	0.305	0.00161	0.126	0.93	0.147	19.2	0.350	0.135	0.169	0.30	1.52	0.335	Dunes	17
10	2.0	0.51	0.406	0.00088	0.107	0.98	0.096	19.0	0.485	0.117	0.115	0.26	1.93	0.282	Dunes	10
16	1.90	0.40	0.333	0.00158	0.130	1.19	0.095	21.6	0.384	0.140	0.110	0.57	4.05	0.365	Dunes	16
8	3.1	0.65	0.490	0.00081	0.115	1.19	0.0735	21.3	0.606	0.128	0.091	0.22	2.51	0.291	Dunes	8
27	2.1	0.40	0.333	0.00135	0.122	1.31	0.070	24.3	0.380	0.131	0.080	1.00	7.9	0.367	Dunes	27
3	3.0	0.56	0.438	0.00086	0.110	1.34	0.054	23.3	0.517	0.120	0.064	0.027	0.30	0.320	Dunes	3
28	2.64	0.48	0.387	0.00116	0.120	1.39	0.059	23.4	0.450	0.129	0.068	0.91	8.9	0.390	Dunes	28
5	3.5	0.63	0.479	0.000866	0.115	1.39	0.055	21.2	0.579	0.126	0.066	0.48	6.3	0.347	Dunes	5
32	4.15	0.73	0.535	0.00082	0.119	1.42	0.056	26.0	0.668	0.133	0.070	0.56	8.7	0.323	Dunes	32
1	4.45	0.78	0.561	0.00088	0.126	1.43	0.062	14.2	0.713	0.142	0.079	0.55	9.2	0.300	Dunes	1
6	4.0	0.69	0.513	0.00088	0.121	1.45	0.056	17.9	0.632	0.134	0.069	0.54	8.2	0.327	Dunes	6
15	2.70	0.45	0.368	0.00150	0.133	1.50	0.063	20.8	0.425	0.143	0.073	1.22	12.4	0.430	Dunes	15
30	5.8	0.94	0.640	0.000555	0.107	1.54	0.038	25.8	0.504	0.095	0.048	-	-	0.290	Dunes	30
34	8.85	1.38	0.816	0.00065	0.131	1.60	0.054	25.4	0.909	0.138	0.060	0.33	11.0	0.249	Dunes	34
7	5.5	0.84	0.591	0.00088	0.130	1.64	0.050	22.9	0.755	0.147	0.064	0.63	13.0	0.344	Dunes	7
33	7.2	1.03	0.673	0.00061	0.115	1.75	0.0346	26.5	0.865	0.130	0.044	0.56	15.1	0.283	Dunes & Sand Bar	33
29	5.8	0.60	0.461	0.00121	0.134	2.41	0.0248	25.3	0.519	0.142	0.028	1.06	23.0	0.573	Flat	29
31	4.2	0.41	0.340	0.00123	0.116	2.56	0.0164	26.4	0.350	0.118	0.017	1.64	25.8	0.738	Flat	31
26	7.1	0.69	0.513	0.00125	0.144	2.58	0.025	24.7	0.589	0.154	0.029	1.41	37.5	0.575	Flat	26
25	8.1	0.78	0.561	0.00124	0.150	2.60	0.0266	24.6	0.662	0.163	0.031	1.61	49	0.553	Flat	25
18	7.40	0.69	0.513	0.00156	0.161	2.68	0.029	22.8	0.600	0.174	0.034	1.94	53	0.603	Flat	18
20	6.7	0.61	0.467	0.00166	0.158	2.74	0.0266	22.5	0.532	0.169	0.030	1.93	48	0.670	Flat	20
23	7.4	0.65	0.490	0.00183	0.170	2.84	0.0288	26.2	0.568	0.183	0.033	1.69	47	0.695	Flat	23
22	9.1	0.76	0.586	0.00170	0.179	2.99	0.0287	20.2	0.698	0.195	0.034	1.74	59	0.661	Flat	22
19	9.0	0.75	0.545	0.00167	0.171	3.00	0.026	21.8	0.639	0.185	0.030	1.83	62	0.644	Flat	19
35	7.2	0.56	0.437	0.00160	0.150	3.22	0.0173	25.6	0.465	0.155	0.018	2.48	67	0.786	Flat	35
36	7.6	0.53	0.419	0.00210	0.168	3.60	0.0174	26.1	0.448	0.174	0.019	3.78	107	0.915	Flat	36

Notes:

* The runs are arranged in order of increasing velocity.

** The temperatures listed are approximate averages of Barton and Lin data.

#D = Mean grain diameter

= Standard deviation; value listed above is the average of two values, 0.045 mm (March 1954) and 0.037 mm (July 1954).

Length of flume = 70 feet.

APPENDIX C

GRAPHICAL SOLUTION OF EINSTEIN-BARBAROSSA EQUATIONS FOR DETERMINATION OF r' AND r''.

As explained in Chapter VI, Sec. C, Einstein and Barbarossa (16) in their analysis of river channel roughness divide both the shear velocity U_* and hydraulic radius r into two parts, one for the so-called grain resistance, the other for dune or bar resistance. In mathematical notation, these relations were expressed by Eqs. 6, 9, 10 and 11 as

$$r = r' + r'' \tag{C-1}$$

$$U_*^2 = u_*'^2 + u_*''^2 \tag{C-2}$$

$$u_*' = \sqrt{g\, r' S} \tag{C-3}$$

$$u_*'' = \sqrt{g\, r'' S} \tag{C-4}$$

Now the separation of r into r' and r'' can never be directly observed, but must be calculated from some assumed or derived relationships. Einstein and Barbarossa suggest Eq. 12, i.e.:

$$\frac{U}{u_*'} = 5.75 \log_{10} \left(12.27 \frac{r'}{K_s} x\right), \tag{C-5}$$

in which the correction factor x is given by a graph (16, Fig. 2) as a function of K_s/δ' as in Eq. 13, which is

$$x = f_1\left(\frac{K_s}{\delta_1}\right) = f_1\left(\frac{K_s\, u_*'}{11.6\nu}\right) \tag{C-6}$$

where δ' is the thickness of the laminar sublayer defined by Einstein as $11.6\ \nu/u_*'$. The equivalent sand roughness K_s is taken as D_{65} by Einstein.

The second main relationship involves both r' and r'' in the following way:

$$\frac{U}{u_*''} = f_2(\psi') = f_2\left(\frac{\rho_s - \rho}{\rho}\ \frac{D_{35}}{r'S}\right) \tag{C-7}$$

To determine this function from field observations, Einstein and Barbarossa first computed r', u_*' and x from Eqs. C-3, C-5, and C-6, and then u_*''

by Eq. C-2; next, calculated values of U/u''_* were plotted against ψ' and a curve was fitted to the points by eye to define the function f_2 in Eq. C-7.

The objective of this appendix is merely to show how the above calculations may be facilitated in order that large quantities of laboratory and field data can be checked easily against the curve proposed by Einstein and Barbarossa. An evaluation of the assumptions and results of their roughness analysis has already been presented in Chap. VI, Sec. C.

The difficulty of the above procedure is that Eqs. C-3, C-5, and C-6 have to be solved by trial and error to determine r'. Substituting Eqs. C-3 and C-6 into Eq. C-5, one obtains

$$\frac{U}{\sqrt{g\,r'S}} = 5.75 \log_{10} \; 12.27 \left(\frac{r'}{K_s}\right) f_1\left(\frac{K_s \sqrt{g\,r'S}}{11.6\,\nu}\right) \qquad \text{(C-8)}$$

where as before the function f_1 is defined by a curve. Basically there are three parameters involved:

(a) $$\frac{U}{u'_*} = \frac{U}{\sqrt{g\,r'S}}$$

(b) $$\frac{r'}{K_s}$$

(c) $$\frac{K_s \sqrt{g\,r'S}}{11.6\,\nu}$$

The solution of Eq. C-8 for r' is laborious because r' appears in all three of these parameters, so that none of them is known directly before the trial-and-error solution is started. It is found more convenient to change the parameters above to

(A) $$\frac{U}{u'_*} = \frac{U}{\sqrt{g\,r'S}}$$ (same as (a)).

(B) $$\frac{U}{\sqrt{g K_s S}} = (a)\sqrt{b}$$

(C) $$\frac{U^3}{g\,\nu\,S} = 11.6\,(a)^3\,(b)\,(c)\,.$$

Consequently, one may write

$$\frac{U}{\sqrt{g\, r' S}} = f_3\left(\frac{U}{\sqrt{g K_s S}}, \frac{U^3}{g \nu S}\right) \qquad (C\text{-}9)$$

Now when r' is unknown, but U, S, and K_s are all known, the second and third parameters can be calculated directly and the first parameter involving r' is readily determined by Eq. C-9, without resort to trial and error.

Figure 40 is a graph of this function (Eq. C-9) derived from the Einstein-Barbarossa formulas. To accomplish this it was first necessary to construct a working graph as follows:

(1) Replace $\frac{r'}{K_s} x$ in Eq. C-5 by its identical equivalent $\left(\frac{U}{\sqrt{g K_s S}} \sqrt{x} \div \frac{U}{u'_*}\right)^2$.

(2) Select various values of $\frac{U}{u'_*}$ and compute corresponding values of $\frac{U\sqrt{x}}{\sqrt{g K_s S}}$ and plot a graph of the relation between these two parameters (not shown). Using this graph the calculation of points for the construction of Fig. 40 proceeded in the following way:

(3) Select a convenient value of $\frac{U}{\sqrt{g K_s S}}$.

(4) Select a convenient value of x.

(5) From working graph (item 2 above) find the value of $\frac{U}{u'_*}$ corresponding to the value of $\frac{U}{\sqrt{g K_s S}} \sqrt{x}$ (from (3) and (4)).

(6) From x, find $\frac{K_s}{\delta'}$ by the Einstein-Barbarossa curve (16, Fig. 2, or 23, Fig. 4).

(7) Compute $\frac{U^3}{g \nu S} = \left(\frac{K_s}{\delta'}\right)(11.6)\left(\frac{U}{u'_*}\right)\left(\frac{U}{\sqrt{g K_s S}}\right)^2$.

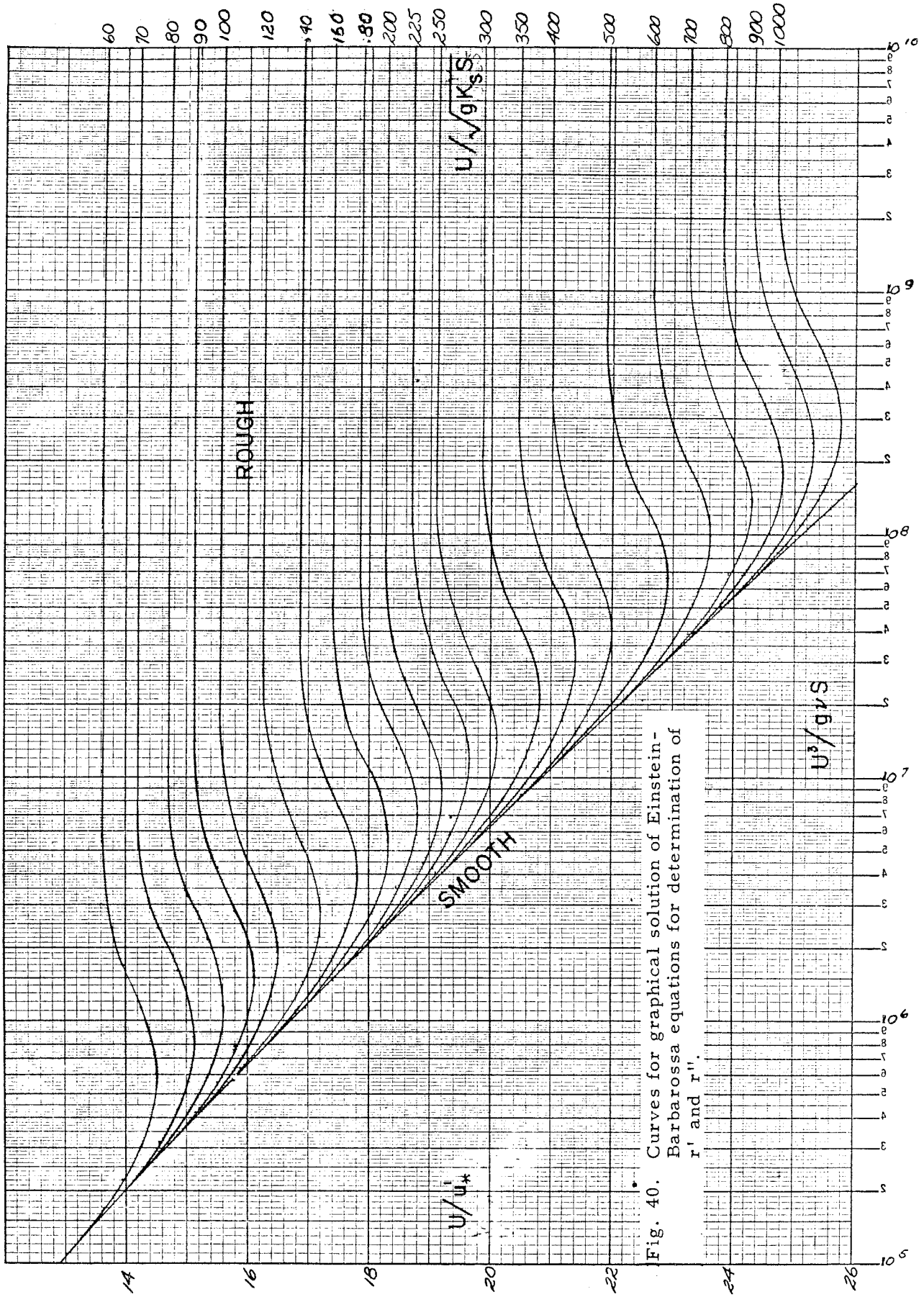

Fig. 40. Curves for graphical solution of Einstein-Barbarossa equations for determination of r' and r''.

(8) Repeat for various points; plot and draw curves as shown in Fig. 40.

The similarity of Fig. 40 to the common pipe-friction diagram is surprising. To emphasize this similarity, the ordinate scale has been inverted so that the higher values of f' (i.e., lower values of U/u'_*) are toward the top of the graph. The sloping line on the left is for channels which are smooth (with respect to the grain resistance only) as indicated by the fact that it is the limit as $\frac{U}{\sqrt{g\,K_s\,S}} \rightarrow \infty$ (or $K_s \rightarrow 0$) with $\frac{U^3}{g\,\nu\,S}$ fixed. Similarly, the horizontal lines at the right represent the rough channel regime where U/u'_* ceases to be a function of $U^3/g\nu S$.

To illustrate the use of Fig. 40, consider Run 2-1 as an example. Since a side-wall correction has been made, the hydraulic radii r, r' and r'' are replaced by r_b, r'_b, and r''_b which apply to the bed section only. From Tables 5 and 6 it is found that:

$U = 1.28$ fps
$S = 0.00278$
$r_b = 0.231$ ft
$U_{*b} = 0.144$ fps
$T = 25.5^{\circ}C$
$K_s = D_{65} = 0.155$ mm $= 0.00051$ ft
$D_{35} = 0.123$ mm $= 0.00040$ ft

The kinematic viscosity for this temperature is $\nu = 0.955 \times 10^{-5}$ ft^2/sec. First, one evaluates the parameters (B) and (C) above:

$$\frac{U}{\sqrt{g\,K_s\,S}} = \frac{1.28}{\sqrt{32.2 \times 0.00051 \times 0.00278}} = 189$$

$$\frac{U^3}{g\,\nu\,S} = \frac{1.28^3}{32.2 \times 0.955 \times 10^{-5} \times 0.00278} = 2.45 \times 10^6 .$$

Next from Fig. 40 is obtained

$$\frac{U}{u'_*} = 18.2 ,$$

whence

$$u'_* = \frac{1.28}{18.2} = 0.0703 \text{ fps}$$

and

$$r'_b = \frac{u_*^2}{gS} = \frac{(0.0703)^2}{32.2 \times 0.00278} = 0.055 \text{ ft.}$$

Therefore,

$$r''_b = r_b - r'_b = 0.231 - 0.055 = 0.176 \text{ ft.}$$

The quantity u''_* may be computed from Eq. C-4 (or C-2) as

$$u''_* = \sqrt{g\, r''_b\, S} = \sqrt{32.2 \times 0.176 \times 0.00278} = 0.125 \text{ fps}$$

From this is found

$$\frac{U}{u''_*} = \frac{1.28}{0.125} = 10.2$$

The computations are concluded by calculating

$$\psi' = \frac{\rho_s - \rho}{\rho} \frac{D_{35}}{r'_b S} = 1.65 \frac{0.00040}{0.055 \times 0.00278} = 4.32 .$$

These last two quantities are the ordinate and abscissa, respectively, in Figs. 27, 28, and 29; this particular point is plotted on Fig. 27.

In summary, this appendix has shown how the problem of determining r' by the Einstein-Barbarossa equations can be solved much more easily using the parameters (A), (B) and (C) in conjunction with Fig. 40, instead of by the trial and error procedure originally suggested by these investigators.

LIST OF SYMBOLS

A	=	area of cross section
a	=	distance from stream bed to point of reference for suspended load equation
b	=	width of flume (rectangular channel)
C	=	Chezy coefficient = $U/\sqrt{rS}$
c	=	point concentration at the distance y from the bed
c_a	=	point concentration at $y = a$
c_{md}	=	sediment concentration at mid-depth ($y = d/2$)
$\overline{C}$	=	sediment discharge concentration, or concentration of sediment in a sample of the discharge = G/Q (weight per unit volume)
D	=	grain diameter
D_g	=	geometric mean sieve diameter
D_s	=	mean sedimentation diameter
D_{35}	=	grain size for which 35% of sand is finer (similarly for D_{50}, D_{65}, etc.)
d	=	mean depth of flow
F	=	Froude number = $U/\sqrt{gd}$
f	=	Darcy-Weisbach friction factor for channel = $8(U_*/U)^2$
f'	=	part of f associated with grain resistance
f''	=	part of f associated with dune or bar resistance
f_b	=	friction factor for bed alone, calculated from sidewall correction procedure = $8(U_{*b}/U)^2$
f_w	=	friction factor for walls
G	=	total sediment discharge = $\overline{C}Q$ (weight per unit time)
g	=	gravitational acceleration
K_s	=	equivalent sand roughness ($= D_{65}$)
k	=	von Karman universal constant
$k_{c\ell}$	=	von Karman constant at the centerline of a rectangular channel

LIST OF SYMBOLS (cont'd)

m = slope of velocity profile (units of velocity per cycle)

n = Manning's roughness coefficient

P_f = power required to overcome hydraulic resistance to flow

P_s = power required to suspend sediment in entire cross-section

P'_s = power required to suspend sediment in a thin layer near the bed

p = wetted perimeter

Q = discharge (volume per unit time)

q = discharge per unit width = Q/b

q_s = sediment discharge per unit width = G/b

R = Reynolds number = $4Ur/\nu$

R_w = Reynolds number for wall section = $4Ur_w/\nu$

r = hydraulic radius = $bd/(b + 2d)$

r_b, r_w = hydraulic radii for bed and wall sections of flow, obtained by side-wall correction procedure

r' or r'_b = part of r or r_b associated with grain resistance

r'' or r''_b = part of r or r_b associated with dune or bar resistance ($r'' = r - r'$; $r''_b = r_b - r'_b$) .

S = slope of energy grade line

S' = part of slope associated with grain resistance

S'' = part of slope associated with dune or bar resistance

S_f = slope of flume

T = temperature of water

U = mean velocity = Q/bd

U_* = shear velocity for whole channel = $\sqrt{\tau_o/\rho}$ = $\sqrt{grS}$

U_{*b} = shear velocity for bed only = $\sqrt{gr_bS}$

u = velocity at distance y up from the bed

$\bar{u}$ = mean velocity on a vertical section

LIST OF SYMBOLS (cont'd)

$\bar{u}_{c\ell}$ = mean velocity on the centerline vertical of a rectangular channel

u_* = shear velocity for two-dimensional flow = $\sqrt{\tau_o/\rho} = \sqrt{gdS}$

$u_{*c\ell}$ = shear velocity on the centerline of a rectangular channel

u'_* = shear velocity for grain resistance only = $\sqrt{gr'_b S}$

u''_* = shear velocity for dune or bar resistance only = $\sqrt{gr''_b S}$

w = settling velocity of sand grains

x = parameter for transition from rough to smooth walls in logarithmic friction formula

y = distance up from the bed of the stream

z = exponent in suspended load equation (see Eq. 23)

β = ratio of turbulent diffusion coefficient for sediment to that for momentum

γ_s = unit weight of sand grains

γ = unit weight of water

δ' = thickness of laminar sublayer = $11.6\,\nu/u_*$

ν = kinematic viscosity of water

ρ = mass density of water

ρ_s = mass density of sand particles

σ_g = geometric standard deviation of sand-size distribution

τ_o = mean shear stress on the boundary of a channel

τ'_o = part of bed shear stress associated with grain resistance

τ''_o = part of bed shear stress associated with dune or bar resistance

ψ' = Einstein's dimensionless parameter for relative intensity of shear on representative particle (D_{35})

REFERENCES

1. Gilbert, G. K., "The Colorado Plateau Province as a Field for Geological Study", Amer. Journal of Science, July-Aug. 1876.

2. Hooker, Elton Huntington, "The Suspension of Solids in Flowing Water", Trans. Amer. Soc. of Civil Engineers, Vol. 36, p. 239, Dec. 1896.

3. Latham, Baldwin, Minutes of Proceedings Institute of Civil Engineers, Vol. 71 (1886), p. 46. See also Ref. 2, p. 288.

4. McMath, R. E., "Silt Movement by the Mississippi", Van Nostrand's Engineering Magazine, 1883, p. 36. See also footnote Ref. 2, p. 289.

5. Gilbert, Grove Karl, "The Transportation of Debris by Running Water", U. S. Geological Survey, Prof. Paper 86, 1914.

6. Buckley, A. B., "The Influence of Silt on the Velocity of Water Flowing in Open Channels", Minutes of Proc. of Institute of Civil Engineers, Vol. 226, p. 183, 1922-23, Pt. II.

7. Vanoni, Vito A., "Transportation of Suspended Sediment by Water", Trans. A.S.C.E., Vol. 111, p. 67-133, 1946.

8. Vanoni, Vito A., "Some Effects of Suspended Sediment on Flow Characteristics", Proc. 5th Hydr. Conf., State Univ. of Iowa, Studies in Engineering, Bul. 34, 1953.

9. Brooks, Norman H., "Mechanics of Streams with Movable Beds of Fine Sands", Proc. A.S.C.E., Vol. 81, Separate No. 668, April 1955.

10. Ali, Said M., and Albertson, Maurice L., "Some Aspects of Roughness in Alluvial Channels", Dept. of Civil Eng., Colorado A. and M. College, Fort Collins, Colorado, Aug. 1953, revised Aug. 1956.

11. Barton, James R. and Lin, Pin-Nam, "A Study of Sediment Transport in Alluvial Channels", Rep. No. 55 J. R. B. 2, Civil Eng. Dept., Colorado A. and M. College, Fort Collins, Colorado, Mar. 1955.

12. Leopold, Luna B., and Maddock, Thomas, Jr., "Relation of Suspended Sediment Concentration to Channel Scour and Fill", Proc. of 5th Hydr. Conf., State Univ. of Iowa, Studies in Eng., Bul. 34, 1953.

13. Eden, Edwin W., "A Study of Bed Movement and Hydraulic Roughness Changes in the Lower Mississippi River", M. S. Thesis, Dept. of Mechanics and Hydraulics, State University of Iowa, June 1938.

14. Carey, Walter C., and Keller, M. Dean, "Systematic Changes in the Beds of Alluvial Rivers", Journal of Hydraulics Div., A.S.C.E., Vol. 83, No. HY4, Aug. 1957.

REFERENCES
(cont'd)

15. Harrison, A. S., "Study of Effects of Channel Stabilization and Navigation Project on Missouri River Levels: - Memorandum No. 18, Sediment Characteristics of the Missouri River, Sioux City to the Mouth", Cmaha District Corps of Engineers, U. S. Army, unpublished report, Jan. 1954.

16. Einstein, Hans A., and Barbarossa, Nicholas L., "River Channel Roughness", Trans. A.S.C.E., Vol. 117, 1952, p. 1121-1146.

17. Vanoni, Vito A., "Experiments on the Transportation of Suspended Sediment by Water", Ph.D. Thesis, Calif. Inst. of Tech., 1940.

18. Brooks, Norman H., "Laboratory Studies of the Mechanics of Streams Flowing over a Movable Bed of Fine Sand", Ph.D. Thesis, Calif. Inst. of Tech., 1954.

19. Johnson, J. W., "The Importance of Side-Wall Friction in Bed-Load Investigations", Civil Eng., Vol. 12, No. 6, June 1942, pp. 329-331.

20. Vanoni, Vito A. and Brooks, Norman H., "Laboratory Studies of Dunes in Streams", manuscript in process.

21. Ismail, Hassan M., "Turbulent Transfer Mechanism and Suspended Sediment in Closed Channels", Trans. A.S.C.E., Vol. 117, 1952, p. 409.

22. Brooks, Norman H., Closing Discussion of Reference 9, Journal of Hydraulics Div., A.S.C.E., Vol. 83, No. Hy2, Paper 1230, April 1957.

23. Einstein, H. A., "The Bed-Load Function for Sediment Transportation in Open Channel Flows", U. S. Dept. of Agr., Soil Conservation Service, Tech. Bul. No. 1026, Sept. 1950.

24. Kalinske, A. A. and Hsia, C. H., "Study of Transportation of Fine Sediments by Flowing Water", Univ. of Iowa, Studies in Engrg., Bul. No. 29, 1945.

25. Barton, James R., Discussion of Reference 9, Proc. A.S.C.E., Vol. 81, Paper No. 841, Nov. 1955, pp. 9-11.

26. Laursen, Emmett, "An Investigation of the Total Sediment Load", Iowa Inst. of Hyd. Research, State Univ. of Iowa, June 15, 1957.

27. Einstein, H. A. and Chien, Ning, Discussion of Reference 9, Proc. A. S. C. E., Vol 81, Paper No. 841, Nov. 1955, pp. 10-27.

28. Keulegan, Garbis, H., "Laws of Turbulent Flow in Open Channels", Research paper 1151, Jour. of Research, National Bureau of Standards, Vol. 21, 1938, pp. 707-741.

REFERENCES
(cont'd)

29. Meyer-Peter, E. and Muller, R., "Formulas for Bed-Load Transport", Internatl. Assn. for Hydr. Structures Res., Proc. 2nd Meeting, Stockholm, 1948, pp. 39-65.

30. Einstein, H. A. and Chien, Ning, "Can the Rate of Wash Load be Predicted from the Bed-Load Function?", Trans. Amer. Geophysical Union, Vol. 34, 1953, pp. 876-882.

31. Straub, Lorenz G., "Terminal Report on Transportation Characteristics of Missouri River Sediment", Univ. of Minn., St. Anthony Falls Hydraulic Lab. in cooperation with the Missouri River Div., Corps of Engrs., U. S. Army, M.R.D. Sediment Series No. 4, April 1954.

32. Lane, E. W., Carlson, E. J. and Hanson, C. S., "Low Temperature Increases Sediment Transportation in Colorado River", Civil Engineering, Vol. 19, No. 9, Sept. 1949, pp. 45-46.

33. Rouse, Hunter, "Modern Conceptions of the Mechanics of Fluid Turbulence", Trans. A.S.C.E., Vol. 102, 1937, p. 535.

34. Lane, E. W. and Kalinske, A. A., "The Relation of Suspended to Bed Material in Rivers", Trans. Amer. Geophysical Union, Vol. 20, Part IV, 1939, pp. 637-641.

35. Leopold, Luna B. and Maddock, Thomas, Jr., "The Hydraulic Geometry of Stream Channels and Some Physiographic Implications", U. S. Geological Survey, Professional Paper 252, 1953.

36. Chien, Ning, "The Present Status of Research on Sediment Transport", Trans. A.S.C.E., Vol. 121, 1956, p. 833.

37. Leopold, Luna B. and Wolman, M. Gordon, "Floods in Relation to the River Channel", Publ. No. 42, International Assn. of Hydrology, Dijon, France, 1956.

38. "Sediment Characteristics Study of Missouri River at Omaha, Nebraska", U. S. Engineer Office, Omaha, Nebr., unpublished report 1951.

39. Einstein, H. A., and Chien, Ning, "Second Approximation of the Suspended Load Theory", Univ. of Calif., Series 47, Issue No. 2, Berkeley, Calif., Jan. 31, 1952.

40. Nomicos, George N., "Effects of Sediment Load on the Velocity Field and Friction Factor of Turbulent Flow in an Open Channel", Ph.D. Thesis, Calif. Inst. of Technology, Pasadena, Calif., 1956.

41. Einstein, H.A., "Formulas for the Transportation of Bed Load". Trans. A.S.C.E., Vol. 107, 1942, pp. 561-577.

42. Rouse, Hunter, "Elementary Mechanics of Fluids", J. Wiley and Sons, New York, 1946.